Ionospheric Research

NSF Grant GP-5611

Scientific Report

on

"Model Studies of Low Energy Plasma in the

Outer Magnetosphere"
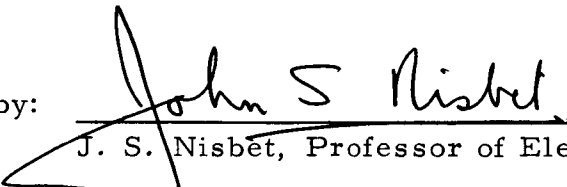
by

J. M. Grebowsky

March 15, 1968

Scientific Report No. 317

Submitted by: _____

J. S. Nisbet, Professor of Electrical Engineering

Approved by: _____

A. H. Waynick, Professor of Electrical Engineering
and Director, Ionosphere Research Laboratory

Ionosphere Research Laboratory

The Pennsylvania State University

College of Engineering

Department of Electrical Engineering

TABLE OF CONTENTS

ABSTRACT

The motion of low energy plasma in the outer magnetosphere is considered. In particular, theoretical plasma models are set up to describe the motion of plasma along a magnetic field line, as the plasma and the "frozen-in" field follow the convection pattern inherent to the "open" model of the magnetosphere. The component of the electric field parallel to the earth's magnetic field lines plays a significant role in this investigation.

At interconnection of the interplanetary and earth field lines on the day side of the earth, two dissimilar plasmas merge. The electrons are considered to rapidly interdiffuse. Due to the small thermal velocities of the low energy protons, however, the protons must be considered in the light of the past history of the parallel electric field.

Using model distribution functions the electron density is determined at every point along the open field lines as a function of the local electrostatic potential. A study of the proton motion indicates that a minimum of electrostatic potential may occur near the magnetopause. Therefore, electrons trapped between the potential minimum and the magnetic mirror had to be included in the analysis. Given the proton density at all points along an open field line, the derived density — potential profiles are used to determine the parallel electric field variation along the field line.

At reconnection on the night side, proton streams traveling along magnetic field lines away from the earth collide at the

equator. It is hypothesized that plasma shocks then form which travel away from the equator, along magnetic flux tubes towards the polar ionospheres as the closed field line formed by reconnection moves towards the day side. The shocks are studied for the simple case in which the ordered proton motion is completely randomized by their passage.

CHAPTER 1

INTRODUCTION

1.1 General Statement of the Problem

The problem to be considered is the motion of the essentially neutral, low density, low energy plasma, consisting of mainly electrons and protons, which exists in the outer reaches of the earth's magnetic field. In this spatial regime, electric fields are believed to exist which have components both parallel and perpendicular to the magnetic field lines. Hence an analysis of the plasma motion will also entail an analysis of the different types of electric fields which are present.

This thesis is an attempt to develop plasma models which describe a few aspects of the plasma environment at large geocentric distances.

1.2 Origin and Importance of the Problem

During the past decade, satellites and rockets have probed the outer reaches of the earth's geomagnetic environment. Scientific instruments carried by these vehicles have begun to furnish a detailed mapping of the magnetic fields and high energy plasmas existing in the neighborhood of the earth. Thus far, however, because of experimental limitations, very few direct measurements have been made of the very low energy (of the order of a few electron volts), low density (a few particles per cubic centimeter) plasma found in this spatial region. Hence, lacking experimental data,

theoretical models are needed in order to determine the probable

spatial and temporal distribution of the low energy, low density

plasma.

Although considerable theoretical research has been done con-

cerning the effects, on a plasma, of electric field components per-

pendicular to the magnetic field direction, the parallel component

is usually neglected due to the assumption of a large (essentially

infinite) electrical conductivity parallel to the magnetic lines of

force. In the case of a medium or high density plasma this assump-

tion requires a vanishingly small parallel electric field because

the current is directly proportional to the electric field and in

the same direction.

In a low density plasma (that is, a plasma for which the mean

free path is much greater than the characteristic length of the

spatial region considered) the current density and electric field in

the direction of the magnetic field are not simply related and the

concept of conductivity has no meaning (Alfvén and Fälthammer, 1963).

Therefore electric field components parallel to the magnetic field

lines may occur in the outer reaches of the earth's magnetic field

where the plasma is of low density. This study will explore the

effects of these "parallel E fields" on the plasma motion.

1.3 The Earth's Magnetic Field Configuration

The earth, with its dipole-like magnetic field, is immersed

in a stream of neutral plasma emitted from the sun. Chapman and

Ferraro (1931, 1932, 1933) approximated this situation by a perfectly

conducting, field-free sheet approaching a magnetic dipole. Induced

currents in the conducting sheet modify the dipole field as is shown in Figure 1. The model of Chapman and Ferraro confines the earth's magnetic field to the earth side of the sheet, forming a geomagnetic cavity. These investigators had assumed that the interplanetary plasma flow, and hence the geomagnetic cavity, existed only during magnetic storms.

Later studies by Biermann (1951) on the tails of comets, and theoretical studies by Parker (1958, 1960) on the hydrodynamic expansion of the solar corona indicated that the sun emitted a continuous stream of charged particles. This was confirmed experimentally by the satellites Lunik 2 and Lunik 3 (Gringauz et al., 1960) and by Explorer 10 (Bonetti et al., 1963). The existence of a continual "solar wind" implied the continual existence of a geomagnetic cavity, which is indeed the case as shown by direct measurements of the geomagnetic field by the satellites Explorers 10, 12, 14, 18, and 21.

With no interplanetary magnetic field, the earth's field is contained completely within the magnetospheric boundary, where the term magnetosphere refers to that part of the earth's environs in which the motion of ionization is dominated by the geomagnetic field. If the solar plasma is warm, the tail of the cavity will close at a great distance from the earth on the night side due to the thermal pressure overcoming the magnetic pressure. The "closed" model of the magnetosphere refers to a field configuration in which the field lines form a closed system and connect every point in one hemisphere to every point in the opposite hemisphere. This model is shown in Figure 2.
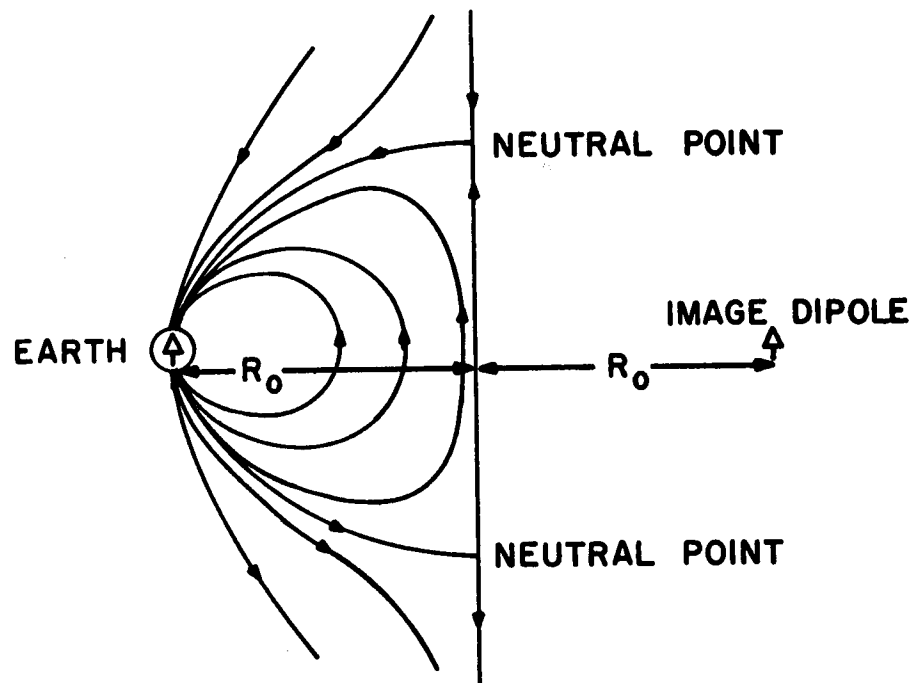
FIGURE I. FIELD CONFIGURATION FOR A DIPOLE
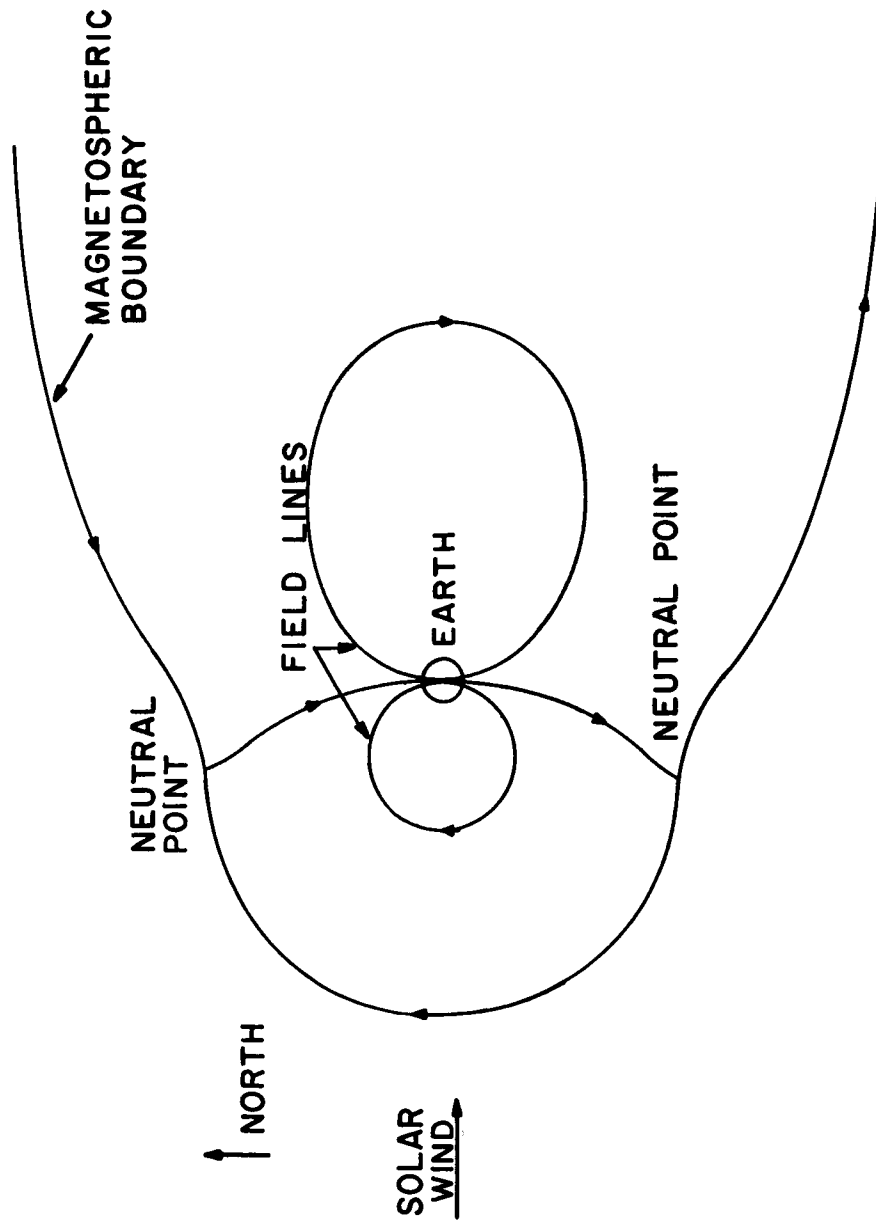APPROACHED BY A PERFECTLY
CONDUCTING SHEET

FIGURE 2. CLOSED MODEL OF THE MAGNETOSPHERE

Using Pioneer 5 data, Coleman et al. (1960) detected a small interplanetary field of the order of a few gammas. Thereupon, Dungey (1961) developed the "open" model of the magnetosphere in which field lines originating in one hemisphere may not terminate in the opposite hemisphere, but instead connect to the interplanetary field (see Figure 3). This configuration results only if the interplanetary field has a southward component. One of the many interesting facets of this model is that the open field lines allow a direct path by which interplanetary charged particles may enter into the magnetosphere.

It is hard to escape the conclusion that the geomagnetic field lines are "frozen" to the plasma in the magnetosphere (Levy et al., 1963; Dungey, 1966). The plasma motion and the corresponding field line motion in the open model are indicated by the arrows in Figure 3. A more detailed description of the motion is seen in Figure 4 where a time sequence of the motion of an individual field line is shown (the motion takes place in the direction of increasing label numbers). Since the situation is assumed to be steady, Figure 4 can also be considered as the total field and flow morphology at a given time. Dungey's model allows the solar field lines to merge with the earth's field on the day side of the earth. The resulting open field lines are then dragged by the solar wind through the tail to a current sheet and are reconnected into the night side of the magnetosphere. The resulting closed field line (labeled 8 in Figure 4) then drifts around the earth to the day side and towards the
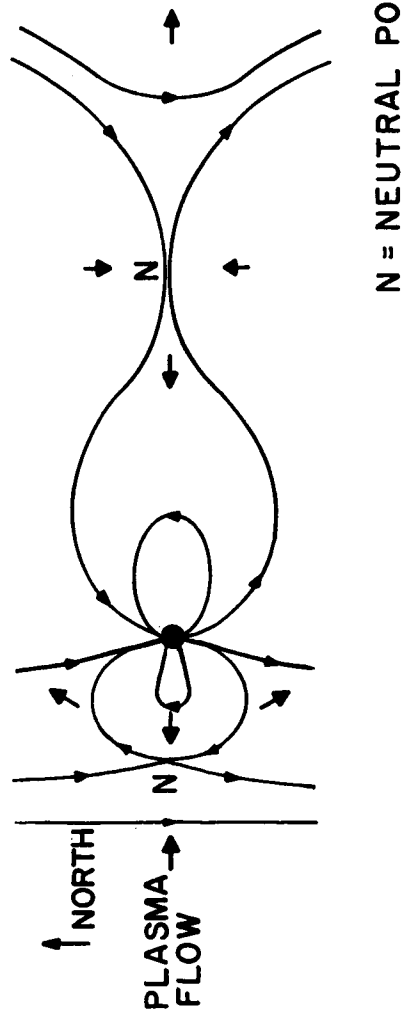
FIGURE 3. OPEN MODEL OF THE MAGNETOSPHERE

N = NEUTRAL POINT
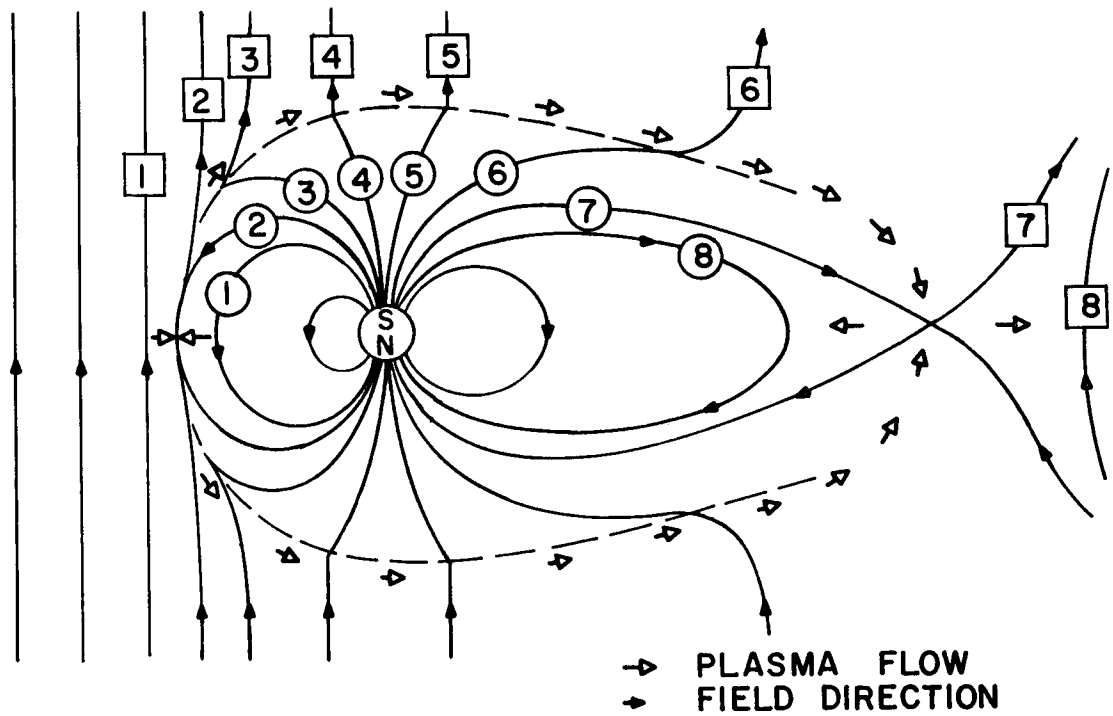
FIGURE 4. RECONNECTION CYCLE (FROM LEVY et al; 1963)

magnetopause (i.e., the boundary of the magnetosphere) where the cycle begins again.

Although there is still some question, the open model of the magnetosphere appears to be widely supported today. This model agrees qualitatively with the DS current system (Dungey, 1961) and appears capable of explaining some aspects of the auroral morphology (Speiser, 1964; 1967). Experimentally, it has been supported by the positive correlation found between geomagnetic disturbances and the southward component of the interplanetary field (Fairfield and Cahill, 1966; Wilcox et al., 1967; Schatten and Wilcox, 1967). Also, measurements of the magnetic field component normal to the magnetospheric boundary current layer (the magnetopause) by Sonnerup and Cahill (1967) provide evidence that field lines of the earth connect to interplanetary field lines at least during the main phase of a magnetic storm. In the face of this evidence, the open model will be assumed in the work to follow.

In addition, since the solar wind velocity (300 to 600km/s) is greater than the Alfvén velocity, a collisionless magneto-hydrodynamic bow shock forms in a manner somewhat analogous to the shock wave formed by supersonic flow past a blunt body in gas dynamics. This shock wave was detected by Explorers 12 and 18 at about 14 to 16 earth radii near the subsolar point on the day side of the earth; whereas, the subsolar point of the magnetopause is on the average at only 10 earth radii. The region between the shock and the magnetopause is called the magnetosheath and is characterized by a well thermalized plasma and a magnetic field which is
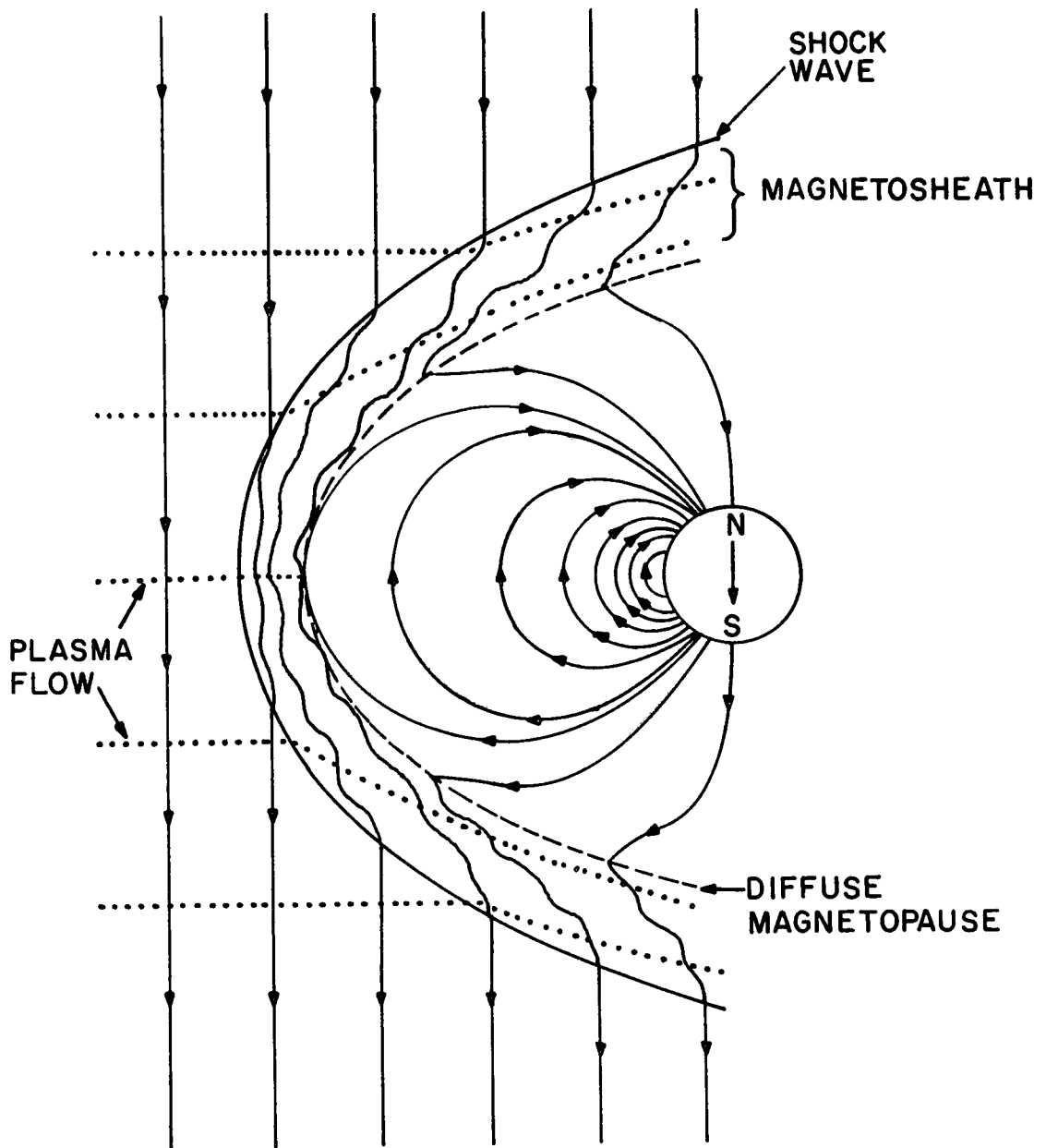
FIGURE 5. OPEN MODEL WITH SHOCK

somewhat turbulent compared to the magnetospheric field. For a southward interplanetary field, the field topology with regards to the shock is as shown in Figure 5.

1.4 Previous Studies of Magnetospheric Ambient Plasma

Lightning discharges produce audio frequency electromagnetic disturbances which propagate through the magnetosphere in the "whistler" mode along magnetic shells with enhanced ionization. From the dispersion characteristics of these waves which are measured by ground based stations, it is possible to obtain electron densities in the equatorial plane.

Studying whistlers, Carpenter (1963) discovered a very abrupt decrease of electron density with increasing distance from the earth at an equatorial geocentric distance of approximately 4 earth radii. This region of rapid decrease is known as the "plasmapause" or "whistler knee." A sharp decrease has also been detected by low energy plasma probes on board space vehicles (Gringauz, 1963; Taylor et al., 1965; Whipple and Troy, 1965). The knee is essentially field aligned and separates, according to Carpenter's (1966) more recent measurements, an inner region (plasmasphere) of density 100 electrons/ cc from the outer region (trough) where the density may be as low as 1 electron/cc (see Figure 6a). Carpenter's results also indicate that the knee possesses the dawn-dusk asymmetry shown in Figure 6b.

The plasmasphere corresponds to a plasma region in which the constituent ions and electrons are in diffusive equilibrium; whereas, the trough consists of a collisionless plasma which is not in
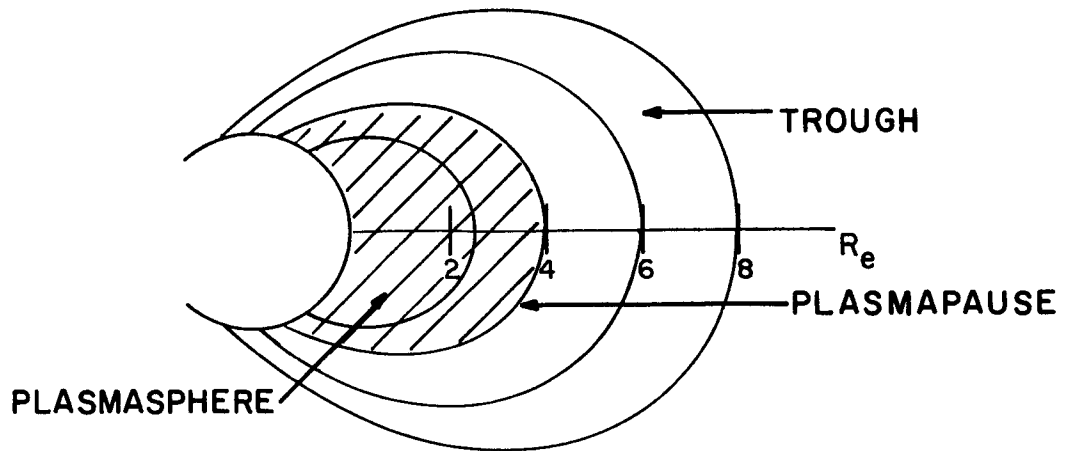
FIGURE 6a. MERIDIAN CROSS SECTION OF MAGNETOSPHERE
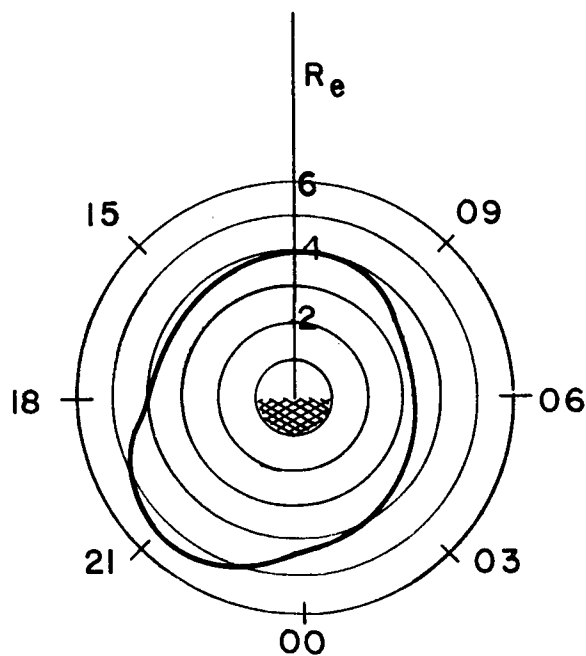
FIGURE 6b. PLASMAPAUSE IN EQUATORIAL PLANE
AS A FUNCTION OF TIME

equilibrium (Angerami and Carpenter, 1966). The distinct change in plasma behavior across the plasmapause appears to correspond to a change in the nature of the magnetic field circulation process as will be seen in the next paragraph.

The convection model described previously did not include the tendency of the magnetospheric plasma to rotate with the earth. If the plasma motion due to the earth's rotation is superposed on the convection motion previously assumed, the magnetospheric lines of force are separated into two distinct groups: those that open to interplanetary space during the convective motion and those that always remain closed. On field lines of the former group, the plasma density will be less than the value expected on the basis of equilibrium theory because the plasma can escape to interplanetary space when these field lines are open, whereas the rate of replenishment from the ionosphere is low. On field lines of the latter group, plasma escape is always prevented by closed field lines so that diffusive equilibrium will prevail. Nishida (1966) showed that the plasmapause appears to correspond to the boundary surface between these two groups of field lines. More recent computations by Brice (1967) also lend support to this explanation of the plasmapause.

1.5 Parallel Electric Fields in the Magnetosphere

In the outer magnetosphere, the mean free paths of the ions and electrons are greater than the size of the magnetosphere (approximately 10 earth radii). The Debye length, on the other hand, is only of the order of meters. Hence, this region can be considered

as a low density plasma in which the principle of quasineutrality is valid; that is, the ions and electrons have the same numerical density everywhere except in thin Debye sheaths.

Alfvén and Fälthammer (1963) showed that the concept of electrical conductivity has no meaning in such a plasma since the electric field and current density are generally not proportional. In fact, these authors studied a low density plasma of protons and electrons in a magnetic mirror configuration, when each kind of particle has a well defined velocity common to all particles of that kind. Their study proved that the electric field parallel to the magnetic field lines vanishes locally only if the ions and electrons have the same pitch angle. This can be demonstrated by an example. Consider a magnetic bottle in which is contained a collisionless plasma. Let all of the protons in the bottle have 0 degrees pitch angle and all of the electrons a pitch angle less than 90 degrees in the equatorial plane. The 0 degree particles cannot be reflected by the magnetic mirror at all, so they must be contained by an electric potential well in order to ensure quasineutrality. Thus, an electric field parallel to the magnetic field must arise which will make the mirror point of the electrons the same as that of the protons.

Alfvén's study was for a very simple plasma distribution. However, Persson (1963) showed that, in general, the parallel electric field vanishes in a steady state only if the velocity-integrated pitch angle distributions of the electrons and positive ions are identical. If they are not, then there is an electric

field determined from the velocity distributions and the principle

of quasineutrality. In a low density plasma these principles re-

place Poisson's equation (Block, 1966).

In the outer magnetosphere these parallel electric fields

must be taken into account when considering the motion of the low

energy charged particles. In determining the parallel field the

important quantity is plasma density. Hence the low energy particles

are likely to be more important than the high energy particles be-

cause the former are more sensitive to the field and also contribute

more to the particle density. In fact, any charge density due to

high energy particles can probably be nullified by low energy par-

ticles with only a slight change in the parallel electric field

(Dungey, 1966).

1.6 Specific Statement of the Problem

The distribution of low energy particles in the outer magneto-

sphere and their motion are to be considered in this thesis. In

particular, the plasma motion along a field line, as it follows the

circulation described in Section 1.3, will be considered for a time

period after the field line has just passed through the day (or

night) neutral point where two dissimilar plasmas meet. Using

approximate plasma models, the results of this study will describe

a few aspects of the outer magnetosphere which might be expected

of the open model of the magnetic field configuration.

In principle, there exists an exact model of plasma flow

along a field line which is valid for the entire circulation cycle.

A truly rigorous model would have a characteristic period equal to the period of the circulation (approximately one day). However, due to the many different plasma processes which may occur, the complexity of the mathematical analysis required, and the lack of direct measurements of this medium, it is not feasible at the present time to devise an accurate model with this cyclic character. We must then be content with some approximate models described below.

CHAPTER II

MOTION OF PLASMA ALONG OPEN FIELD LINES

2.1 General Description of the Model

At reconnection on the day side of the earth, magnetospheric

plasma of ionospheric origin meets a higher temperature plasma of

magnetosheath origin. These dissimilar plasmas will interdiffuse

along the open field line formed at reconnection, as the plasma

and the magnetic field lines follow the convection pattern described

in the introduction. This situation is depicted qualitatively in

Figure 7 which shows a flux tube and its enclosed proton plasma at

various stages in the circulation cycle. The protons of ionospheric

origin are characterized by the temperature T_e and those of magneto-

sheath origin by T_s (the subscripts e and s are indicative of the

earth and sun respectively). The shaded region in the figure

corresponds to the interdiffusion region, which expands along the

field lines as the night side is approached.

An electron of energy 0.3 ev (this energy is typical of the

thermal plasma under consideration) travels 10 earth radii (Re) in

one minute - a time much shorter than the characteristic time of

the field line circulation (approximately one day). Hence, the

electrons will interdiffuse very rapidly and can be considered by

neglecting the variation of the parallel electric field with time.

The protons, on the other hand, due to their lower velocities must

be considered in the light of the past history of the electric

field. The parallel E field is assumed to be that static field
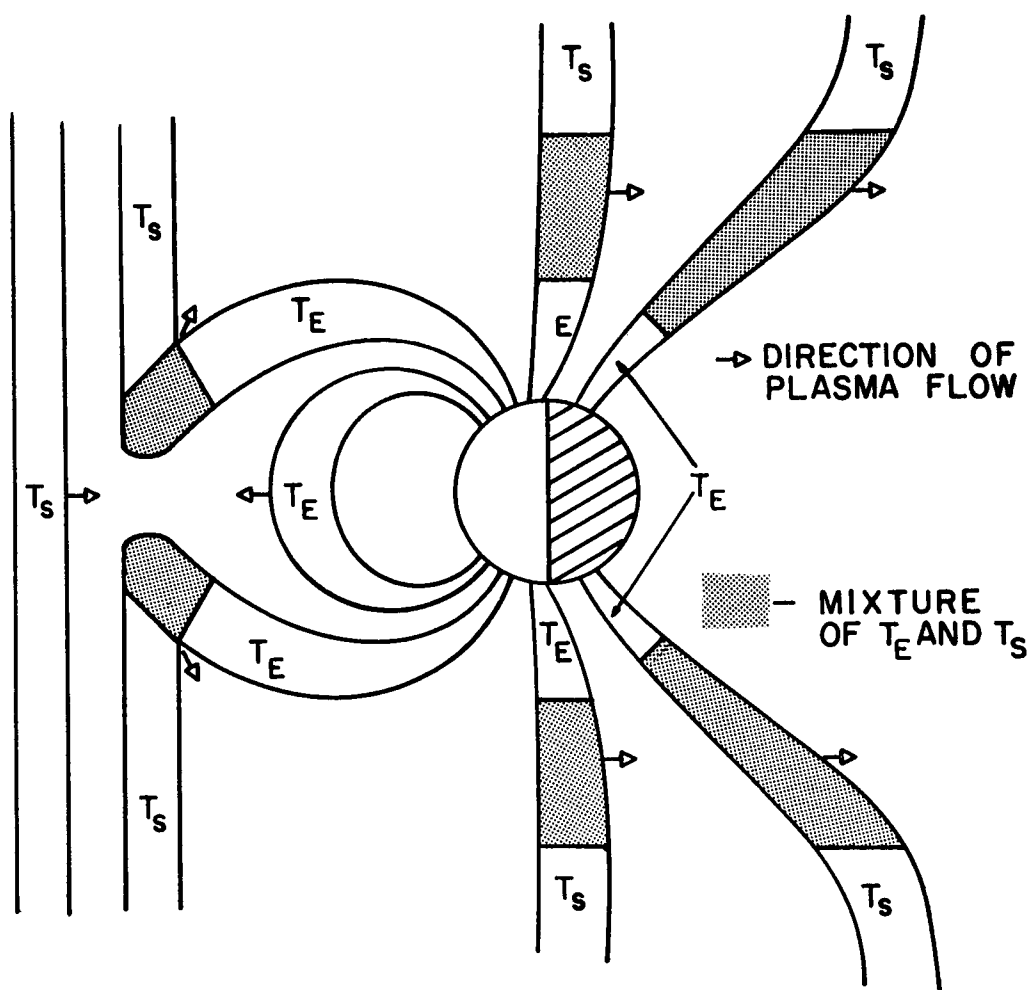
FIGURE 7. CIRCULATING FLUX TUBES AND ION
TEMPERATURES

which makes the electrons have the same density as the protons at every point along the circulating field line considered.

2.2 Basic Assumptions of the Gross Motion

The guiding center of a nonrelativistic charged particle of mass m and charge e, moving under the influence of external electric and magnetic fields of magnitude E and B respectively, obeys the following equations of motion (Alfvén and Fälthammer, 1963):

$$u_{\perp} = - \frac{\underset{\sim}{B}}{eB^2} \times (e\underset{\sim}{E} - \mu \ \text{grad} \ B - m \frac{d\underset{\sim}{u}}{dt})$$

and   (2-1)

$$\frac{d}{dt} (m\underset{\sim}{u})_{11} = (e\underset{\sim}{E} - \mu \ \text{grad} \ B)_{11} \ .$$

In equations 2-1 the subscripts 11 and $\perp$ denote the components of a vector parallel and perpendicular to the magnetic field. The velocity $u_{\perp}$ (the perpendicular component of the guiding center velocity) is to be distinguished from the spiralling velocity $v_{\perp}$. Also, the magnetic moment $\mu = \frac{1}{2}mv_{\perp}^2/B$ is an invariant of the motion for the plasmas and field configurations under consideration. It is to be noted that the MKS system of units is used throughout this thesis.

When the centrifugal force due to motion along a curved field line is explicitly determined and substituted for the inertial term (the last term in the first of equations 2-1), and when curl B vanishes, the equation of motion for the perpendicular component of the guiding center velocity becomes (see Alfvén and Fälthammer, 1963):

$$\underset{\sim}{u}_L = - \frac{\underset{\sim}{B}}{eB^2} \times \left[e\underset{\sim}{E} - \mu \left(1 + 2 \frac{u_{11}^2}{v_L^2}\right) \text{grad } B \right] \cdot \qquad (2\text{-}2)$$

From equation 2-2 the ratio of the magnetic drift velocity to the electric field drift velocity is of the order of magnitude V/EL where V is the volt equivalent of the particle's energy and L a characteristic length. For the low energy, low density particles in the outer magnetosphere, this quantity is much less than one. Therefore, the magnetic drift term can be ignored and the equations of motion can be written as

$$\underset{L}{u} = - \frac{\underset{\sim}{B}}{B^2} \times \underset{\sim}{E} \qquad \text{or} \qquad \underset{\sim}{E}_L + \underset{\sim}{u} \times \underset{\sim}{B} = 0 \qquad (2\text{-}3)$$

and

$$\frac{d}{dt} (m\underset{\sim}{u}_{11}) = (e\underset{\sim}{E} - \mu \text{ grad } B)_{11} \cdot \qquad (2\text{-}4)$$

Having determined the equations of motion applicable to low energy magnetospheric ions, it is now possible to determine the conditions under which these particles can be considered as "frozen to" the magnetic lines of force. Using equation 2-3 the rate of change of magnetic flux F through a contour moving with the guiding centers of the plasma can be shown to be (Fälthammer, 1964)

$$\frac{dF}{dt} = - \int \int \text{curl } \underset{\sim}{E}_{11} \cdot \underset{\sim}{dS} \qquad (2\text{-}5)$$

where S is the area of the contour. Thus if curl $\underset{\sim}{E}_{11}$ vanishes, the particles behave as though attached to the magnetic lines of force. This condition is valid for the models to be considered since the

parallel E field will be assumed to be a conservative field. Detail-
ed measurements of the magnetospheric E and B fields are required in
order to determine how valid this assumption is.

Assuming that the low energy plasma is frozen to the magnetic
field, the evolution of plasma motion along a line of force can be
considered as it follows the circulation pattern described previous-
ly (Dungey, 1966). The parallel component of the ion velocity will
develop according to equation 2-4 and the perpendicular component
is determined from equation 2-3.

2.3 Magnetic Field Model

As an open field line is swept towards the night side of the
earth by the solar wind, its spatial configuration changes, as is
apparent in Figure 4. Since the plasma motion along an open field
line is to be considered for only a short time period after re-
connection on the day side, this field variation can be ignored.
That is, the variation of B along the open field lines is assumed
to be a spatial and temporal invariant.

In the magnetosheath, Fairfield (1967) has indicated that the
magnetic field may be more ordered than the interplanetary field.
The magnetosheath field is of the order of 10 to 20 gammas. On the
earth side of the magnetopause, the field is essentially dipolar.
Hence, the magnetic field along a field line extending from the
earth to the day side reconnection point should be dipolar and should
approach an essentially constant value in the magnetosheath. Later
a dipole field will be used for calculations, but at present, it is
more convenient if the magnetic field is chosen to be of the form

$$B = a \, e^{-\beta(S-1)} + b$$

where a, b and β are constants and S is the distance along the field

line from the earth in earth radii (Re). The constants are deter-

mined from the following conditions:

    1. at S = 1 Re, B = 6×10^4 gammas

    2. at S = 2 Re, B = 10^3 gammas

    3. as S → ∞, B → 10 gammas.

The value of B chosen at 1Re is approximately the auroral zone value,

that at 2Re is an approximate dipole value at high latitudes. It

must be emphasized that although the form chosen for the field is

not very accurate it is simple enough in form for convenient numerical

calculations and it becomes essentially constant at great distances

corresponding to the magnetosheath. Evaluating the constants, the

magnetic field formula is:

$$B = 6 \times 10^4 \, e^{-4.1 \, (S-1)} + 10 \text{ (gammas)}. \qquad (2.6)$$

2.4 Ionospheric Electrons

    By ionospheric electrons is meant those electrons which have

traveled upwards along the open flux tube under consideration from

the base level of the tube in the ionosphere where they were produced

by photoionization processes. Below the base level (i.e. in the

upper ionosphere) the distribution of electrons is controlled by

collisions and will be described by the Maxwell-Boltzmann distribu-

tion function. Ignoring collisions above the base level (i.e. in

the magnetosphere) and considering only those electrons whose

trajectories pass through the base level (i.e. those in the loss cone), Liouville's theorem is appropriate and the ionospheric electrons are all characterized by the same distribution function. (Particles trapped between two magnetic mirrors or a magnetic and electric mirror are not considered--for such particles, collisions are probably important (Dungey, 1966) and the Fokker-Planck equation must be used. In the next chapter trapped electrons will be considered in a simple situation.)

Let the electron's electric potential energy in the conservative parallel field E_{11} be denoted by ϕ, where ϕ is a function of position on the field line. The Maxwellian distribution function for the electrons in this conservative force field is (Chapman and Cowling, 1964):

$$f = n_o \left(\frac{m}{2 \pi k T} \right)^{3/2} e^{-mv^2/2kT} e^{-\phi/kT} \qquad (2\text{-}7)$$

where ϕ is the potential energy with respect to the potential energy at the ionospheric base level and n_o is the base level electron density.

Since only those electrons which are within the loss cone of the base are being considered, at any given point along the field line the electron's parallel and perpendicular velocities must satisfy the inequality:

$$v_{11}^2 - \left(\frac{B_o}{B} - 1 \right) v_{\perp}^2 + \frac{2\phi}{m} \geq 0 \qquad (2\text{-}8)$$

where B_o is the base level magnetic field and B is the field at the point under consideration. This relation is derived by assuming an

invariant magnetic moment, conservation of energy, and $v_{11}^2 \geq 0$. It defines mathematically the loss cone hyperboloid (Persson, 1965) at every point on the field line. The loss cones for positive and negative potential energies are shown in Figure 8.

In order to determine the electron density at a point, given the potential, the distribution function is integrated over the allowed velocity range. For a positive potential energy (i.e. an electron in a region of negative potential) let $\alpha = \dfrac{B_o}{B} - 1$, $\gamma = \dfrac{m}{2kT}$, and $\Phi = \dfrac{2|\phi|}{m}$. Then the density of the electrons in the loss cone is given by:

$$n = n_o \left(\frac{\gamma}{\pi}\right)^{3/2} 2\pi \int_{-\infty}^{\infty} \int_o^{\left(\frac{v_{11}^2 + \Phi}{\alpha}\right)^{\frac{1}{2}}} e^{-\gamma(v_{11}^2 + v_L^2 + \Phi)} v_L \, dv_L \, dv_{11}$$

where the upper limit for v_L is obtained from equation 2-8 and the factor of 2π arises from integration over the axial angle. The integral is easily evaluated to yield:

$$n = n_o \left[1 - \sqrt{1 - \frac{B}{B_o}} \; e^{-\frac{B}{B_o - B} \gamma \Phi} \right] e^{-\gamma \Phi} . \qquad (2\text{-}9)$$

It must be emphasized that this equation is valid for a positive potential energy only. Also, at the base, the potential, as defined, vanishes and the density is just n_o.

Next, the case of a negative electrostatic potential energy must be considered. The distribution function is now given by

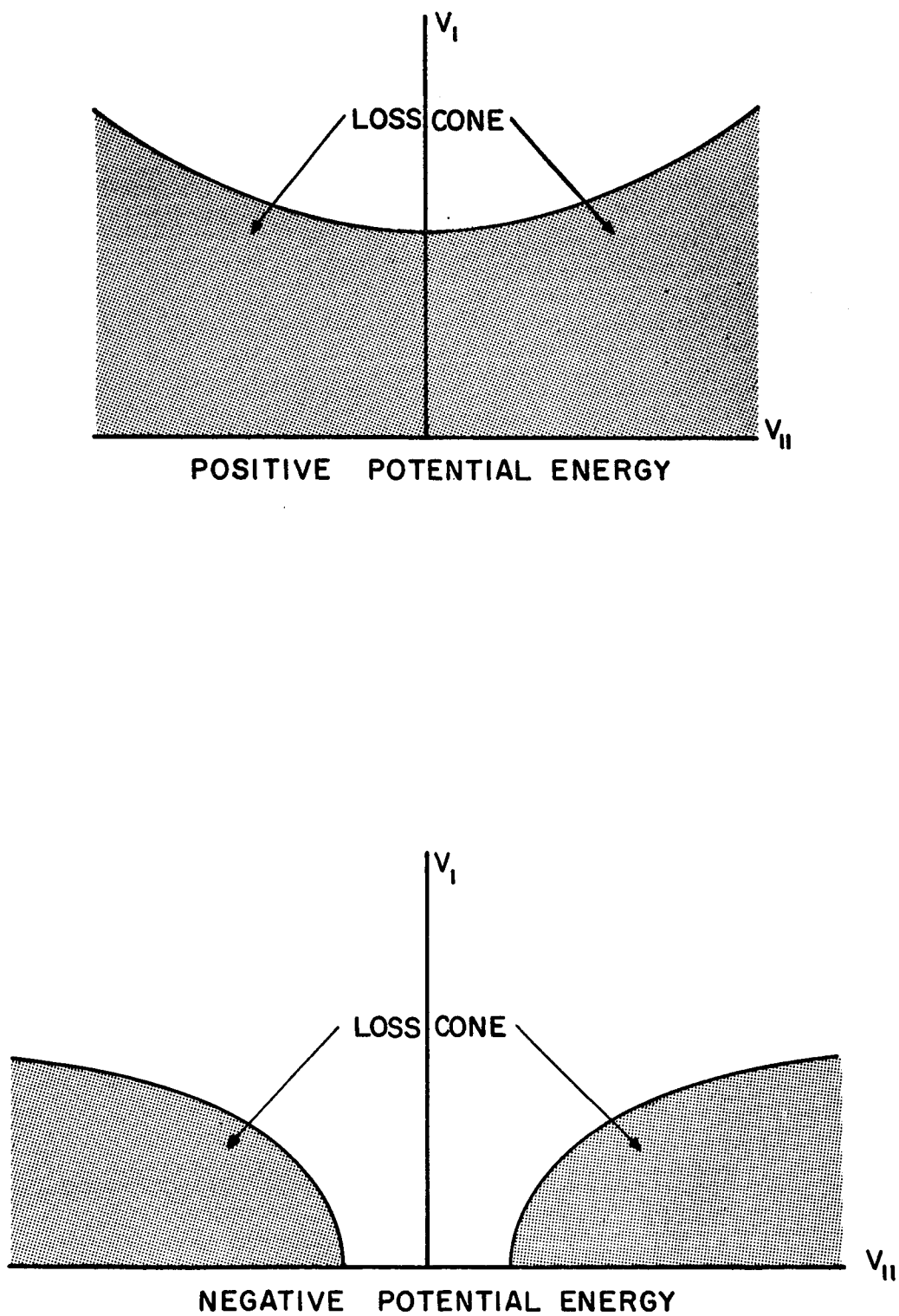$$f = n_o \left(\frac{m}{2\pi kT}\right)^{3/2} e^{-mv^2/2kT} e^{|\phi|/kT}$$

FIGURE 8. LOSS CONE HYPERBOLOIDS FOR ELECTRONS

where Boltzmann's factor is now an increasing exponential function

of the electrostatic potential energy. The loss cone boundary for

v_L is again given by equation 2-8 but the parallel velocity is not un-

restricted (see the lower half of Figure 8). In order to have a

positive kinetic energy, conservation of energy requires that v_{11}^2

be greater than or equal to Φ. The density integral is now:

$$n = n_0 \left(\frac{\gamma}{\pi}\right)^{3/2} 2\pi \left[\int_{\sqrt{\Phi}}^{\infty} \int_0^{(\frac{v_{11}^2 - \Phi}{\alpha})^{\frac{1}{2}}} + \int_{-\infty}^{-\sqrt{\Phi}} \int_0^{(\frac{v_{11}^2 - \Phi}{\alpha})^{\frac{1}{2}}} \right]$$

$$e^{-\gamma(v_{11}^2 + v_L^2 - \Phi)} v_L \, dv_L \, dv_{11} \cdot$$

Performing the integration and rearranging terms, the electron density

in a region of positive potential is

$$n = n_0 \left[1 - \text{erf}(\sqrt{\gamma \Phi}) - \sqrt{1 - \frac{B}{B_0}} \, e^{-\frac{B}{B_0 - B} \gamma \Phi} \left\{ 1 - \text{erf}\left(\sqrt{\frac{\gamma \Phi B_0}{B_0 - B}}\right) \right\} \right] e^{\gamma \Phi} \cdot$$

$$(2\text{-}10)$$

Equation 2-10 is valid for a negative potential energy only.

The electron density as a function of electrostatic potential

energy is plotted in Figure 9. The potential is a multiple-valued

function of the electron density for small values of $\frac{B_0}{B}$ (i.e. near

the base level) and small potentials. The depth of the valleys will

be reduced when electrons of interplanetary origin are included.

The choice of the proper potential corresponding to a density

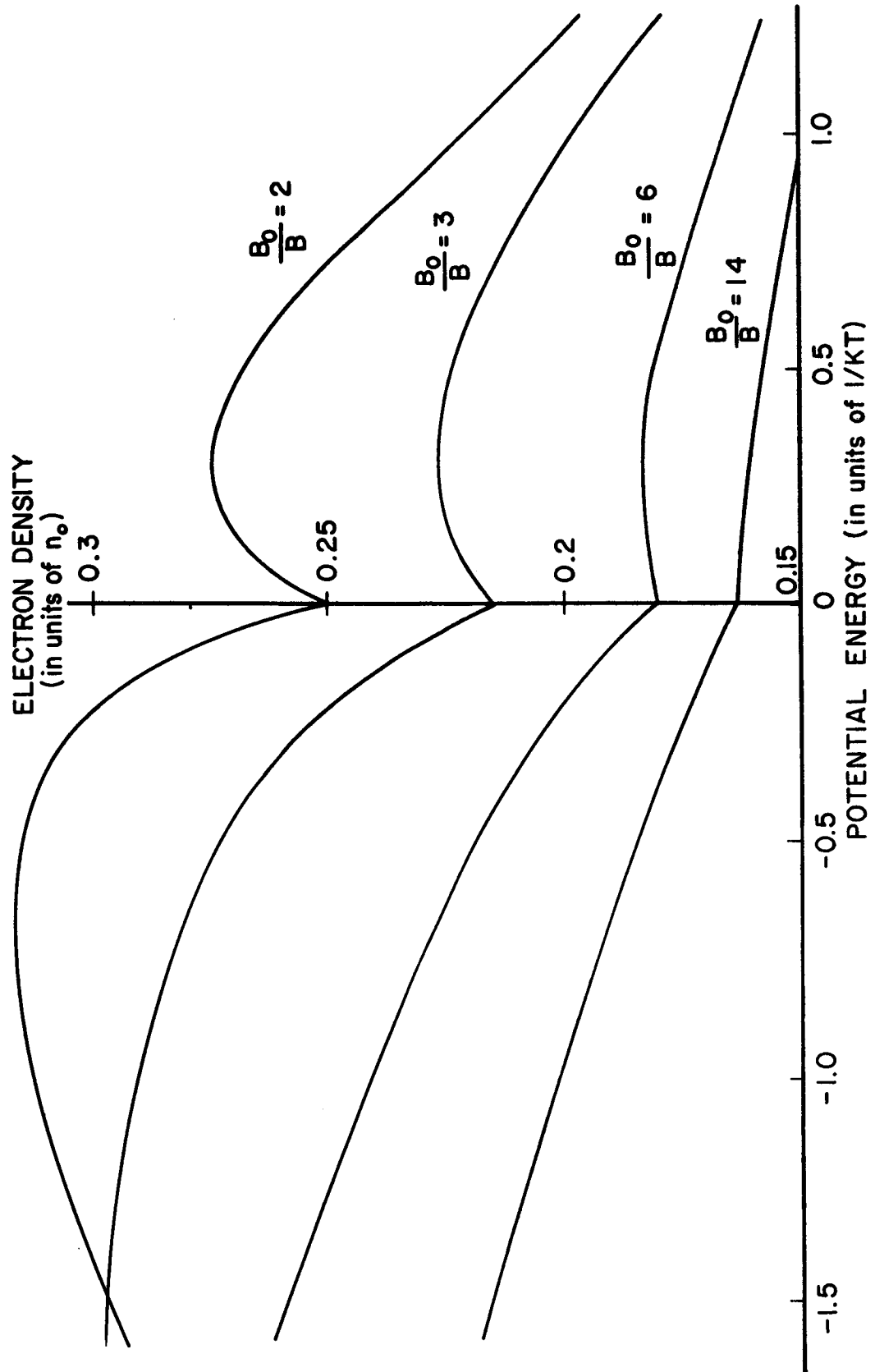specified in the multiple-valued region must be made in the light of

FIGURE 9. IONOSPHERIC ELECTRONS

the fact that no discontinuities of density or potential are allowed along the field line.

2.5 Interplanetary Electrons

Along an open field line there are contributions from two sources -- the ionosphere and interplanetary space. The electrons of interplanetary origin will now be considered.

Again, it is assumed that the interplanetary electrons, due to their large thermal velocity, are in equilibrium along the field line and are immersed in a quasistatic electric field. The base level of the interplanetary electrons is to be taken at a point in the magnetosheath near the magnetospheric bow shock, in order to avoid the necessity of applying the complicated shock relations to this problem. This assumption restricts the application of the present analysis to that section of the open field line which lies on the earth side of the shock. The density at this interplanetary base level is taken to be Cn_o where n_o is the ionospheric base level density considered previously and C is a multiplicative constant. The temperature of those electrons whose trajectories pass through the interplanetary base level is τT where T is the temperature of the ionospheric electrons and τ is a constant.

Under the above assumptions and noting that the magneto-sheath electrons are well thermalized due to their passage through the shock, the distribution function of the electrons of inter-planetary origin is Maxwellian with the form:

$$f = Cn_o \left(\frac{m}{\tau 2\pi kT}\right)^{3/2} e^{-\frac{mv^2}{2k\tau T} - \frac{\phi}{kT\tau}}$$

where ϕ is again the potential energy with respect to the ionospheric base level. It is implicitly assumed that the ionospheric and interplanetary base levels have the same potential -- this assumption will be removed in the next chapter.

Using Liouville's theorem, those electrons which traveled from, or can travel to, the magnetosheath base level can be described as Maxwellian with the above distribution. Reflected particles (more accurately, electrons reflected by the magnetic mirror) were ignored in the calculations of the ionospheric electron component because they did not come from the ionospheric base level and hence, did not satisfy Liouville's theorem. However, electrons from the interplanetary base level can be reflected by the converging field lines and still be considered Maxwellian with the interplanetary temperature. Thus, these particles must be taken into account. It must be emphasized that due to the assumed lack of collisions, particles in the loss cone cannot become trapped nor vice versa.

Consider those interplanetary electrons which travel along the field line toward the earth. Integrating the above distribution function over half of velocity space, the total electron density ignoring those reflected particles which are traveling away from the earth is $\frac{1}{2} Cn_o e^{-\phi/\tau kT}$. To this must be added the density of particles which are reflected closer to the earth -- this is just the density of particles outside of the loss cone. That is,

$n = \frac{1}{2} Cn_o e^{-\phi/\tau kT} + n$ (outside the loss cone). But n (outside) = $\frac{1}{2} Cn_o e^{-\phi/\tau kT} - n$ (inside the loss cone). Therefore, it follows that the density of interplanetary electrons at any point along the open field line is given by:

$$n = Cn_o e^{-\phi/\tau kT} - n \quad \text{(inside loss cone)} \qquad (2\text{-}11)$$

where n (inside) is calculated in a manner identical to that used in the previous section. It should be noted that only positive loss cone velocities (i.e. particles approaching the earth) are considered here, whereas, both positive and negative values were considered in the previous section. To find the total electron density at any point only ionospheric electrons which travel away from the earth are considered. The previous loss cone densities calculated are valid if a factor ½ is applied.

Evaluating equation 2-11 for both positive and negative potentials and adding the results to equations 2-9 and 2-10 (including the factor ½) yields the total electron density along the field line. For a positive potential the density is given by

$$n = Cn_o \exp(\gamma\phi/\tau) + P(1) + CP(\tau) \qquad (2\text{-}12)$$

where

$$P(\tau) = \frac{n_o}{2}\left[1 - \text{erf}\left(\sqrt{\gamma\phi/\tau}\right) - \sqrt{1 - \frac{B}{B_o}}\, e^{-\frac{B\,\gamma\,\phi}{(B_o - B)\tau}}\left\{1 - \text{erf}\left(\sqrt{\frac{\gamma\,\phi\,B_o}{(B_o - B)\tau}}\right)\right\}\right]e^{\frac{\gamma\phi}{\tau}}.$$

For a negative potential the density is given by

$$n = Cn_o \exp(-\gamma\phi/\tau) + N(1) - CN(\tau) \qquad (2\text{-}13)$$

where

$$N(\tau) = \frac{n_o}{2}\left[1 - \sqrt{1 - \frac{B}{B_o}}\, e^{-\frac{B\,\gamma\,\phi}{(B_o - B)\tau}}\right]e^{-\gamma\phi/\tau}$$

In the above equations $\Phi = \frac{2|\phi|}{m}$ and $\gamma = \frac{m}{2kT}$. Thus, $\gamma\Phi = \frac{|eV|}{kT}$ where

V is the electrostatic potential. The quantity $\frac{eV}{kT}$ is plotted against

the electron density in Figure 10 for the assumed values $\tau = 9$ and

$C = 0.3$. These values of τ and C imply that the electron density in

the magnetosheath adjacent to the shock is approximately one-third

that of the density at the base of the field line in the polar region.

These values were chosen with a certain proton model in mind--see

the next section. Varying the values of these two parameters changes

the scales of the density-potential profiles but does not change the

general shape as shown in Figure 10. Given the proton density at

any point, the principle of quasineutrality in conjunction with the

figure, yields the electrostatic potential. These computations are

valid for any type of magnetic field configuration which has a field

magnitude that is a monatonically decreasing function of the distance

along a field line from the magnetic mirror.

2.6 Proton Distributions

Given the proton density at any point along the field line,

equations 2-12 and 2-13 can be inverted numerically to yield the

electric field potential. This technique will now be used to explore

a simple model of the charged particle motion and the parallel

electric field development along an open field line which has just

reconnected on the day side of the earth.

Since the characteristic time of the low energy proton motion

in the magnetosphere is comparable to the period of circulation of

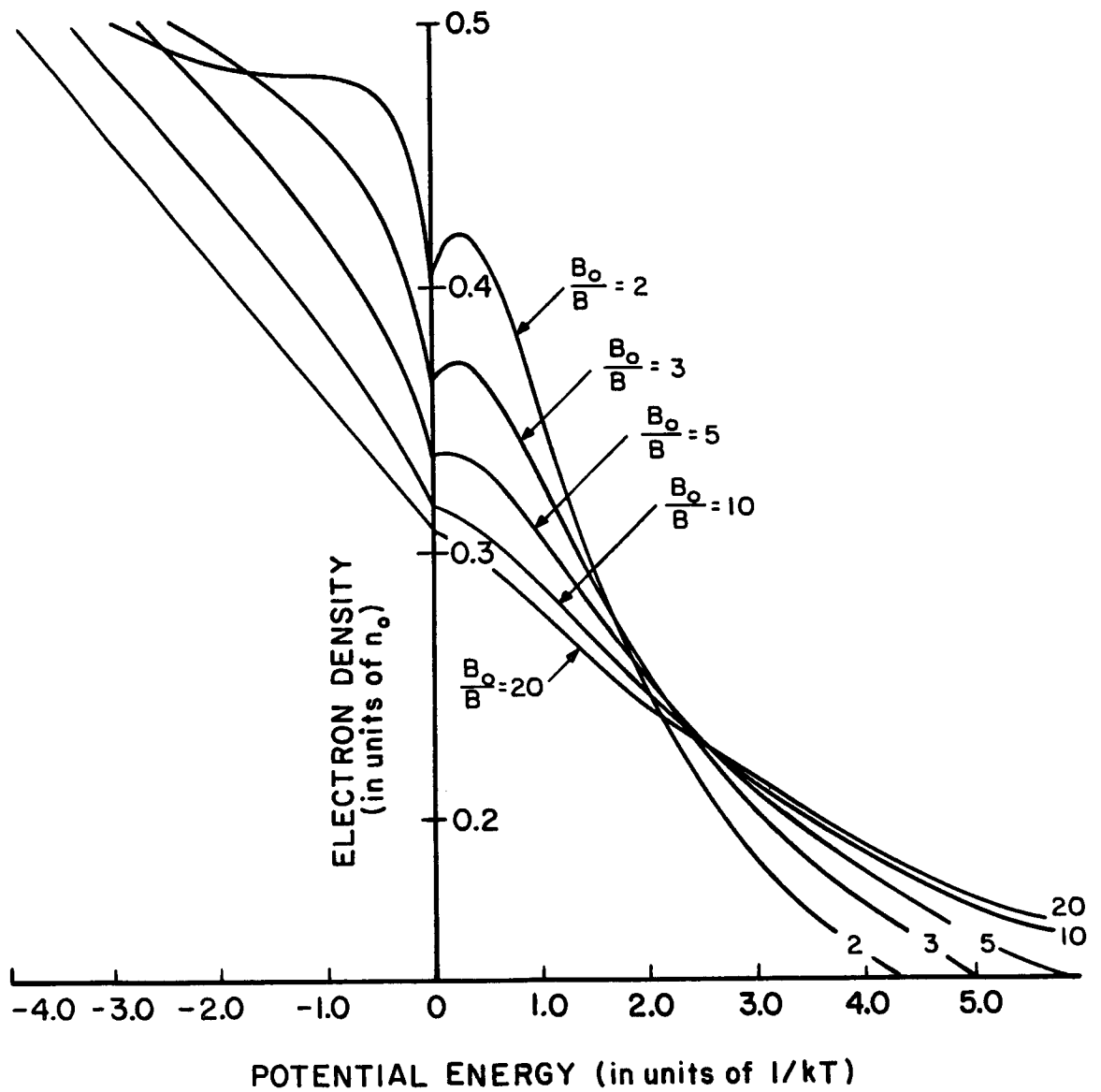the field lines (Dungey, 1966), the past history of the parallel

FIGURE 10. TOTAL ELECTRON DENSITY

electric field cannot be ignored for the protons as was done for the electrons. The development of the proton distribution function with time must now be considered. For computational ease it will be assumed that the distribution functions describing protons of ionospheric and magnetospheric origin are steplike. That is, the distribution function is assumed to have a nonzero constant value in a finite region near the origin in velocity space and vanishes outside of this region. This corresponds to replacing the characteristic bell shaped curve of the Maxwellian distribution by a rectangular shaped profile.

The prime requirement that a distribution function must satisfy is that integration of the function over all of velocity space must yield the density,

i.e.
$$n = \int_{-\infty}^{\infty} \int_{-\infty}^{\infty} \int_{-\infty}^{\infty} f \, dv_x \, dv_y \, dv_z$$

or
$$n = 2\pi \int_{0}^{\infty} \int_{-\infty}^{\infty} f v_{\perp} \, dv_{11} \, dv_{\perp} \, .$$

It shall be assumed that the maximum value of the corresponding Maxwellian distribution is the nonzero value of the step function. The step function is then

$$f = \frac{1}{2\pi} \, n \, \left(\frac{M}{2\pi kT} \right)^{3/2} \quad \text{for } |v_{\perp}| \lesssim v_1 \text{ and } |v_{11}| \lesssim v_1$$

and $f = 0$ outside this region, where the boundary velocity v_1 is determined by integrating over all velocity space. Then

$$n = n \; (\frac{M}{2\pi kT})^{3/2} \int_0^{v_1} \int_{-v_1}^{v_1} v_{\perp} \; dv_{11} \; dv_{\perp}$$

or

$$n = n \; (\frac{M}{2\pi kT})^{3/2} v_1^3$$

Thus, a good value for the boundary velocity is $v_1 = (\frac{2\pi kT}{M})^{\frac{1}{2}}$ where M is the proton mass.

If the velocity boundaries defining the distribution are constant, the distribution function for protons of ionospheric origin is given by

$$f = \frac{1}{2\pi} \; n_1 \; (\frac{M}{2\pi kT})^{3/2} \quad \text{for} \quad |v_{11}|, \; |v_{\perp}| \; \stackrel{<}{=} \; v_1^{IO} \qquad (2\text{-}14)$$

where

$$v_1^{IO} = (\frac{2\pi kT}{M})^{1/2} \text{ and } f = 0 \text{ elsewhere;}$$

and that for interplanetary protons is

$$f = \frac{1}{2} \; Dn_1 \; (\frac{M}{2\pi kT})^{3/2} \quad \text{for} \quad |v_{11}|, \; |v_{\perp}| \; \stackrel{<}{=} \; v_1^{IN} \qquad (2\text{-}14)$$

where

$$v_1^{IN} = (\frac{2\pi kT}{M})^{1/2} \quad \text{and } f = 0 \text{ elsewhere.}$$

T is the ionospheric proton density (assumed identical to that of the electrons), τ T is the temperature of the interplanetary protons, n_1 is the ionospheric proton base level density and Dn_1 is the density of the interplanetary base, where τ and D are multiplicative constants.

The ionospheric base level proton density n_1 is not the same as the ionospheric base level electron density n_o considered earlier. This is due to the fact that protons are not the only positive ions which exist near the earth or near the shock, whereas the present analysis assumes protons are the only positive ions present. Such an assumption is only valid in regions away from both base levels. Thus the base level density n_1 is less than n_o.

It has been assumed above that the velocity perpendicular to the magnetic field has the same boundary as the parallel velocity. It shall be assumed that this boundary remains invariant with the values given in equations 2-14. However, due to the electric field parallel to the magnetic field, the parallel velocity boundary changes with time. If v_U and v_L denote the upper and lower parallel velocity boundaries respectively, then the proton density is given by the sum of the ionospheric density

$$n = n_1 \left(\frac{M}{2\pi kT}\right)^{3/2} \frac{(v_1^{IO})^2}{2} (v_U^{IO} - v_L^{IO}) \qquad (2\text{-}15)$$

and the interplanetary density

$$n = Dn_1 \left(\frac{M}{2\pi kT\tau}\right)^{3/2} \frac{(v_1^{IN})^2}{2} (v_U^{IN} - v_L^{IN}) \qquad (2\text{-}15)$$

where the superscript IO indicates ionospheric values and IN interplanetary values.

Since collisions are being ignored, the temperatures of the interplanetary particles and ionospheric particles remain distinct for all time. However, as the protons move along the field line,

the perpendicular velocity boundary of the distribution function should change with time due to the conservation of the magnetic moment. If a small enough time interval is considered during which a particle travels a distance over which the field changes only slightly, the perpendicular velocity boundary may be considered a constant at a fixed point.

2.7 Time Development

At the point of day side reconnection (see Figures 4 and 7) the proton velocity boundaries are as shown in Figure 11, corresponding to the values of equations 2-14 where $D = 0.3$ and $\tau = 9$. The ionospheric protons are bounded by $\pm v_1^{IO}$, and the interplanetary protons with a temperature $9T$ are bounded by $\pm v_1^{IN} = 3v_1^{IO}$. The boundaries of the distribution function correspond to the limiting values of the proton motion. Therefore, to calculate the boundary changes with time, equation 2-4 is applied to the individual protons making up the boundary. Along a circulating field line this equation is

$$\frac{dv_{11}}{dt} = - \frac{e}{M} \frac{\partial V}{\partial S} - \frac{\mu}{M} \frac{\partial B}{\partial S} . \qquad (2\text{-}16)$$

In this equation V is the electrostatic potential and μ the magnetic moment which is equal to $\frac{1}{2} \frac{Mv_\perp^2}{B}$. Since the boundary of the perpendicular velocity is a constant and μ is an invariant, the following calculations are valid for only small time increments and/or slowly varying magnetic fields. The magnetic moment, although
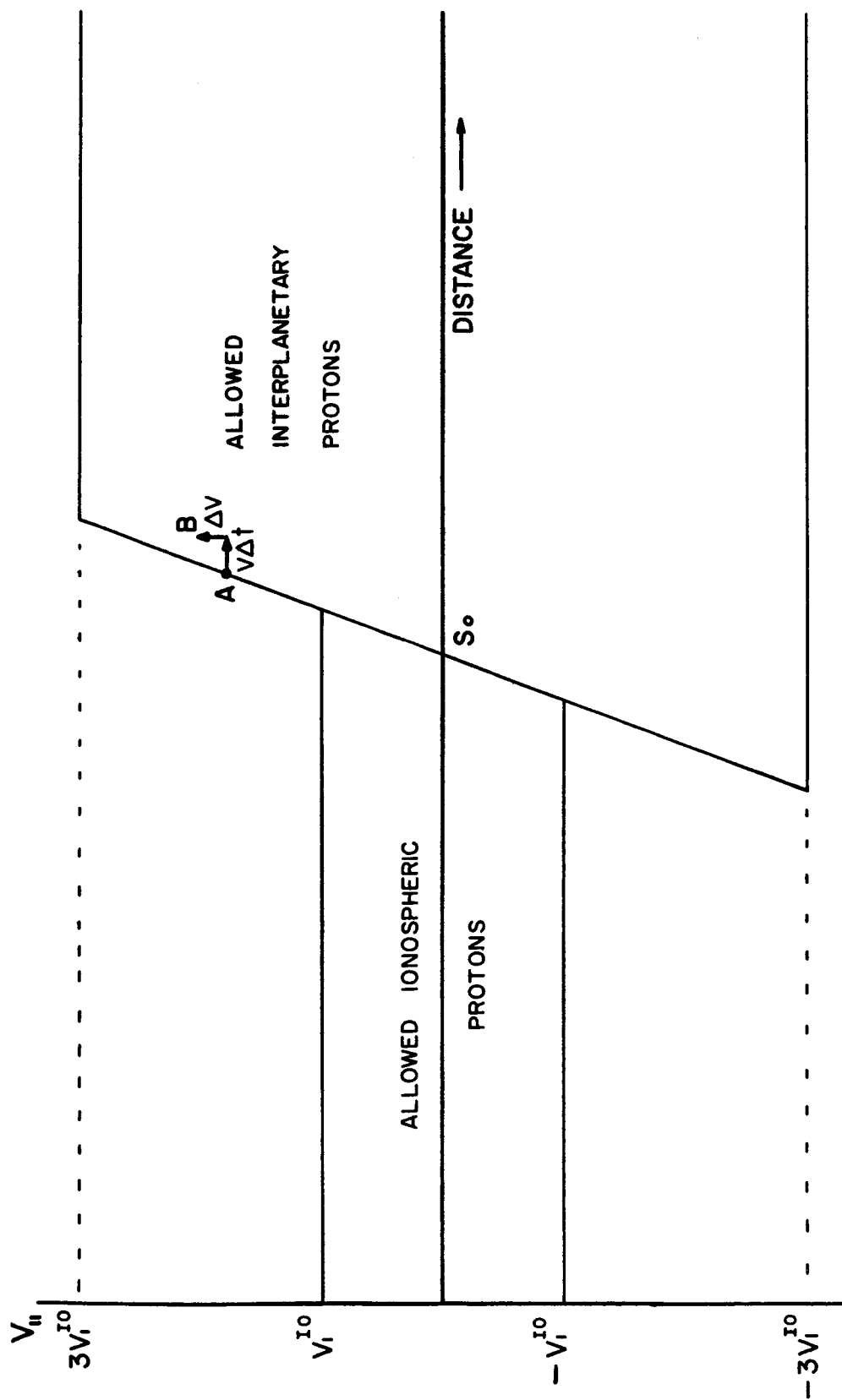
FIGURE II. PROTON VELOCITIES AT t=0

invariant for each individual proton, must vary with distance along the field line.

Consider point A with parallel velocity v in Figure 11. In a time Δt this point (or proton) moves a distance $v\Delta t$ away from the earth where a positive velocity corresponds to motion in this direction. In this time to a first approximation, the velocity changes, according to equation 2-16, to

$$v + \Delta v = v + (- \frac{e}{M} \frac{\partial V}{\partial S} - \frac{\mu}{M} \frac{\partial B}{\partial S}) \Delta t - v \frac{\partial v_{11}}{\partial S} \Delta t \quad (2-17)$$

where $\frac{\partial V}{\partial S}$, μ, and $\frac{\partial B}{\partial S}$ are evaluated at $S = \frac{S_i + S_f}{2}$ (see Figure 11).

It is assumed that during the process of reconnection, the interplanetary and ionospheric protons interdiffuse slightly near the magnetopause, which initially has its centroid at the point S_o as seen in Figure 11. This region of interdiffusion will widen with time along the field line as it is swept towards the night side (see Figure 7). The assumed interdiffusion initially yields a non-vanishing finite slope of the v_{11}- distance plot near S_o. The slope of the distribution boundary in this region is taken as two (the units are those used in Figure 11). Future experimental data will decide whether or not there is some interdiffusion during the re-connection process, and if so, how much.

The gradient of the magnetic field required in the equation of motion is easily obtained by differentiating the exponential function of equation 2-6 which was used as the model for the magnetic field variation along the field line.

Next, a scheme is needed to evaluate the electric field. Initially, the proton distribution of Figure 11 is assumed. At any point along the field line the proton density is determined using equations 2-15. From the principle of quasineutrality, the electron density is then known, and equations 2-12 and 2-13 are used to determine the electric potential corresponding to the parallel E field along the magnetic field line. These latter equations cannot be solved explicitly for the electric potential as a function of density. They must be solved numerically. The Newton iteration scheme (Booth, 1955) was used to calculate the potential corresponding to a given electron density. The potential gradient in the equation of motion is then determined by the method of finite differences. The derivative $\frac{\partial V}{\partial S}$ is replaced by $\frac{V(S_f) - V(S_i)}{S_f - S_i}$ where $S_f = S+0.001$, $S_i = S-0.001$ and all quantities in this expression are in earth radii.

The magnetic moment of a boundary proton at a given point on the field line is that of a proton with the perpendicular velocity v_1^{IO} or v_1^{IN} depending upon whether an ionospheric or interplanetary proton is considered. Since the magnetic moment is also a function of B, it will vary spatially along the field line but not temporally.

Since all quantities on the right-hand side of equation 2-17 are known initially, the evolution of the velocity boundaries in a finite time increment may be approximated by the technique developed at the beginning of this section. The new boundary velocities are then known and the process can be repeated for further time intervals.

In order to perform the actual numerical computations, two numerical parameters must be fixed: T the ionospheric base level temperature and the base level of the field line. Since distances of the order of 10 Re are being considered, the base level can be assumed to be at the earth, i.e. B_o = B(S=1Re). The temperature, on the other hand, at high latitudes in the upper ionosphere usually ranges between 1000 and 3000 degrees Kelvin (Geisler and Bowhill, 1965) and is essentially the same for both the protons and electrons. The lower temperature will be used in these calculations and the ionospheric particles are taken to be isothermal along the field line. Choosing a higher temperature would only change the magnitude of the results but would not change the general form.

2.8 Computations

The 7074 IBM computer of the Pennsylvania State University Computation Center was used. Due to the complicated nature of the resulting proton velocity distributions, it was found that the calculations could not be performed in an automatically computed self consistent iteration scheme. After each iteration the data had to be scanned by hand in order that the interval between sample points could be varied depending upon the complexity of the region being considered. Also, care had to be taken that no multiple upper and lower velocity boundaries were ignored.

For a temperature of 1000 degrees, the ionospheric proton velocity boundary (v_1^{IO}) is approximately 7 km/sec. A proton with this velocity travels a distance of 0.1 Re in 88 seconds. This time

interval is selected for the computations because it is large enough to keep computing time at a minimum and is small compared to the circulation period of the flux line ($\sim$ 1 day). The largest distance interval used is 0.1 Re. This interval was selected only for regions in which the density and hence, the electric potential were constant over a considerable range.

The effects of the relationship between the base level electron (n_o) and ion (n_1) densities must now be considered. Previously, it was shown that the proposed model of densities in the outer magnetosphere requires that n_1 be less than n_o. Due to the deficiency of proton density at the ionospheric base level, n_1 must be chosen such that the potential at or near the base becomes negative, because adding the deficient density will cause an increase in potential, whereas, the potential at the base must vanish. The base potential vanishes because it is the reference potential for the entire field line. Figure 12 depicts the initial potential profile for two values of n_1. It is seen that raising the base level ion density does not greatly disturb the general functional form of the potential or the corresponding parallel electric field. Increasing the density only shifts the potential curve upward and does not affect the relative values. In the following calculations, the value $n_1 = 0.5n_o$ is selected. Experimental measurements are needed in order to determine whether or not this is a truly realistic value.

A few important characteristics of the initial electric potential profile along a reconnected field line, as shown in
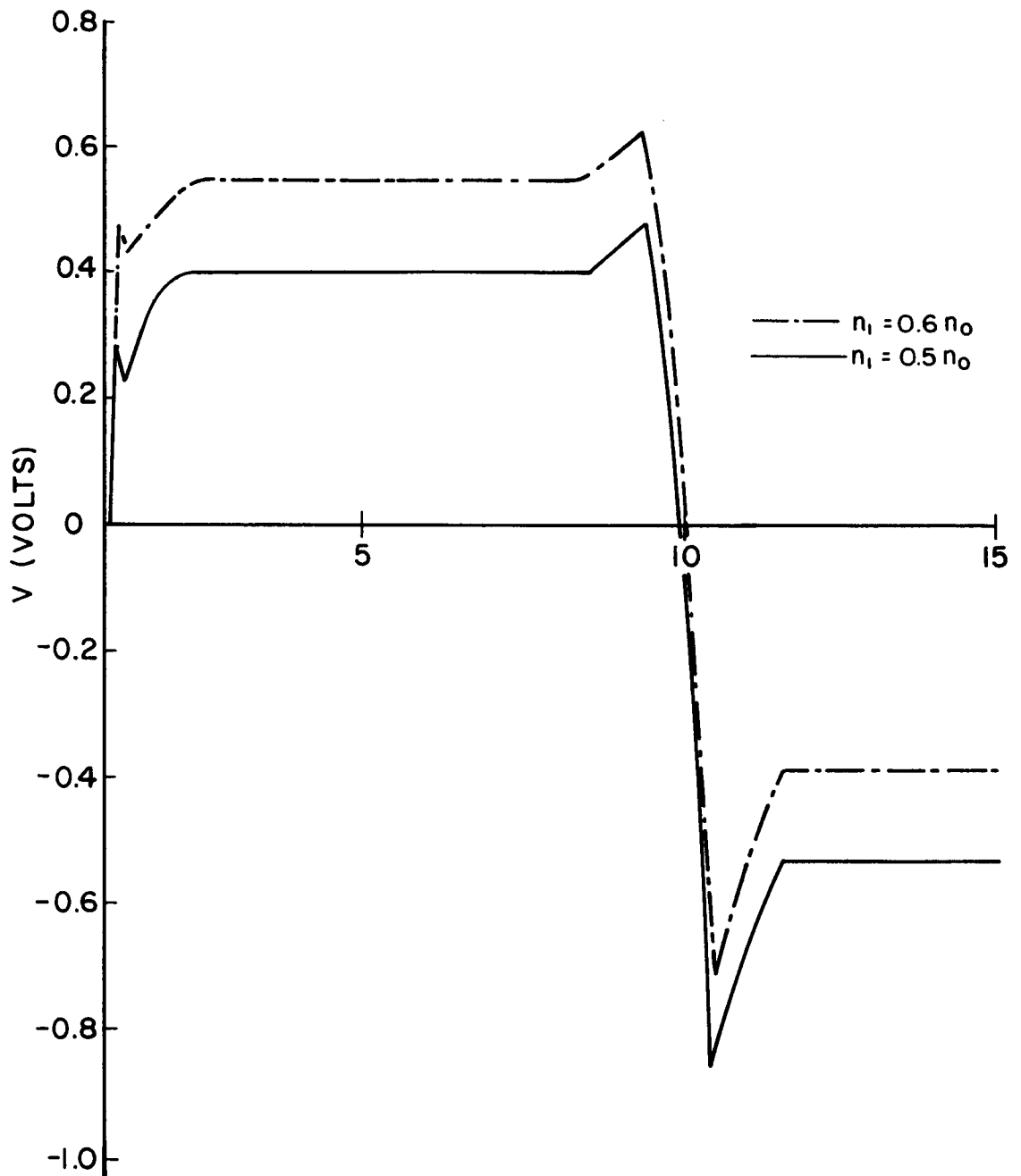
FIGURE 12. INITIAL POTENTIAL CONFIGURATIONS

Figure 12, should be noted. First, near the ionospheric base level, there is a large oscillation in the electric potential. This is due to the rapid decrease of the magnetic field in this region and to the oscillatory nature of the electron density-potential profile in this region (see Figure 10). The present analysis really breaks down in this region due to the fact that the entire proton population is not considered and because the perpendicular velocity boundary will in actuality change with time in this region. Therefore, this model shall only be considered at great distances from the earth.

It can also be seen that the potential decays from a positive value on the earth side of the interdiffusion region to a negative value in the magnetosheath. This suggests that some electrons will be trapped between an electric potential barrier and the low altitude magnetic mirror. In the present calculations these trapped particles are not taken into account. The potentials considered are of the order of a volt.

The ion velocity configuration after a period of 88 seconds is plotted in Figure 13. The velocity boundaries are normalized with respect to v_1^{10}. It can be seen that the protons are accelerated towards the magnetosheath by the parallel electric field in the interdiffusion region. Outside of the interdiffusion region, there is very little variation in the proton boundary other than a simple translational motion. Since the density is directly proportional to the sum of the widths of the velocity profiles, it follows that the density develops spatial and temporal variations
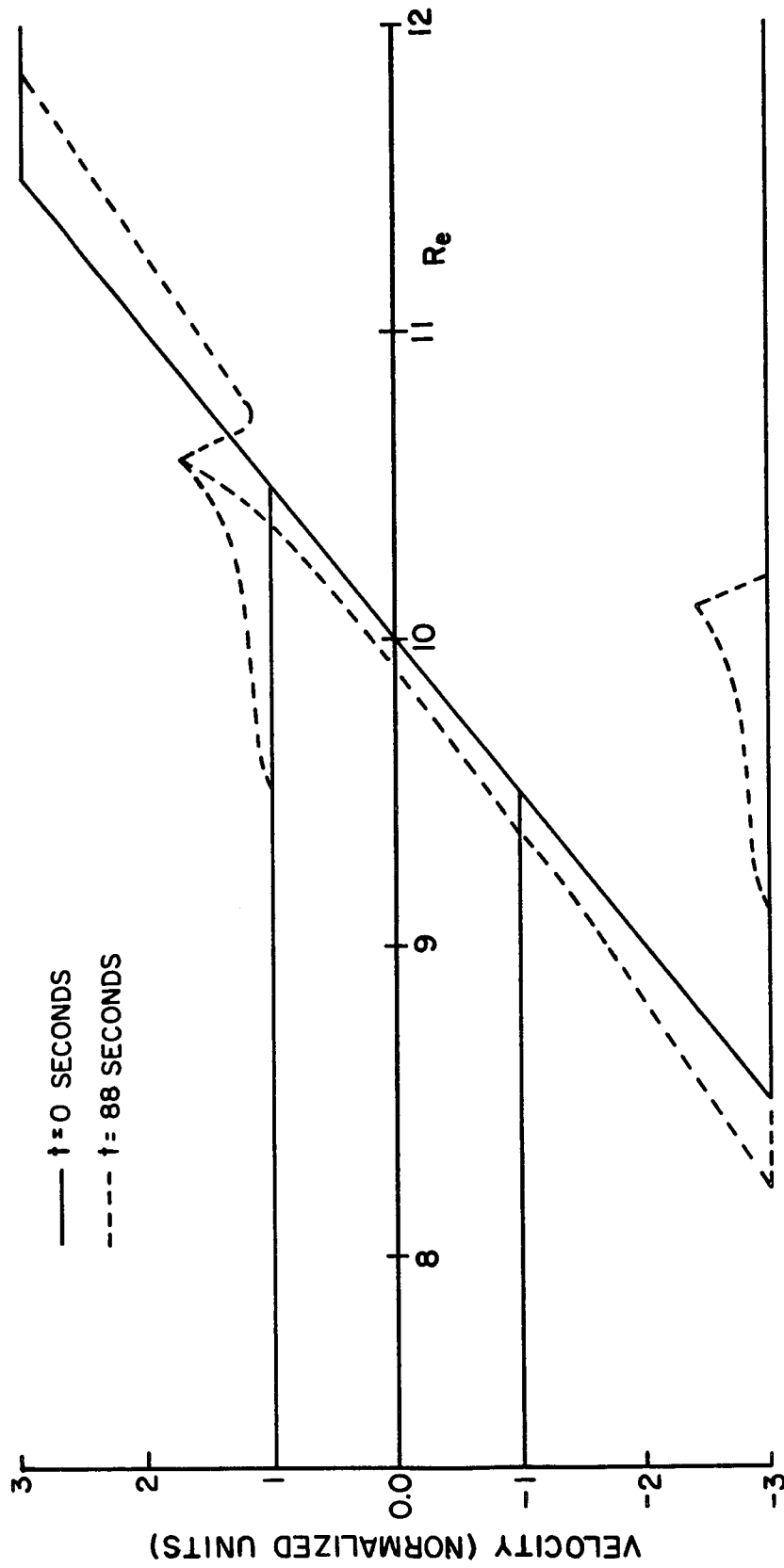
FIGURE 13. ION VELOCITIES—1st ITERATION

in the interdiffusion region as it decreases from the undisturbed magnetospheric value to the assumed constant magnetosheath value.

The potential profile (Figure 14) after the first iteration retains the same form as the initial configuration except that the region of decreasing potential is much wider. As the time increases the potential begins to oscillate and the electric field propagates away from the initial point of reconnection on the field line.

The velocity profiles for further iterations appear in Figures 15 and 16. It is apparent that the number of oscillations increase with time and that the amplitudes can become quite large. It can be seen that the leading edge of the ionospheric particles propagating into the magnetosheath steepens and the electric field associated with this steepening increases with time. Eventually, a discontinuity in density and electric field occurs. Since quasi-neutrality occurs only over distances greater than the Debye length, these discontinuities cannot be analyzed within the framework of the present model. In fact, it may be possible that the inclusion of trapped particles and a more realistic distribution function may not yield such regions.

Due to roundoff errors and the approximate calculations of the field gradients, computations of this type will yield violent oscillations after just a few iterations. A more valid approach would be to perform a series of iterations many times independently and average the results. Such a procedure, however, could not be performed within the time limits allowed for computer computation at the Pennsylvania State University.
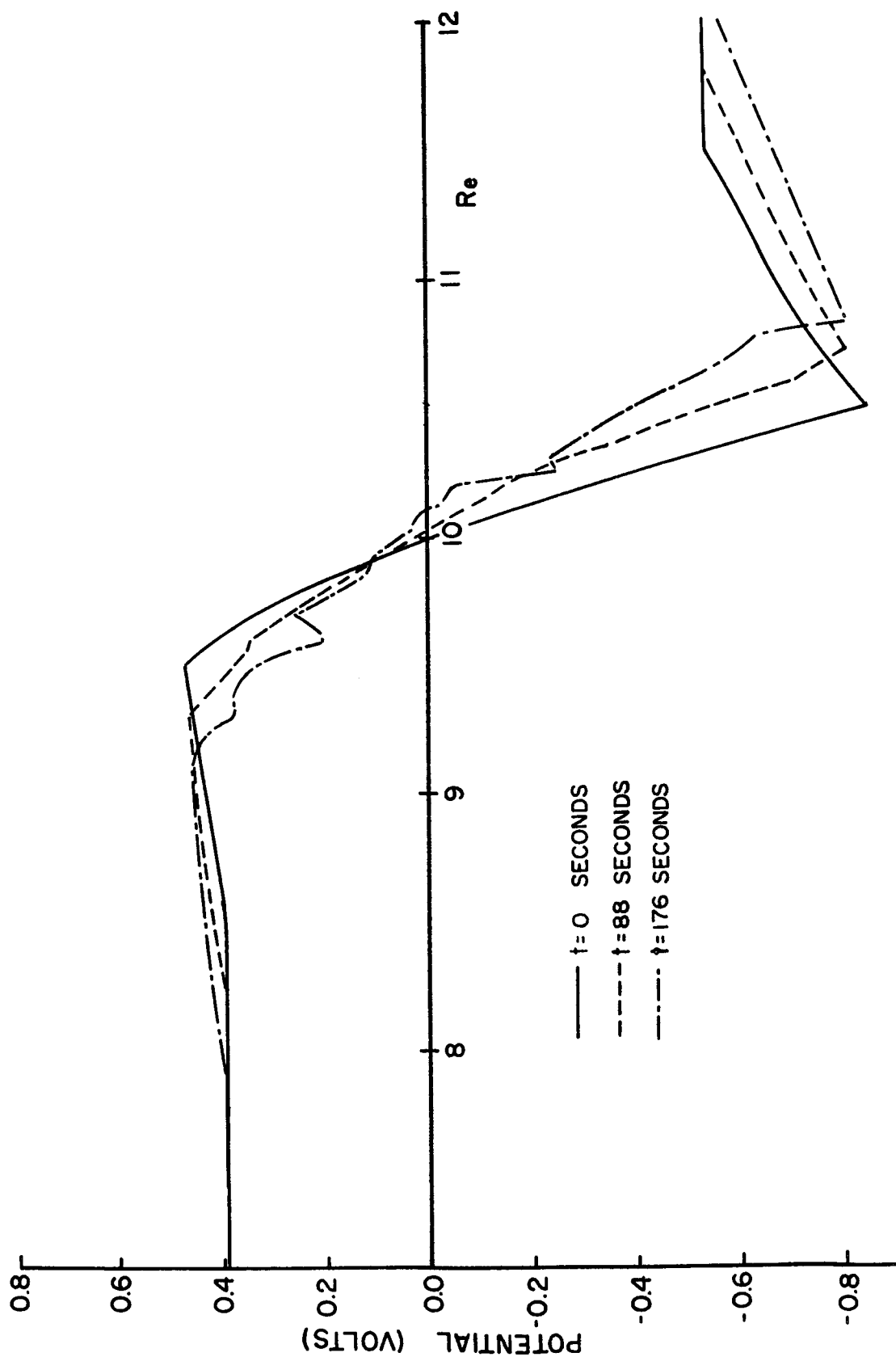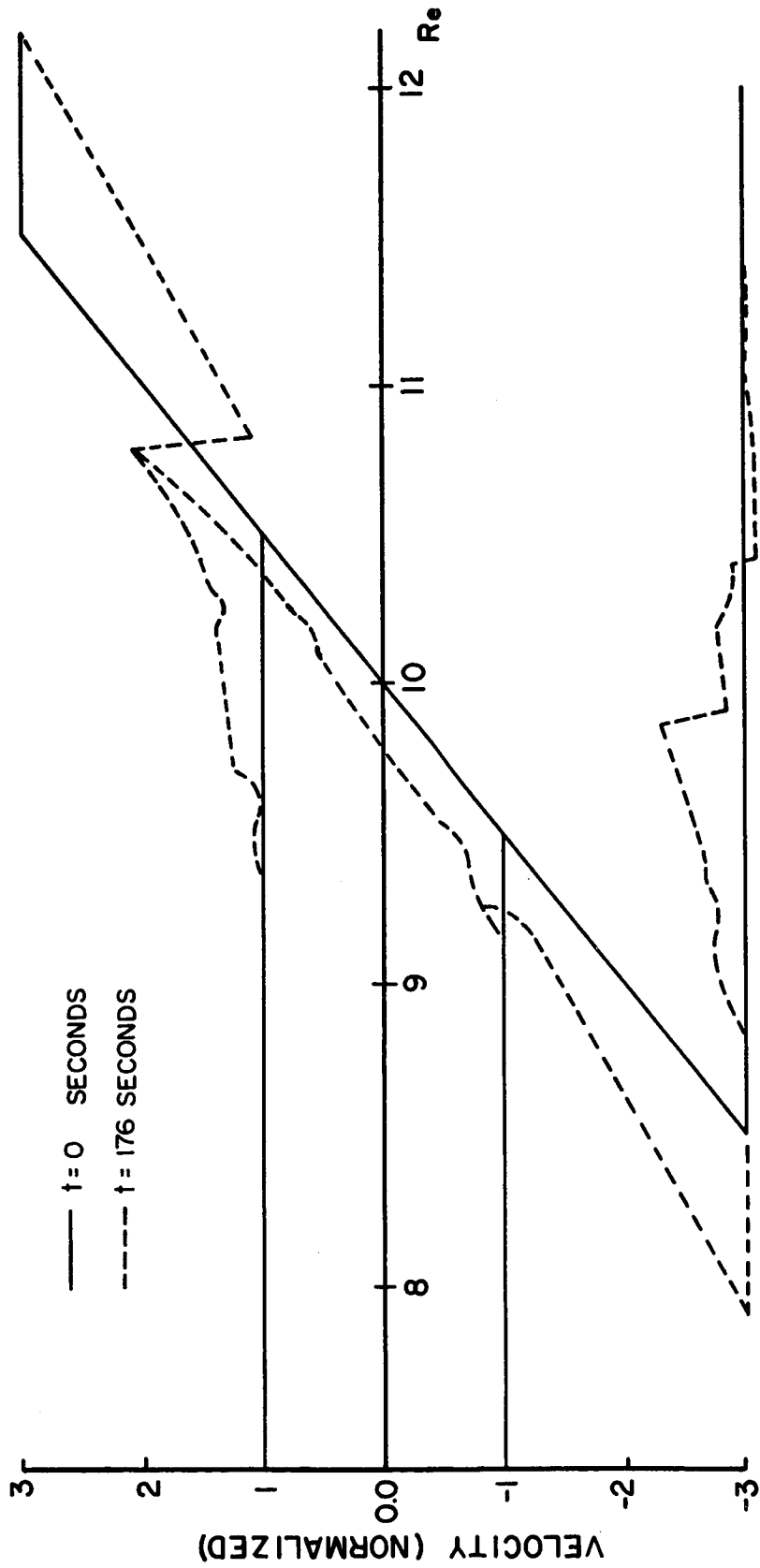
FIGURE 14. POTENTIAL CHANGES
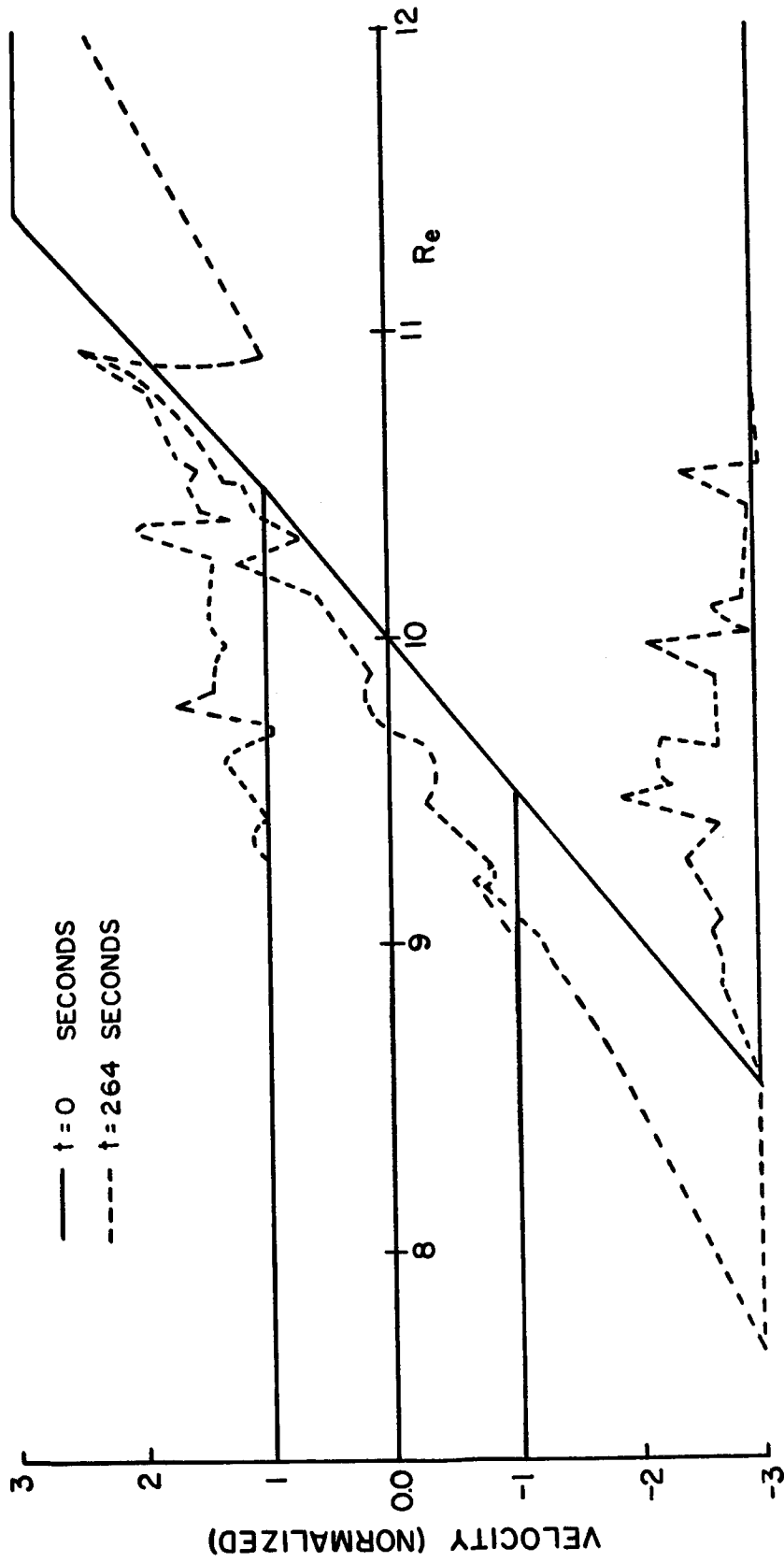
FIGURE 15. VELOCITY PROFILE-2nd ITERATION

FIGURE 16. VELOCITY PROFILE-3rd ITERATION

Similar calculations were performed for the case D = 3, i.e.
when the interplanetary density is three times the magnetospheric
proton density initially. In the light of the exceedingly low
densities measured by whistler studies in the outer magnetosphere,
the magnetospheric density may well be less than the magnetosheath
proton density at reconnection on the day side. The initial poten-
tial configuration for this case appears in Figure 17 and the
velocity profile after one iteration in Figure 18. It is seen that
the potential increases as the field line is traversed in the
direction of interplanetary space. This yields a parallel electric
field which is directed toward the earth. Hence, the protons are
accelerated down the field line, as is seen in Figure 18, in contrast
to the previous situation where the electric field was directed into
the magnetosheath. In general, if D > 1 the protons will be accel-
erated towards the earth; whereas, if D < 1 they will be accelerated
away from the earth. The width of the potential plateau formed in
the case D = 3 (see Figure 17) is dependent upon the initial value
of the boundary velocity gradient.

In the preceding computations, it was assumed that no protons
or electrons are trapped between the magnetic mirror and a potential
barrier or between two potential barriers. The next chapter will
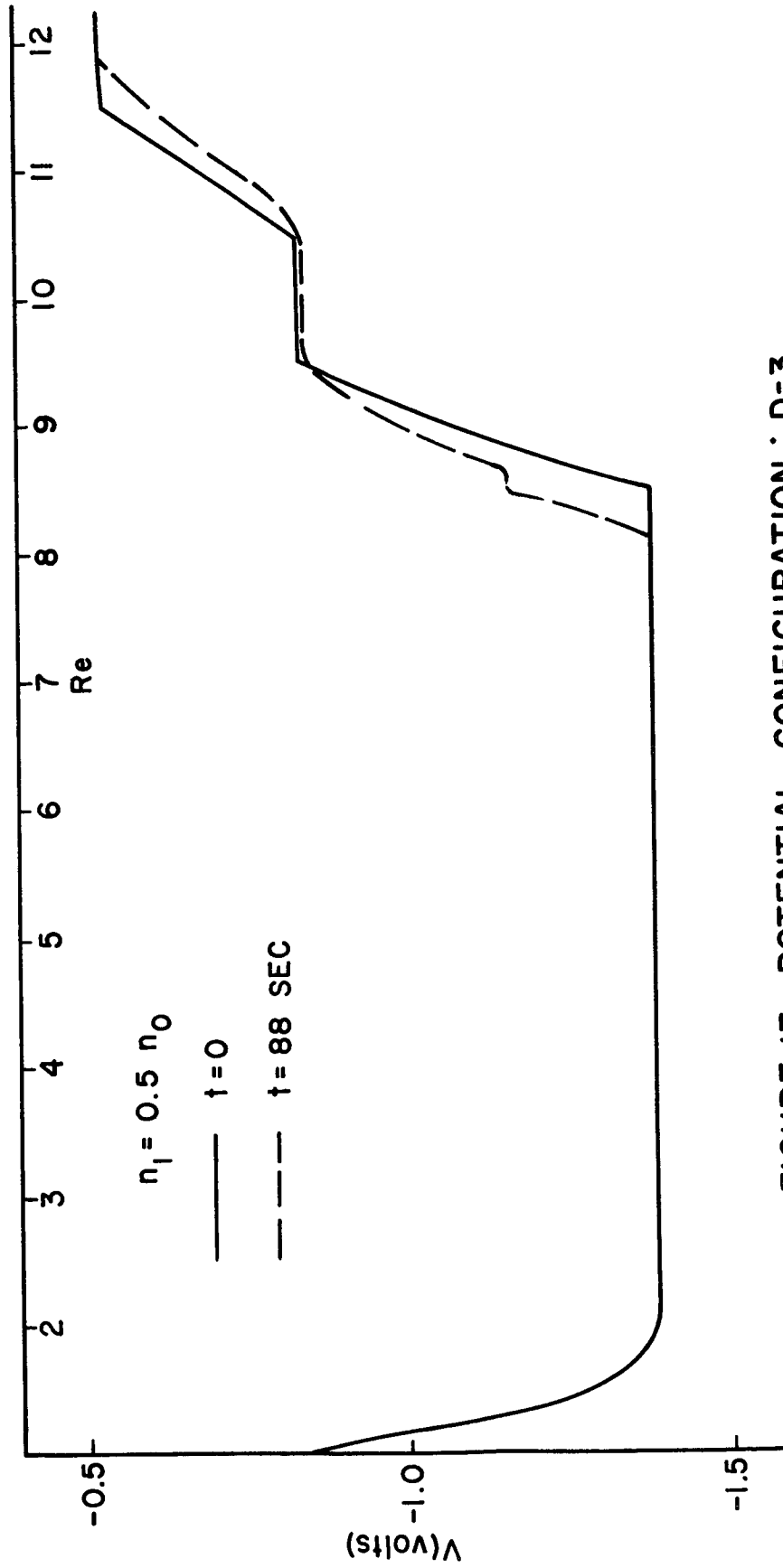show how trapped electrons may be included in the analyses.

FIGURE 17. POTENTIAL CONFIGURATION : D=3
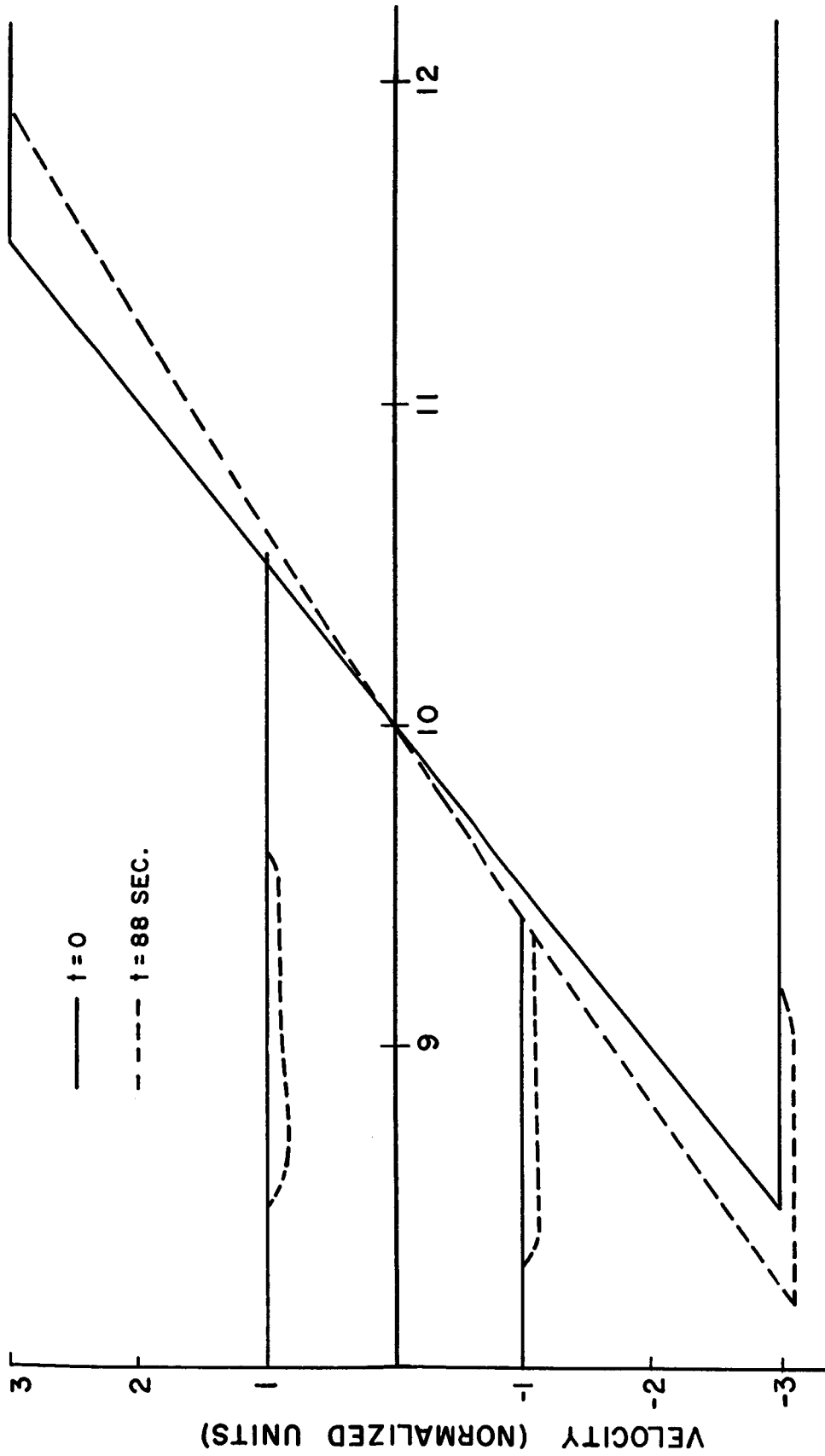
FIGURE 18. VELOCITY PROFILE : D=3

CHAPTER III

ELECTRON DENSITY ALONG AN OPEN FIELD LINE
WITH A POTENTIAL MINIMUM

3.1 Introduction to the Problem

As seen in the previous chapter, when a closed magnetic field line connects to the interplanetary field on the day side to form an open field line, a parallel electric field results in the region of interdiffusion of the ionospheric protons and the hotter magnetosheath protons. If the magnetospheric density is initially less than the magnetosheath density along the field line considered, the electric potential on the magnetosheath side of the interdiffusion region is negative with respect to the potential on the ionospheric side (see Figure 12). The resulting parallel electric field in the inter-diffusion region is, in general, directed outwards from the earth. Hence, some electrons will be trapped between the interdiffusion region and the magnetic mirror formed by the converging field lines near the earth. The present chapter will consider the electron density along an open field line which has one minimum of electro-static potential corresponding to the parallel electric field.

Again, it is to be assumed that collisions are absent, and that the electrons present are Maxwellian with a temperature corre-sponding to the magnetosheath value or the ionospheric value, de-pending upon which base level their trajectories originate in, or depending upon their place of origin. The electrons trapped between the minimum of electric potential and the magnetic mirror will be characterized by the ionospheric temperature because scattering of

electrons into the trap takes place near the ionosphere where most collisions occur, and where electrons of interplanetary origin are very scarce. Hence, the region of velocity space corresponding to trapped electrons is only very weakly coupled to the region of velocity space which contains interplanetary distributions.

Figure 19a depicts typical loss cone configurations at a point on an open field line between a magnetic mirror near the ionosphere and a potential barrier near the magnetopause. The trapped region is that region of velocity space which is outside of both loss cones. This and other configurations will be analyzed in detail in later sections.

The assumption that the trapped particles are of ionospheric origin at time t = 0 is valid at all later times also if the magnitude of the potential minimum does not vary too rapidly with time. However, if the height of the potential barrier increases significantly in a time period which is shorter than the characteristic travel time of an interplanetary electron from the barrier to the ionosphere and back, electrons which had barely sufficient energy to overcome the barrier will become trapped (see Figure 19b). Since the magnetospheric density is small, and because only slow potential variations are allowed in the quasistatic approximation used, this contribution to the trapped particles can be ignored.

The trapped electrons have a bounce time which is short compared to the characteristic time of the reconnection cycle. Hence, the density in the trap can, in principle, be evaluated by using the longitudinal invariant. In this region of velocity space, collisions and

IONOSPHERIC ELECTRONS

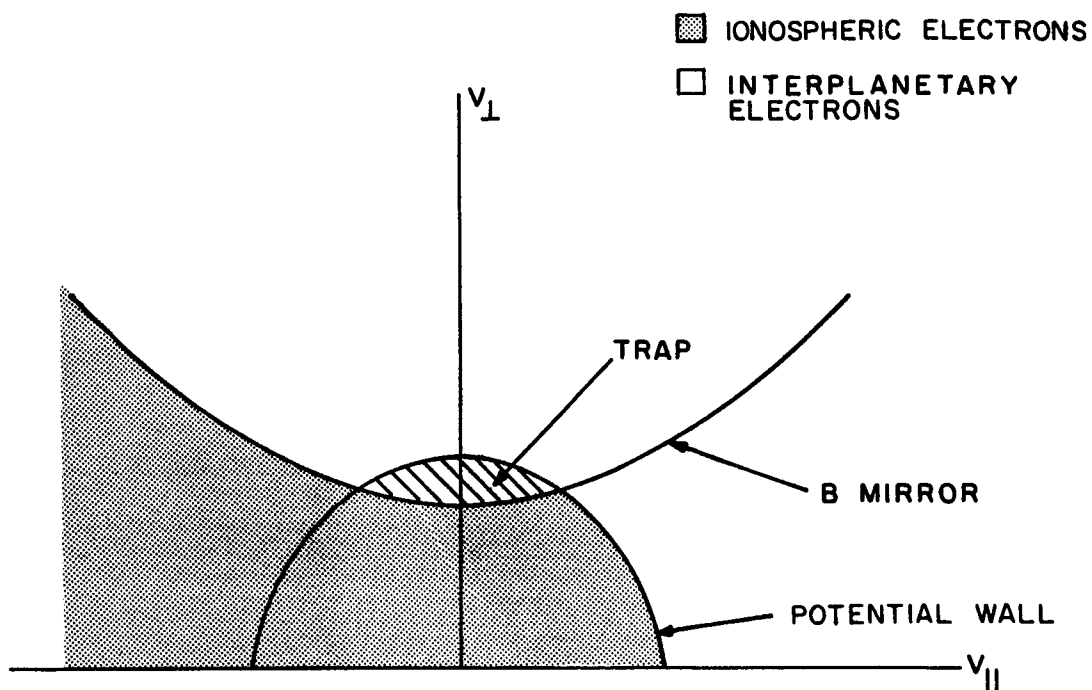INTERPLANETARY ELECTRONS

TRAP

B MIRROR

POTENTIAL WALL

$V_\perp$

$V_\parallel$

FIGURE 19a. TYPICAL LOSS CONE CONFIGURATION

$V_\perp$

— — — HIGHER BARRIER
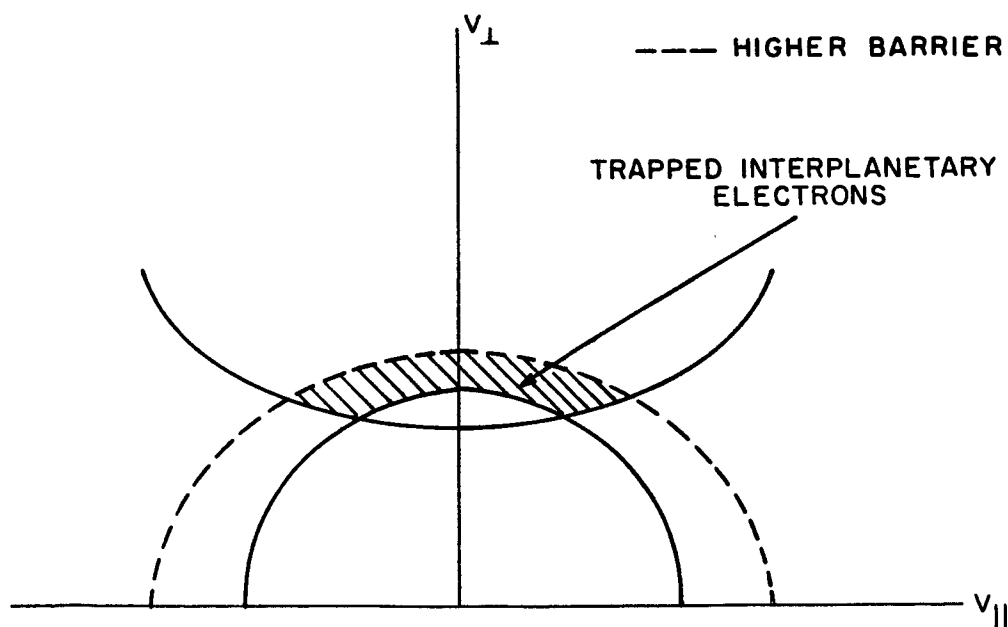
TRAPPED INTERPLANETARY ELECTRONS

$V_\parallel$

FIGURE 19b. TRAPPING DUE TO POTENTIAL CHANGES

the variation of the potential minimum with time are important. Since the interplanetary electrons in the trap can be ignored, the trapped electrons will be in approximate equilibrium with the ionospheric particles and hence, can be characterized by a Maxwellian distribution.

Assuming a conservative parallel electric field, the electron density along a field line is determined by integrating the distribution functions of the electrons over the allowed regions of velocity space as was done in the previous chapter. Previous calculations assumed that the ionospheric and magnetospheric base levels were at the same potential. This stringent condition will be replaced by the more realistic condition that the net electron current along the field direction vanishes.

3.2 Base Level Potentials

In order to specify the relationship between the ionospheric and interplanetary base level potentials, an additional condition must be found. Ideally, the electron current along the field line $\underset{\sim}{j}_e$ should equal the negative of the proton current $\underset{\sim}{j}_p$ (i.e. $\underset{\sim}{j}_e = -\underset{\sim}{j}_p$). However, $\underset{\sim}{j}_p$, as seen in the previous chapter, is small compared to the product of the charge density and the thermal velocity of electrons in the magnetosphere. Hence, a good approximation for the electrons along the field line is $\underset{\sim}{j}_e = 0$. Since the steady state approximation is used for the electrons the divergence of the electron current (div $\underset{\sim}{j}_e$) vanishes. Thus, if the electron current vanishes at one point along the field line, it vanishes everywhere. For convenience this condition of vanishing electron current will be applied at the point

where the electric potential is a minimum. It must now be determined which electrons contribute to the current at the minimum.

Consider the schematic diagram of Figure 20a. This figure depicts the possible trajectories for the electrons along an open field line with a minimum in the electric potential. As can be seen in the figure, there are three general types of trajectories for particles of interplanetary origin: (1) Electrons which pass over the potential barrier and are lost in the ionosphere; (2) Electrons which pass over the barrier but are reflected by the magnetic mirror on the earth side of the minimum; and (3) Electrons which cannot pass over the barrier and hence, must remain on the magnetosheath side of the potential minimum. These trajectories are labeled S_i (i = 1, 2, 3) in Figure 20.

Electrons of ionospheric origin also have three general types of trajectories: (1) Electrons which are reflected by the potential barrier; (2) Electrons trapped between the magnetic mirror and the potential barrier; and (3) Electrons which pass over the barrier and are lost beyond the magnetosheath base level. These trajectories are denoted by E_i (i = 1, 2, 3). (The trajectory labels E and S are suggestive of earth and sun.)

The above classifications were made under the assumptions that there is only one significant potential minimum, and that the magnitude of the magnetic field decreases monotonically along a line of force away from the earth. Thus, there is allowed no potential-potential or magnetic-magnetic trapping. However, if desired, the
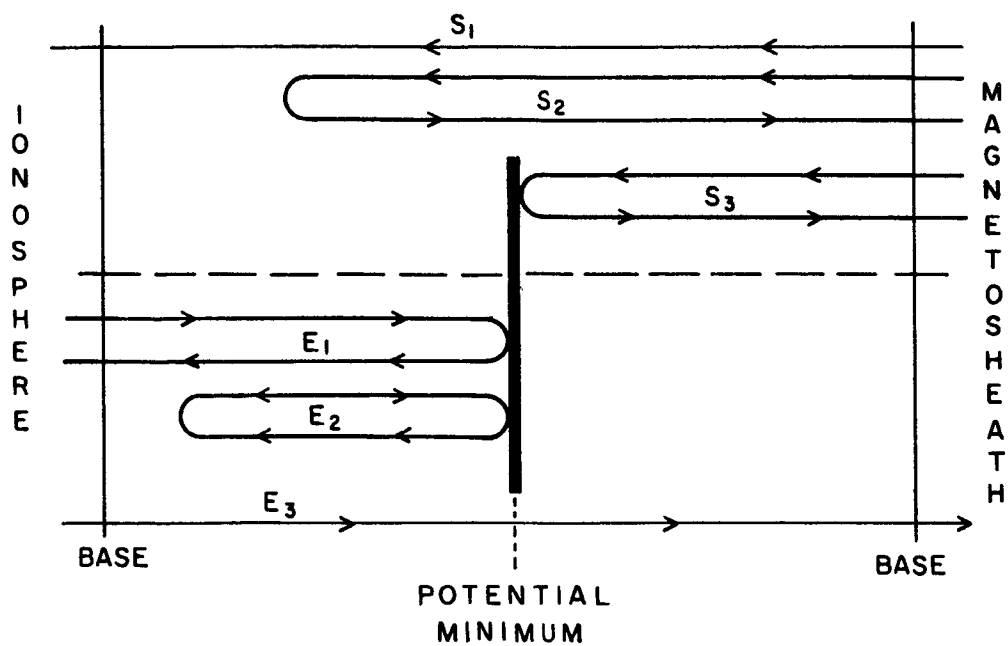
FIGURE 20a. POSSIBLE TRAJECTORIES
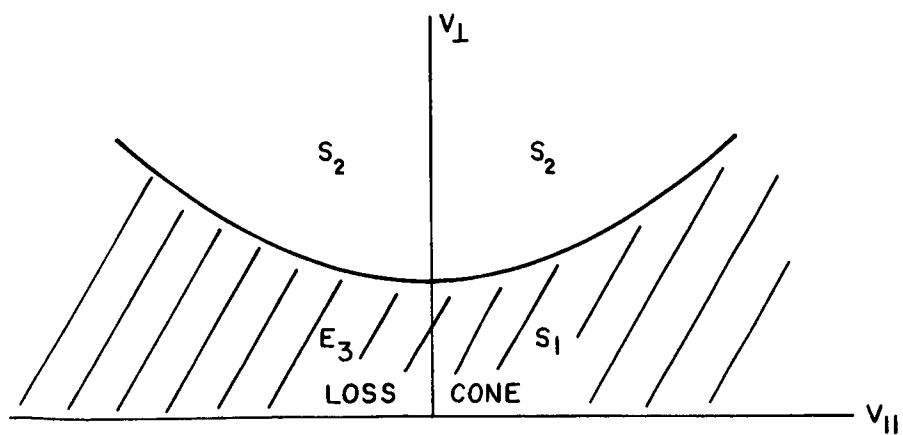
FIGURE 20b. IONOSPHERIC LOSS CONE
AT MINIMUM

same technique employed here could be used to describe the trajectories occuring in the more complicated situations.

Returning to an evaluation of the electron current at the point of potential minimum, it is apparent that not all electron trajectories contribute to the current at this location. Interplanetary electrons of types S_2 and S_3 yield no net current -- nor do ionospheric particles of types E_1 and E_2. Thus, only electrons whose trajectories pass from the ionospheric to the magnetosheath base level must be considered in determining the electron current at the minimum.

The ionospheric loss cone at a given point along a field line is defined as that region of velocity space which contains, at the considered point, only those trajectories which pass through the ionospheric base level. As was done in Chapter 2, the equation for the ionospheric loss cone boundary is determined using the conservation of energy and the first adiabatic invariant, which is the magnetic moment. If the subscript E denotes conditions at the ionospheric base level and the subscript M denotes conditions at the point of minimum potential, then the equation for the ionospheric loss cone boundary at the point of minimum potential is

$$V_{\perp_M}^2 = \frac{v_{11_M}^2 + (\Phi_M - \Phi_E)}{\frac{B_E}{B_M} - 1}$$

where Φ is $\frac{2}{m}$X (Potential Energy) and $\Phi_M - \Phi_E$ is greater than zero because the potential energy of an electron is a maximum at the point of potential minimum. All electrons which have perpendicular

velocities less than the values determined from the above equation possess trajectories which pass through the ionospheric base level. The loss cone hyperboloid and the regions corresponding to the various trajectory types found at the minimum appear in Figure 20b.

The only type of ionospheric trajectory which can reach the minimum is E_3. In Figure 20b it is seen that the region of velocity space occupied by these trajectories consists of the area of the loss cone for which $v_{11} < 0$ (motion towards the earth is defined as positive). Denote this region by A and let B be the region of velocity space corresponding to interplanetary trajectories which pass through the minimum point (B is just the complement of A). The net electron current along the field line at the point of minimum potential in the direction towards the earth is then given by

$$j = \int_A f_E v_{11} \, d\underset{\sim}{v} + \int_B f_s v_{11} \, d\underset{\sim}{v}$$

where

$$f_Y = n_Y \left(\frac{m}{2\pi kT_Y}\right)^{3/2} \exp\left(-\frac{m}{2kT_Y}(v_{11}^2 + v_L^2)\right) \circ$$

$$\exp\left(-\frac{m}{2kT_Y}(\Phi_M - \Phi_Y)\right) \tag{3-1}$$

and Y is a subscript label which indicates base level (i.e. either E or S) conditions.

Since the integrands of the above integrals are odd functions of v_{11} the S_2 trajectories (Figure 20b) do not contribute to the current. Therefore, $j = j_s - j_E$ where

$$
j_Y = \int_0^\infty \int_0^\infty \left(\frac{v_{11}^2 + \Phi_M - \Phi_E}{\frac{B_E}{B_M} - 1} \right)^{1/2} 2\pi \, f_Y \, v_{11} v_{\perp} \, d \, v_{\perp} \, d \, v_{11}
$$

Integrating this expression yields:

$$
j_Y = n_Y \left(\frac{kT_Y}{2\pi m} \right)^{1/2} \left[1 - \frac{B_E - B_M}{B_E} \exp \left(- \frac{m}{2kT_Y} \frac{\Phi_M - \Phi_E}{\frac{B_E}{B_M} - 1} \right) \right] \circ
$$

$$
\exp \left(- \frac{m}{2kT_Y} \left(\Phi_M - \Phi_Y \right) \right). \tag{3-2}
$$

Since the net current vanishes, $j_E = j_S$, and hence from equation 3-2:

$$
n_s \, e^{\frac{m\Phi_s}{2kT_s}} = n_e \left(\frac{T_E}{T_S} \right)^{1/2} e^{\frac{m\Phi_E}{2kT_E}} \frac{F(T_E)}{F(T_S)} \equiv G \tag{3-3}
$$

where

$$
F(T) = 1 - \frac{B_E - B_M}{B_E} \exp \left(\frac{m}{2kT} \frac{\Phi_E}{\frac{B_E}{B_M} - 1} \right)
$$

and where the reference level for the potential scale is taken at the minimum (i.e., $\Phi_M = 0$). This expression yields a relationship between the interplanetary and ionospheric base levels potentials when the base level electron densities and temperatures and the magnetic field at the ionospheric base and at the minimum are specified.

Taking as characteristic values $T_E = 6000°K$, $T_S = 600,000°K$ and assuming that the potential minimum is near the magnetopause so

that B_E/B_M is approximately 1000, equations 3-3 were used to calculate the base level potentials relative to one another as the ratio of base level densities n_e/n_s was varied. The results are plotted in Figure 21. The F factors in equation 3-3 become significantly different from one only near the origin as is demonstrated by the curvature of the potential profiles in Figure 21.

Taking the ratio n_e/n_s to be 100, the electron ionospheric temperature was varied and the changes in the potential profiles were determined (see Figure 22). As shown in the figure, an increase of T_E corresponds to a decrease in the order of magnitude of the interplanetary base level potential as compared to the ionospheric base level potential. This is to be expected since the Boltzmann factor contains the ratio of potential to temperature. In the limit $T_S = T_E = T$ the potential of the ionosphere base is greater than that of the magnetospheric base by the additive factor $kT \ln \dfrac{n_e}{n_s}$. Thus, the potentials of the base levels are equal only when the base level densities and temperatures are equal -- in the physical realm of the magnetosphere this will never occur.

Thus far the relationship between the base level potentials has been derived. In order to determine the explicit values in a given physical situation, it will be assumed that the electron density at the point of minimum potential is known. The relationship between the potentials and the density at the minimum will now be derived.

Consider the regions A and B of velocity space which were defined earlier. A is the region corresponding to trajectories of
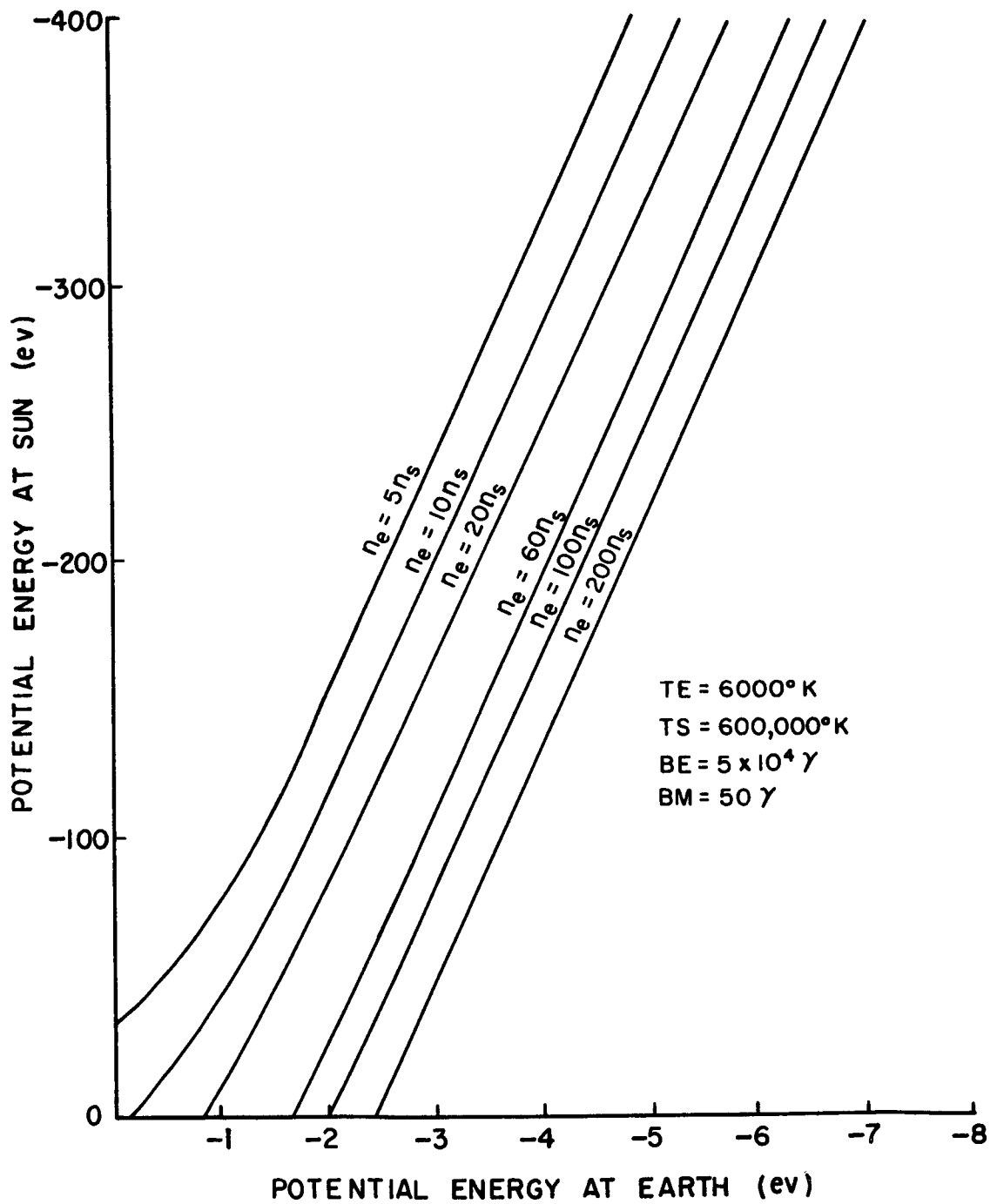
FIGURE 21. EFFECT OF n_e ON $\phi_s - \phi_e$ PROFILE
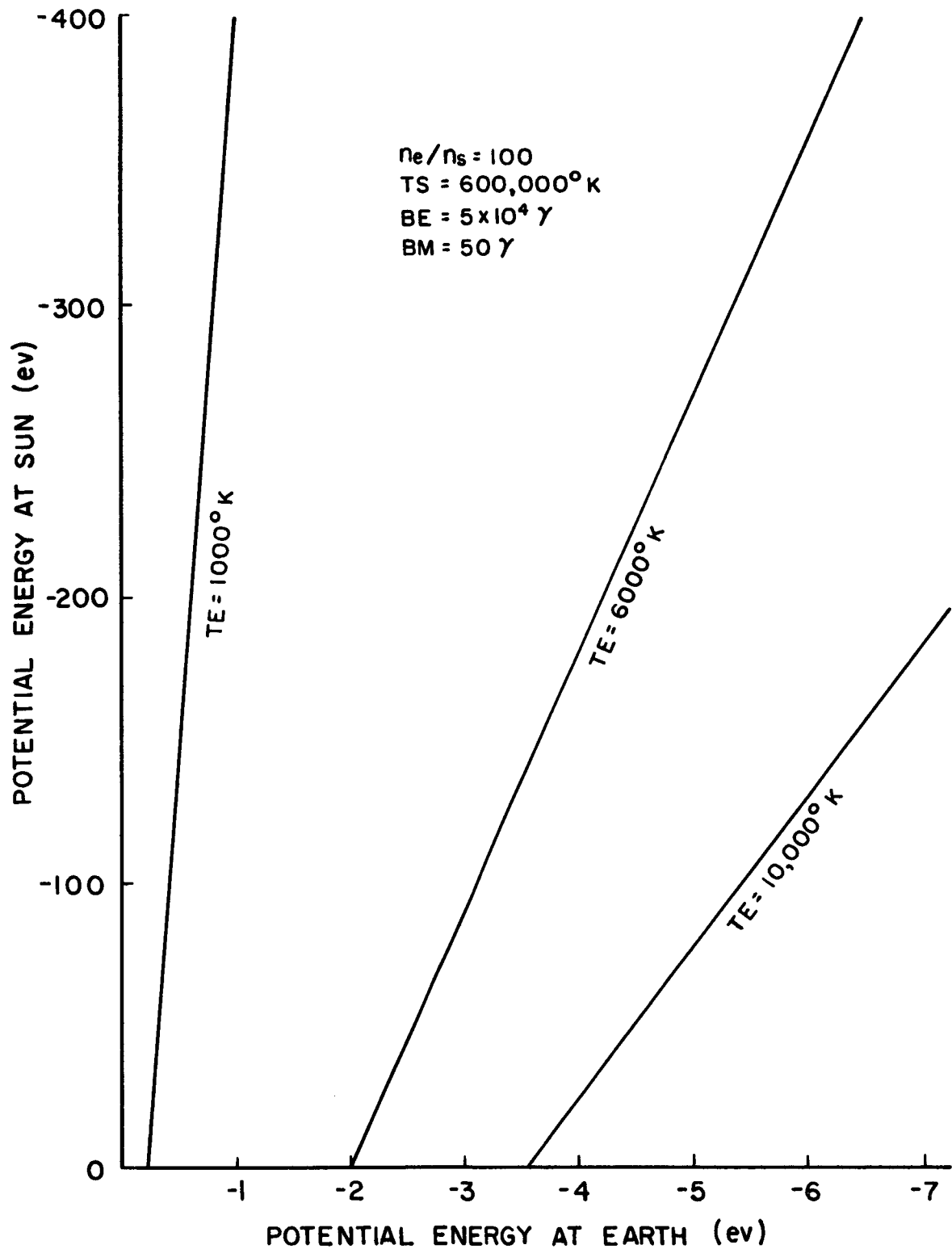
EFFECTS OF IONOSPHERIC TEMPERATURE ON $\phi_s - \phi_e$ PROFILE

FIGURE 22

type E_3 (see Figures 20) and B is the complement of A. The density at the minimum is then given by

$$n_M = \int_A f_E \, d\underset{\sim}{v} + \int_B f_s \, d\underset{\sim}{v}.$$

Since the second integral in this equation can be written as

$$\int_B f_s \, d\underset{\sim}{v} = \int_{\substack{All \\ Space}} f_s \, d\underset{\sim}{v} - \int_A f_s \, d\underset{\sim}{v}$$

the density at the minimum is given by:

$$n_M = 2\pi \int_{-\infty}^{\infty} \int_0^{\infty} f_s \, v_L \, d v_L \, d v_{11} + 2\pi \int_0^{\infty} \int_0^{\left(\frac{v_{11}^2 + \phi_M - \phi_E}{\frac{B_E}{B_M} - 1} \right)^{1/2}}$$

$$(f_E - f_s) \, v_L \, d v_L \, d v_{11}$$

where f is given in equation 3-1. Integrating this expression, the density at the minimum, n_M, is found to be:

$$n_M = G \left[1 - \frac{1}{2} F(T_s) \right] + \frac{n_E}{2} \exp \left(\frac{m}{2kT_E} \phi_E \right) F(T_E) \qquad (3-4)$$

where G and F(T) are, as defined in equation 3-3, functions of only the ionospheric base level potential.

Figure 23 depicts the variation in density at the minimum as a function of the ionospheric potential using the ionospheric base level density as a variable parameter. This figure shows that the density at a fixed base level potential is an increasing function of n_e and at a fixed base level density is an increasing function of the electron potential energy. Physically, this is expected because an
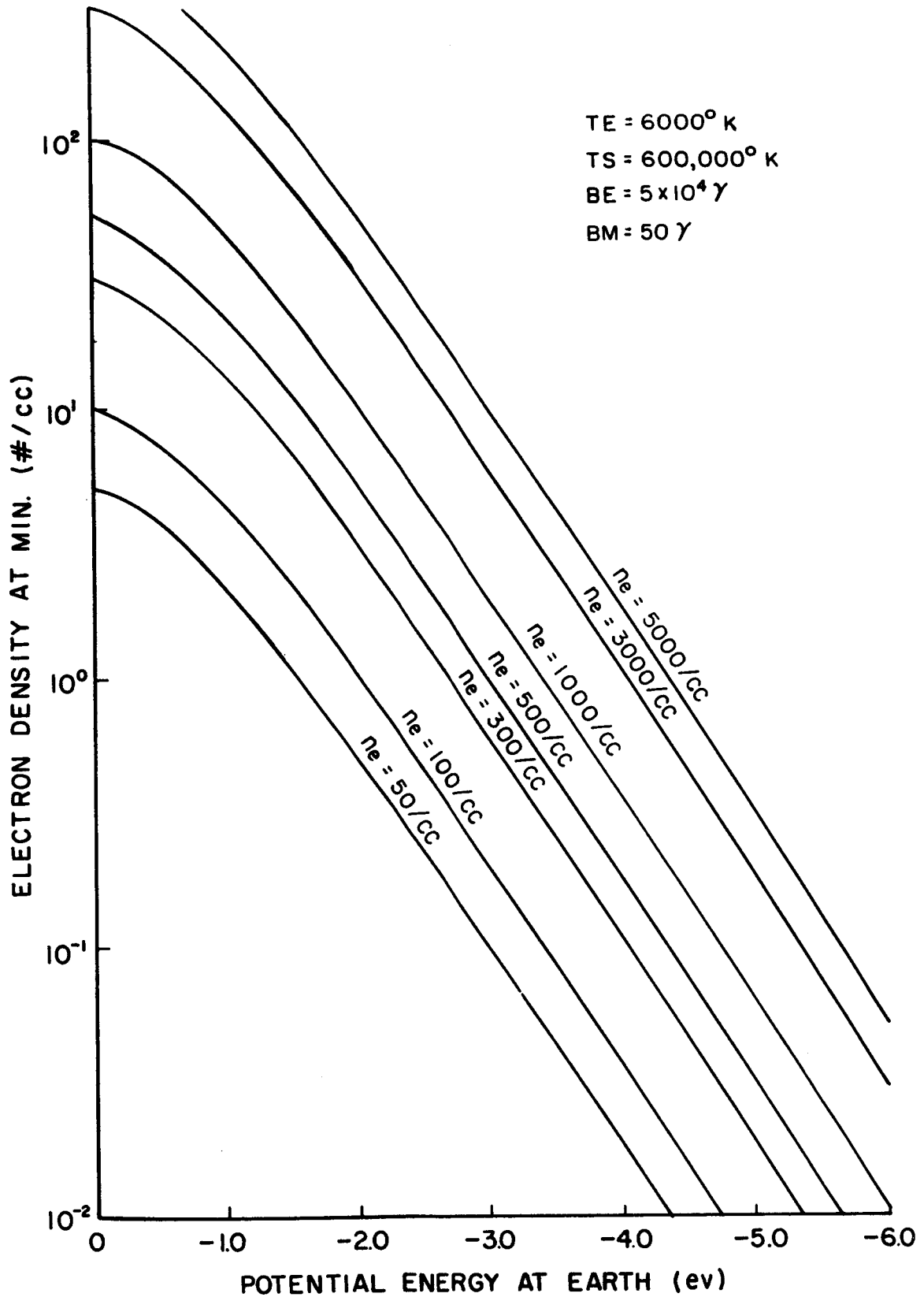
EFFECTS OF IONOSPHERIC DENSITY ON $n_m - \phi_e$ PROFILE

FIGURE 23

increase of density at the base level creates an increase in the number

of electrons available to reach the minimum, and a decrease in potential

energy at the earth increases the potential barrier which the electrons

must surmount in order to reach the minimum.

Figure 24 is a similar plot using the ionospheric temperature

as the variable parameter. Here it is seen that the density, at a

given potential, increases rapidly as the ionospheric temperature

increases. This is expected physically since an increase in tempera-

ture implies an increase in the average energy of the ionospheric

particles, and hence, an increase in the number of electrons which can

overcome the potential barrier.

Figure 23 indicates that there is an upper limit to the electron

density which can exist at the point of minimum potential. This figure

in conjunction with the results of Figure 21 indicates that this limit

is not necessarily the density determined for a vanishing base level

potential. In fact, there could be a nonvanishing lower limit to

the ionospheric base level potentials which are allowed physically.

The density upper limit however occurs either at $\Phi_S = 0$ or $\Phi_E = 0$.

If the ionospheric base level density is greater than 100/cc, as it

probably is in reality, the upper limit of density is obtained from

equation 3-3 by letting $\Phi_S = 0$. This upper limit is found to be

$$n = n_s \left[1 + \frac{1}{2} F(T_s) \left(\left(\frac{T_s}{T_E} \right)^{1/2} - 1 \right) \right]$$

Since $F(T_S)$ is a very small quantity (of the order of B_M/B_E), the

maximum allowable electron density at the point of minimum potential

is approximately equal to n_S. Hence, if the density in the
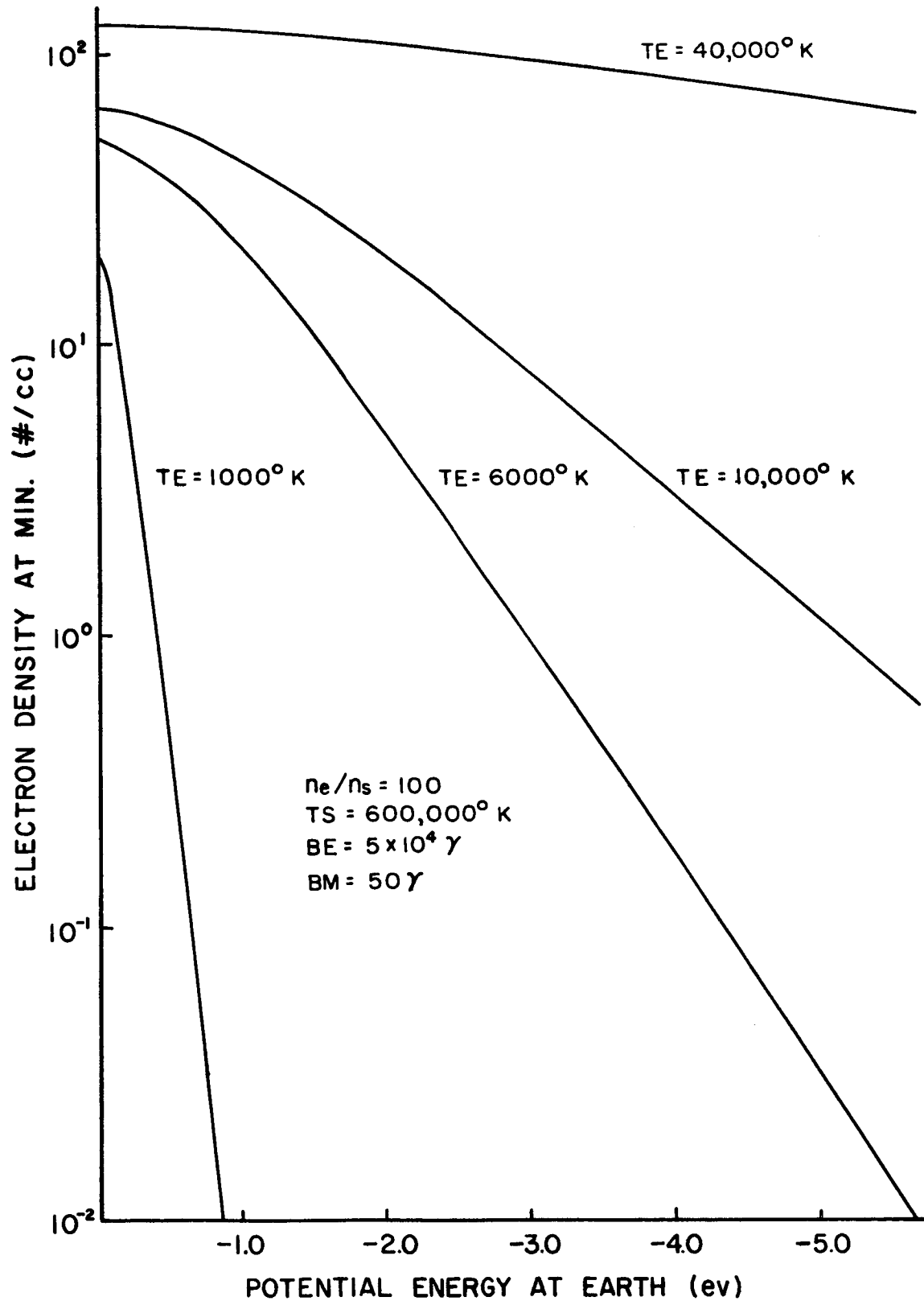
EFFECTS OF IONOSPHERIC TEMPERATURE ON n_m-ϕ_e PROFILE

FIGURE 24

magnetosphere is greater than the magnetosheath density, as was assumed previously, the minimum of potential will probably also correspond to a minimum of electron density.

Another interesting facet of the density at the minimum is that for $T_E = T_S = T$, the density is just $n_s e^{\frac{m\phi_S}{2kT}}$ or equivalently $n_E e^{\frac{m\phi_E}{2kT}}$. This is expected because the equality of base level temperatures creates a symmetrical problem: electrons can be considered as occupying all of velocity space at the minimum and as referred to either one of the base levels (i.e., $f_S = f_E$).

From the preceding results, it is now possible to specify uniquely the base level potentials, given the electron density at the point of minimum potential. For example, if $n_M = n_S = 5$ electrons/ cc (a value characteristic of the medium on the sunward side of the bow shock), $n_E = 100$ electrons/cc, and $T_E = 10^{-2} T_S = 6000^{o}K$, then from Figure 23 or equation 3-4 the ionospheric potential energy is -0.86ev and using equation 3-3 or Figure 21 the interplanetary potential is seen to be zero. If the density at the minimum is changed to $n_M = 0.5$ electrons/cc, the potential energy of the ionospheric base level decreases to -2.4 ev and the interplanetary base potential energy drops to -120 ev. Thus, a technique is now available for the determination of the relative base level potentials. It now remains to determine the electron density distributions along the open field lines. This will be done in the following sections.

3.3 Loss Cone Configurations

In order to determine the density at any point along an open field line with a minimum of electric potential corresponding to the

parallel electric field present, it must be determined to which

regions of velocity space ionospheric electrons belong and to which

regions magnetospheric electrons belong. This initially requires a

knowledge of the equations for the ionospheric loss cone and the

loss cone corresponding to the potential barrier.

The point of minimum potential divides the field line into

two parts: interplanetary and magnetospheric. From the results of

Chapter 2 it is expected that initially at reconnection on the day

side, this point is at the magnetopause. Each point on the field

line can be further classified by its potential relative to the

ionospheric base potential (i.e., $\Phi - \Phi_E \geq 0$ or $\Phi - \Phi_E < 0$). Again

it must be emphasized that the potential energy corresponding to the

minimum of potential is a maximum with respect to the potential

energy values along the field line. Thus, each point on the field

line falls within one of four classifications:

class 1: $\Phi - \Phi_E \geq 0$ $B > B_M$

class 2: $\Phi - \Phi_E < 0$ $B > B_M$

class 3: $\Phi - \Phi_E \geq 0$ $B < B_M$

class 4: $\Phi - \Phi_E < 0$ $B < B_M$.

(NOTE: B_M is the magnetic induction magnitude at the point of the

potential minimum.)

As has been done in previous cases, using the first adiabatic

invariant and conservation of energy, the equations describing the

ionospheric loss cone and the potential minimum loss cone for points

on either side of the minimum can be obtained. There are four specific equations which are obtained:

1. Ellipse:
$$v_\perp^2 = \frac{(\Phi_M - \Phi) - v_{||}^2}{(1 - \frac{B_M}{B})} \quad \text{(minimum loss cone)}$$

2. Hyberbola: (opening upwards)
$$v_\perp^2 = \frac{v_{||}^2 + (\Phi - \Phi_E)}{(\frac{B_E}{B} - 1)} \quad \text{(ionosphere loss cone)}$$

3. Hyperbola: (opening sideways)
$$v_\perp^2 = \frac{v_{||}^2 - (\Phi_E - \Phi)}{(\frac{B_E}{B} - 1)} \quad \text{(ionosphere loss cone)}$$

4. Hyberbola: (opening sideways)
$$v_\perp^2 = \frac{v_{||}^2 - (\Phi_M - \Phi)}{(\frac{B_M}{B} - 1)} \quad \text{(minimum loss cone)}$$

where the quantities in parentheses are assumed to be positive. Therefore, given the relationship between Φ and $\Phi_{E,M}$, and B and $B_{M,E}$, the ionospheric and potential minimum loss cone equations can be determined at a glance from the above equations.

Each of the four classes discussed previously is a region in which the velocity boundaries of the electrons are described by a pair of the preceding equations: the potential minimum loss cone is either 1 or 4 and the ionospheric loss cone is either 2 or 3. For example, for spatial points in class 1, which is a region between the ionosphere and the minimum, the two loss cones are defined by equations 1 and 2 above. The loss cones corresponding to all four classes are

are plotted and labeled in Figure 25. The labels I and M are used to indicate the ionospheric loss cone and the potential minimum loss cone curves respectively.

In order to determine the velocity boundaries of the ionospheric electron and interplanetary electron velocity distributions, it must be known whether or not each pair of curves actually intersect and if so, what is the point of intersection. From geometrical and algebraic manipulations it is easily seen that if there is intersection, the points of intersection are $(v_{11}, v_{\perp})$ where

$$v_{11}^{\ 2} = \frac{B_E - B}{B_E - B_M} \ (\Phi_M - \Phi) \ - \ \frac{B - B_M}{B_E - B_M} \ (\Phi - \Phi_E) \qquad (3-5)$$

and

$$v_{\perp}^{\ 2} = \frac{B}{B_E - B_M} \ (\Phi_M - \Phi_E).$$

The conditions for intersection are then obtained for each class of points. They are tabulated below:

$$
\begin{array}{lccc}
\text{class 1} & \dfrac{\Phi_M - \Phi}{B - B_M} & \geq & \dfrac{\Phi - \Phi_E}{B_E - B} \\[4mm]
\text{and class 2:} & & & \\
\end{array}
$$

$$(3-6)$$

$$
\begin{array}{lccc}
\text{class 3} & \dfrac{\Phi_M - \Phi}{B_M - B} & \geq & \dfrac{\Phi - \Phi_E}{B - B_E} \ . \\[4mm]
\text{and class 4:} & & & \\
\end{array}
$$

It can readily be seen from the class definitions that the conditions for classes 2 and 3 are always satisfied. Hence, there will never be a situation in these classes which will require nonintersecting loss
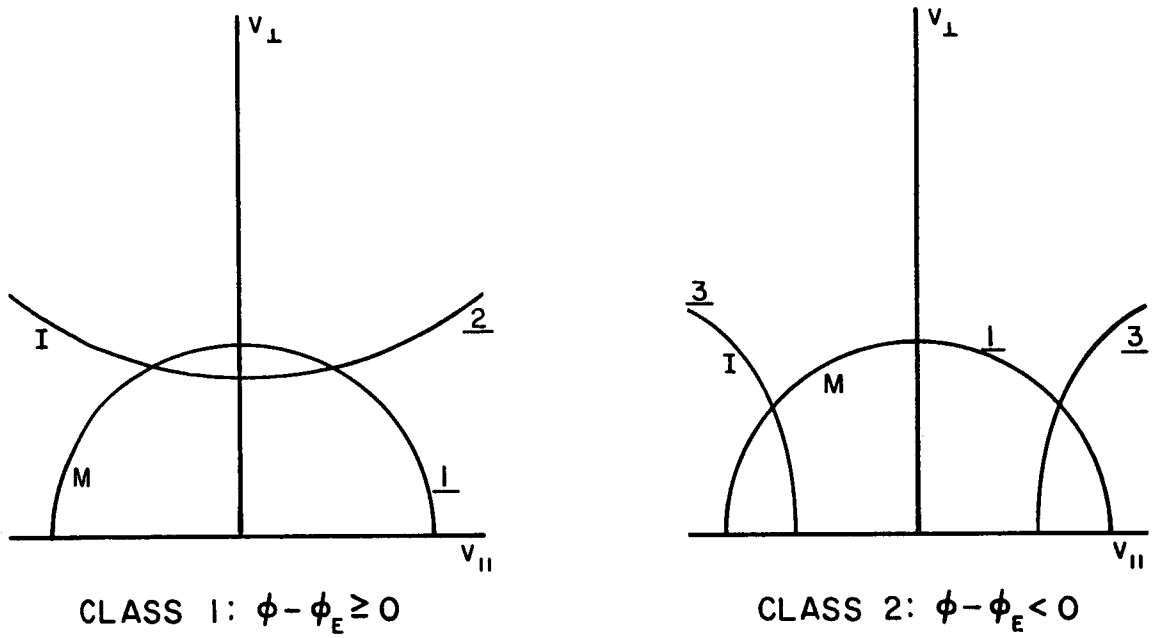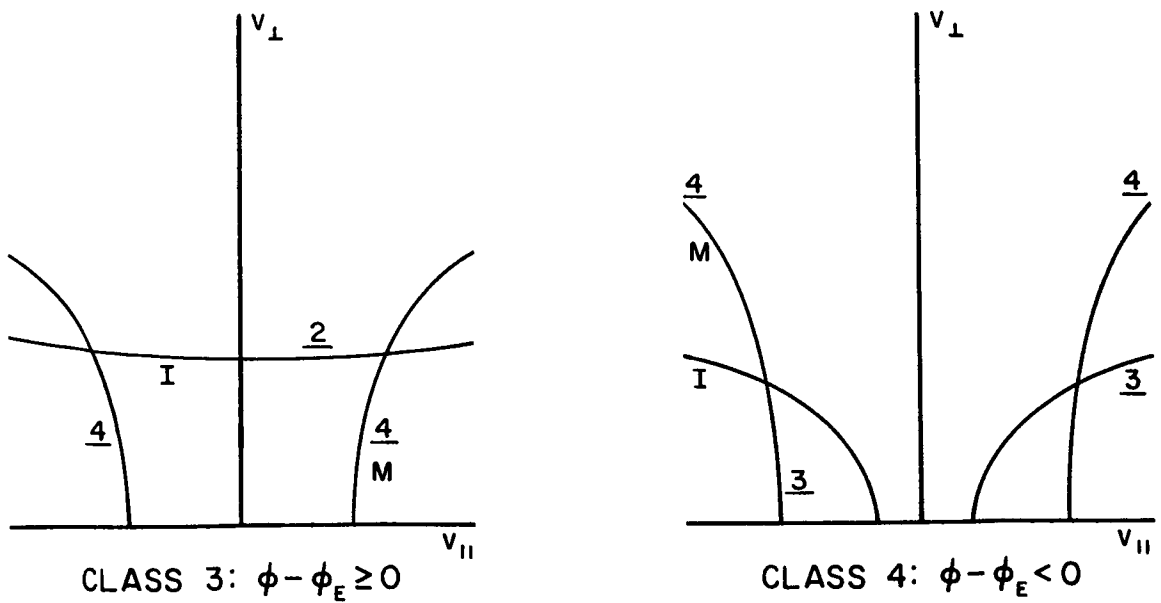
FIGURE 25. LOSS CONE CURVES

cones. However, the nonintersecting cases cannot be ignored for class 1 and class 4 regions.

Thus far, the equations defining the loss cones at a given point along the field line have been determined. Now it must be determined which regions of velocity space are occupied by electrons of ionospheric origin (these electrons have a temperature T_E and a distribution function f_E) and which regions are occupied by magneto-sheath particles (these have a temperature T_S and a distribution function f_S). The distribution functions f_E and f_S are specified by equation 3-1. Electrons of ionospheric origin (this includes those electrons which are trapped between the magnetic and potential mirrors) will be considered first.

In order to interpret positive and negative values of v_{11}, a direction must be defined as positive. The convention will be that $v_{11} < 0$ corresponds to the velocity of a particle which is moving along the field line away from the earth.

The E trajectories defined in Figure 22 correspond to electrons which are characterized by the temperature T_E and the Maxwellian distribution function f_E. On the earth side of the potential minimum all three types of ionospheric trajectories exist. Beyond the minimum in the magnetosheath only one type of ionospheric electron trajectory exists corresponding to electrons which have sufficient energy to overcome the potential wall. The velocity regions occupied by each of these trajectories must now be considered. The total velocity region allowed to ionospheric electrons is then obtained by superposition.

At a given point, the velocities of ionospheric particles with trajectories E_1 originating within the ionospheric base level (i.e., within the ionospheric loss cone) and which are reflected by the potential wall (i.e., outside the minimum loss cone) lie within that region of velocity space which is common to both the ionospheric loss cone and the region outside of the potential minimum loss cone. The velocity regions corresponding to the other trajectories can be similarly deduced.

It is more descriptive and convenient to describe the allowed velocity regions by using the notation of set theory. Let the region of velocity space corresponding to the ionospheric loss cone region be denoted by I and the region corresponding to the minimum loss cone by M. Then the regions corresponding to the three types of ionospheric electron trajectories can easily be determined in terms of these two regions.

The velocity region for electrons whose trajectories originate at the ionospheric base or below it and are reflected by the potential minimum is just $I \cap \tilde{M}$ where $\sim$ denotes the (set) complement. For trapped electrons the corresponding region of velocity space is $\tilde{I} \cap \tilde{M}$, and for ionospheric electrons which arise at or below the ionospheric base with sufficient energy to pass over the potential barrier it is $I(v_{11} \leq 0) \cap M$. Hence, when $B > B_M$ (on the earth side of the minimum), where all three types of E trajectories exist, the velocity region corresponding to electrons of temperature T_E and distribution function f_E is given by $(I \cap \tilde{M}) \cap (\tilde{I} \cap \tilde{M}) \cap [I(v_{11} \leq 0) \cap M]$ or $[I(v_{11} \leq 0) \cap M] \cup \tilde{M}$. Similarly,

when $B < B_M$, the corresponding region is just $I(v_{11} \leq 0) \bigcap M$. Using these relations in conjunction with the actual forms of the loss cones (Figure 25), the explicit regions occupied in velocity space can be obtained. The velocity region occupied by electrons with the distribution function f_E is shown shaded in Figure 26 for intersecting loss cone boundaries and in Figure 27 for nonintersecting boundaries. All four classes are included in the latter figure, but it is to be remembered that points in the second and third classes always have intersecting loss cone boundaries in the physical model under consideration.

Electrons of interplanetary origin which have the temperature T_S and Maxwellian distribution function f_S, could be similarly treated. However, there is a much simpler approach. At any point along the field line all of velocity space is filled by the plasma consisting of ionospheric, trapped, and magnetosheath electrons, and because collisions are assumed nonexistent, all three components occupy disjoint regions in velocity space. Since trajectories which do not come directly from the ionospheric or magnetosheath base levels are by definition trapped and characterized by the temperature T_E, the velocity region occupied by interplanetary electrons is just the complement of that region occupied by the T_E electrons. The unshaded regions in Figure 25 and Figure 26 correspond to electrons of interplanetary origin.

The next section will describe how the preceding results are to be applied in order to determine the electron density - electric potential profile along an open field line.
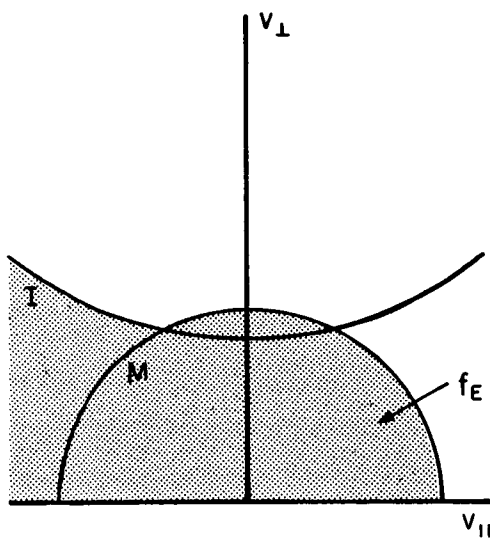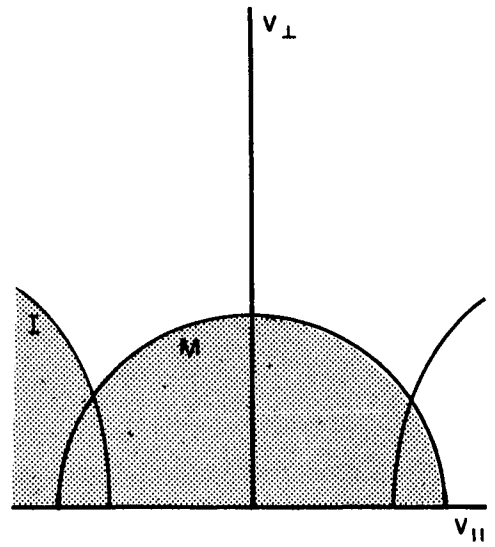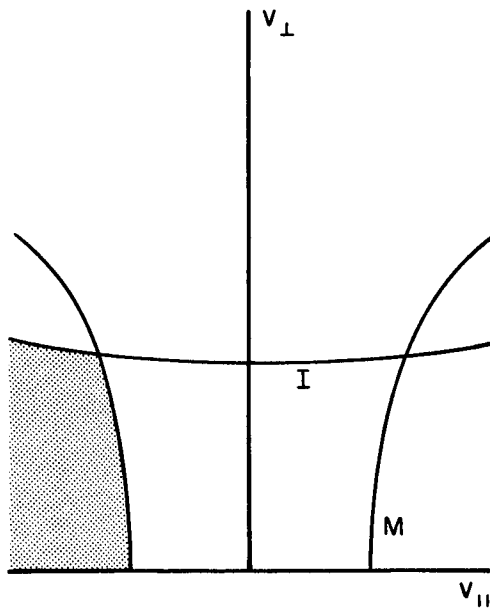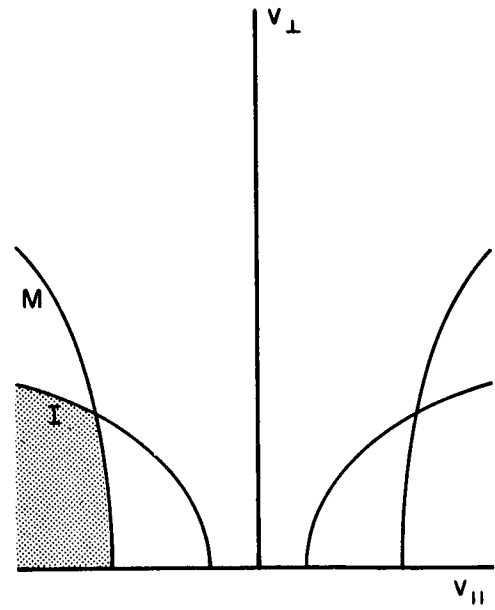
FIGURE 26. INTERSECTING LOSS CONES
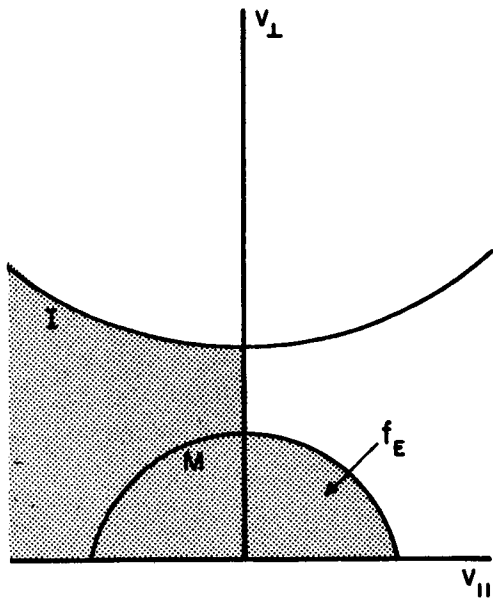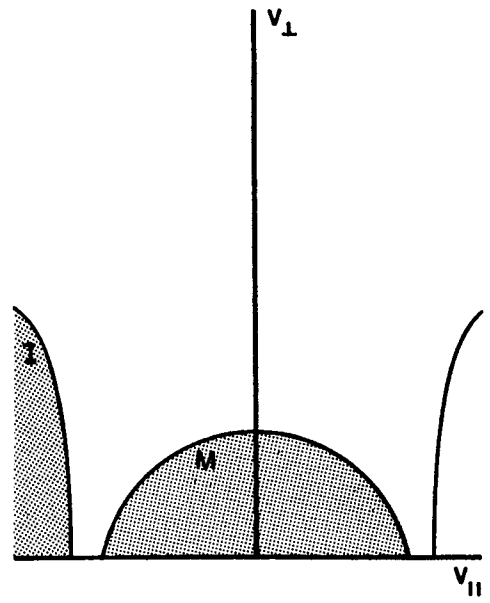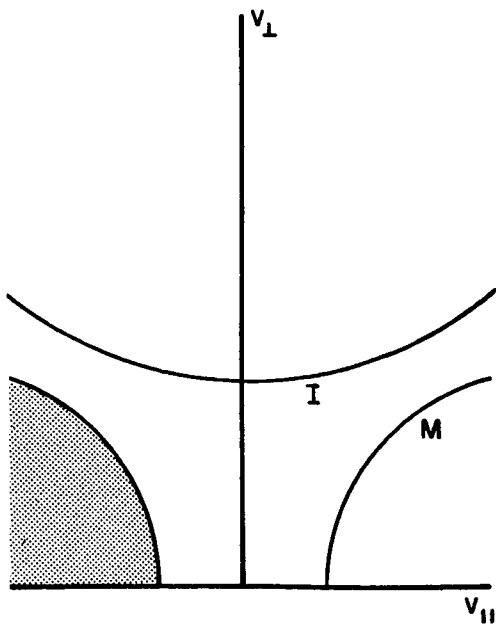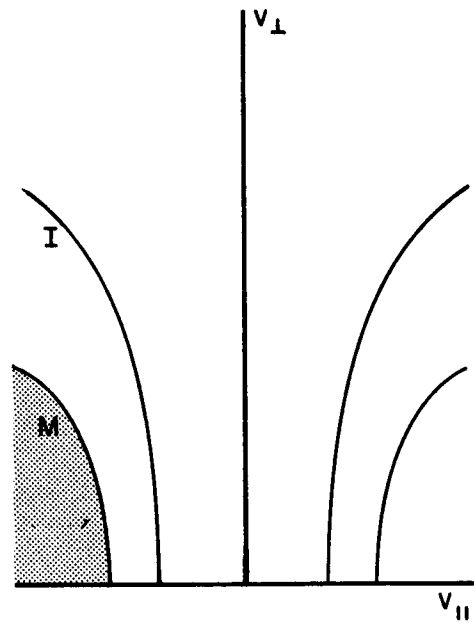
FIGURE 27. NON-INTERSECTING LOSS CONES

3.4 Electron Density Profiles

The velocity regions occupied by electrons with the distribution functions f_E and f_S have been determined for each of the four classes of points defined previously. In order to determine the density at a given point on the field line, the distribution functions are integrated over the corresponding velocity region.

The total electron density is given by:

$$n = \int_{R_E} f_E \, d\underset{\sim}{v} + \int_{R_S} f_S \, d\underset{\sim}{v}$$

where R_A is the allowed velocity region for electrons characterized by the distribution function f_A. Since R_S is just the complement of R_E,

$$\int_{R_S} f_S \, d\underset{\sim}{v} = 2\pi \int_{-\infty}^{\infty} \int_{0}^{\infty} f_S \, v_\perp \, d v_\perp \, d v_{11} - \int_{R_E} f_S \, d\underset{\sim}{v} .$$

Therefore

$$n = 2\pi \int_{-\infty}^{\infty} \int_{0}^{\infty} f_S \, v_\perp \, d v_\perp \, d v_{11} + \int_{R_E} (f_E - f_S) \, d\underset{\sim}{v} .$$

Since f_A (equation 3-1) is proportional to $n_A \exp \left[- \frac{m}{2kT_A} (\Phi - \Phi_A) \right]$, the density can be written in the general form:

$$n = n_S e^{- \frac{m}{2kT_S} (\Phi - \Phi_S)} \left(1 - \frac{1}{2} F (I_c, T_S) \right) + \frac{n_e}{2} e^{- \frac{m}{2kT_E} (\Phi - \Phi_E)} \circ$$

$$F (I_c, T_E) \qquad (3\text{-}7)$$

where $\frac{1}{2}$ F (I_c, T_A) denotes the function obtained in class I by integrating f_A exp $[\frac{m}{2kT_A} (\Phi - \Phi_A)]$ over the velocity region R_E. The subscript c is a dummy label. For intersecting loss cone boundaries c $\equiv$ i and for nonintersecting boundaries c $\equiv$ n. The factor $\frac{1}{2}$ has been drawn from the integrals.

The limits of integration for the required integrals can easily be deduced from Figures 25, 26 and 27 and equations 3-5. Since the determination of F (I_c, T) is a process of straightforward, though tedious integration, only the final results will be given below. The potential energy at the minimum is taken as zero.

Let $A = \sqrt{\frac{m}{2kT}}$, $C_M = \sqrt{\frac{B_M}{B - B_M}}$, $D_M = \sqrt{\frac{B_M}{B_M - B}}$,

$C_E = \sqrt{\frac{B_E}{B_E - B}}$, $P = \sqrt{-\Phi}$, $E_1 = \exp(\frac{A^2 \Phi B}{B - B_M})$ and

$E_2 = \exp - (\frac{A^2 (\Phi - \Phi_E) B}{B_E - B})$. Then the F functions are given explicitly by:

$$F (1_i, T) = 1 + erf (PA) - \frac{E_1}{C_M} [arf (PAC_M) + arf (\alpha AC_M)]$$

$$- \frac{E_2}{C_E} erfc (\alpha AC_E)$$

$$F (1_n, T) = 1 + erf (PA) - \frac{arf (PAC_M)}{C_M} - \frac{E_2}{C_E}$$

$$F (2_i, T) = 1 + erf (PA) - \frac{E_1}{C_M} [arf (PAC_M) + arf (\alpha AC_M)]$$

$$- \frac{E_2}{C_E} erfc (\alpha AC_E) \tag{3-8}$$

$$F(3_i, T) = \text{erfc}(PA) - \frac{E_1}{D_M}[\text{erf}(\alpha \, AD_M) - \text{erf}(PAD_M)]$$

$$- \frac{E_2}{C_E} \, \text{erfc}(\alpha \, AC_E)$$

$$F(4_i, T) = \text{erfc}(PA) - \frac{E_1}{D_M}[\text{erf}(\alpha \, AD_M) - \text{erf}(PAD_M)]$$

$$- \frac{E_2}{C_E} \, \text{erfc}(\alpha \, AC_E)$$

$$F(4_n, T) = \text{erfc}(PA) - \frac{E_1}{D_M} \, \text{erfc}(PAD_M)$$

$$\text{where} \quad \alpha = \sqrt{\frac{B - B_E}{B_E - B_M} \Phi - \frac{B - B_M}{B_E - B_M}(\Phi - \Phi_E)} \ .$$

The notation arf (x) is proposed for the Dawson function which

is $\frac{2}{\sqrt{\pi}} \int_0^x e^{x^2} \, dx$. Erfc (x) is the notation commonly used for

the complement of the error function 1 - erf (x).

Equations 3-8 in conjunction with 3-7 yield the electron

density - electric potential profile on any line of force along which the

magnetic field magnitude varies monotonically, and on which there

is one significant minimum of potential corresponding to the parallel

electric field present.

3.5 Numerical Computations

The 7074 computer of the Pennsylvania State University was

used to obtain the numerical profiles. Dawson's function was

evaluated by interpolating between the tabulated values in the

NBS Handbook of Mathematical Functions (1964). Due to the rapid

divergence of this integral, logarithmic interpolation was used.

For values of x less than 3.2, the error function was evalu-

ated using the expansion:

$$\text{erf}(x) = 1 - (a_1 t + a_2 t^2 + a_3 t^3 + a_4 t^4 + a_5 t^5)e^{-x^2} + \varepsilon(x)$$

where $t = \dfrac{1}{1 + p x}$, $p = 0.3275911$, $a_1 = 0.25482959$, $a_2 = 0.28449673$,

$a_3 = 1.4214137$, $a_4 = 1.4531520$ and $a_5 = 1.0614054$. The absolute

value of the remainder term ε is less than or equal to 1.5×10^{-7}.

For values of x greater than 3.2, a double precision library sub-

program was used to interpolate between the tabulated values of

erfc (x) listed in the NBS Handbook.

The following representative values are chosen for the

physical parameters:

$$T_E = 6000^\circ \text{ K}$$

$$T_S = 600,000^\circ \text{ K}$$

$$n_e = 100 \text{ electrons/cc}$$

$$n_s = 5 \text{ electrons/cc} \quad .$$

At the point of minimum potential it was shown previously that there

is probably a minimum of density also. Hence, a reasonable value for

n_M is 0.5 electrons/cc. These values are rather arbitrary due to the

lack of sufficient measurements of low energy particles in the outer

magnetosphere. Since the immediate concern is the determination of

general characteristics of the density profile, the exact values

for these parameters are not crucial. However, in order to determine the magnitude of the parallel electric field in the magnetosphere it will be essential that these parameters be known exactly. Hopefully, these quantities will be accurately determined in the near future.

For a density at the minimum of 0.5 electrons/cc, the technique developed in Section 3.2 can be used to determine the base level potentials. Using this method, the potentials V are found to be V_E = 2.4 ev and V_s = 120 ev. Thus, the potential of the interplanetary base level is much larger than that of the ionospheric base. This was anticipated in Section 3.2.

Using the above parametric values, the density-potential profile was evaluated for a few points on the field line. The resulting curves are plotted in Figure 28 where the notation R or Ratio is equilvalent to the ratio B_E/B where B_E is the magnitude of the magnetic field at the ionospheric base level. Only the region $0 \leq V \leq 3.5$ ev was plotted. More negative values of the potential energy are uninteresting because the density rapidly becomes a simple exponential function of the potential energy. Expanding the scale would only extend the straight lines which are already apparent in the figure. Also, R is assumed to be 1000 at the point of the minimum -- this value is characteristic of the magnetopause.

As expected the density at V = 0 approaches 0.5/cc as the point considered moves towards the point of the minimum. It is also apparent that the density of 0.5 electrons/cc is the lowest density obtainable on the field line. Therefore, the minimum of potential
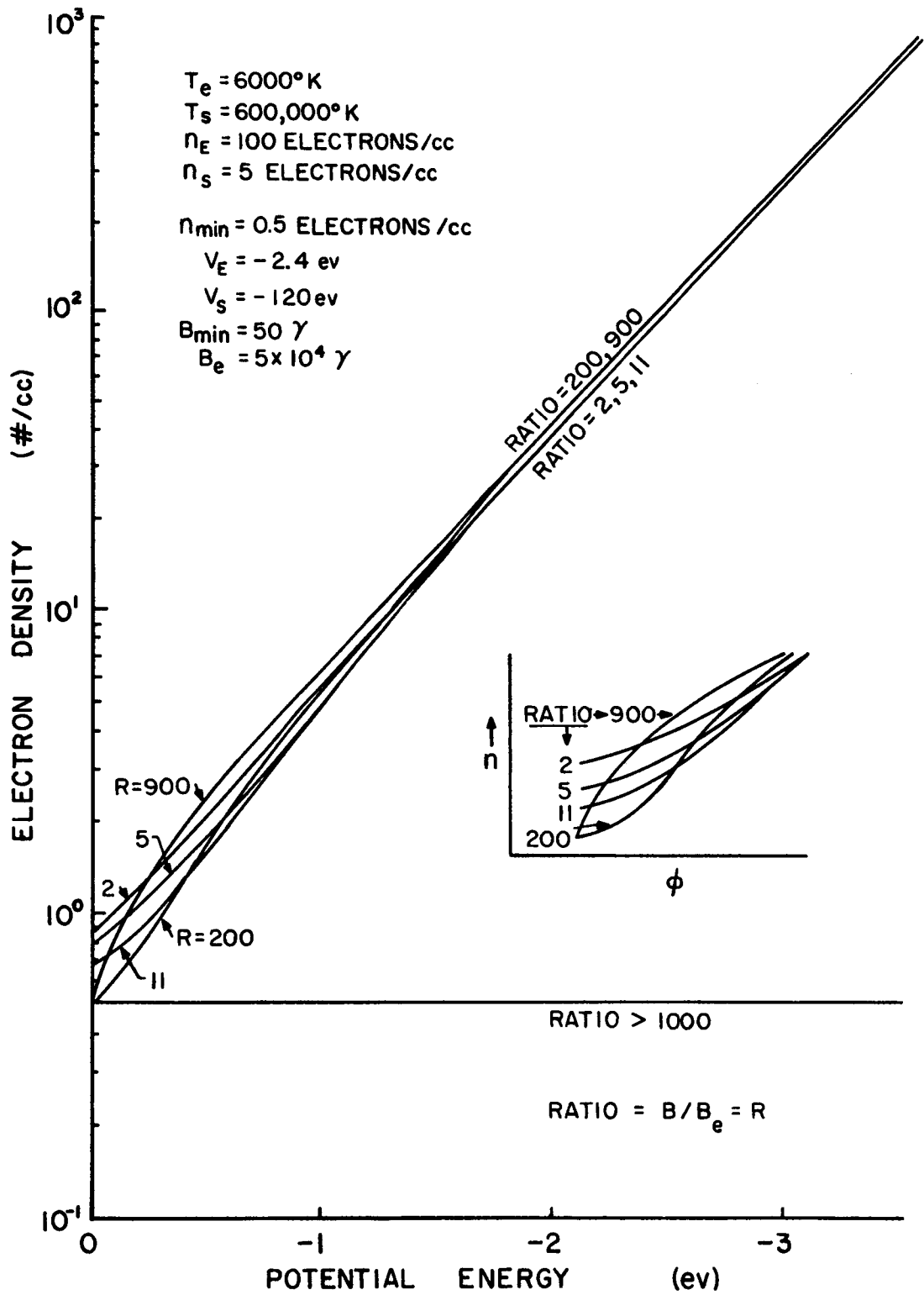
FIGURE 28. ELECTRON DENSITY-
POTENTIAL ENERGY PROFILES

in this case occurs at the same place on the field line as the mini-
mum of electron density. It should be noted that at the minimum
(i.e., at Ratio = 1000), the density profile degenerates into the
single point ($\Phi = 0$, n = 0.5).

On the earth side of the minimum (i.e., points on the field
line with Ratio < 1000) the profiles for V $\leq$ 0.5 ev show an interest-
ing change near Ratio = 200. In this spatial region, the curves in
the semilog plot of Figure 28 change their apparent curvature. At
low altitudes on the field line (i.e., at small values of R) the
profiles are concave upwards; whereas, for points near the minimum
the curves are concave downwards. This change is clearly seen in
the enlarged diagram (not drawn to scale) on the right side of the
figure. This apparent transition corresponds to a change from non-
intersecting class 1 loss cones (see Figure 27), to intersecting
class 1 loss cones (Figure 26) as B increases (i.e., as the point of
the potential minimum on the field line is approached).

Beyond the point of the minimum (i.e., for the points B >
1000) only one density-potential profile is drawn. The computations
indicated that the profiles in this spatial region change insignifi-
cantly from point to point on the open field line. It is seen in
the figure that the electron density varies very slowly with po-
tential at points in this region. If the profile for R > 1000 was
extended to the potential energy of -120 ev (the interplanetary
base level value) it would be found that the density would approach
5 electrons/cc (the interplanetary base level value). Electrons of
ionospheric origin contribute very little to the electron density at

points beyond the minimum. The class 3 and class 4 loss cones (see Figures 26 and 27) which are applicable in this spatial region, contain very few ionospheric electrons. In other words, only those few electrons in the far tail of the Maxwellian distribution function, which describes the ionospheric particles, have sufficient energy to travel over the potential barrier into the magnetosheath. Most of the ionospheric electrons are reflected by the barrier and never reach the region R > 1000.

3.6 Further Considerations

The techniques developed in this chapter are valid for arbitrary monotonic magnetic field configurations. However, the analysis was performed with the physics of the magnetosphere in mind. Logically, having looked at electron motion, it should now follow that the proton motion along an open field line just after reconnection on the day side be considered. The proton model developed in Chapter 2 could be used in conjunction with this electron density model to determine the time development of the parallel electric field, and also the proton motion along a field line as it is swept towards the night side. Such an analysis is prohibited by the exceedingly long computer time required.

Although prohibited by computer limitations from extending the electron density model, it is apparent that a general method has been devised which could be applied to the motion of thermal collisionless plasmas along more complicated magnetic fields. The technique can be extended to consider the density-potential relation

in a field with potential-potential or magnetic-magnetic trapping
if the distribution of the trapped particles is characterized by the
Maxwellian function. Such may be the case in static plasma con-
figurations. Then by measuring the electron density along the magnetic
field lines, the parallel electric field can be determined.

Shifting attention from the day side reconnection to the night
side reconnection process, the next chapter will explore a different
type of model which might describe the plasma motion along closed
field lines which travel towards the day side after having re-
connected on the night side.

CHAPTER IV

NIGHT SIDE ANALYSIS

4.1 General Description of the Model

In previous chapters, the ambient plasma distribution along an open field line on the day side of the earth was considered for a short time period after connection to the solar field. Electrons of ionospheric and interplanetary origin were assumed to interdiffuse immediately along the entire field line due to their large thermal velocities. The protons, on the other hand, had to be analyzed time dependently due to their rather small thermal velocities. These assumptions are relevant also to particles on those closed field lines in the outer magnetosphere which form a part of the circulation cycle. Hence, the electrons can be considered from the quasistatic viewpoint; whereas, the proton motion is dependent upon the past history of the parallel electric field.

The field line circulation on the night side of the earth is depicted in Figure 29 for the region near the reconnection current sheet in the noon-midnight meridian plane. As time increases, a field line and its associated "frozen-in" plasma move in the direction of increasing Roman numerals. Before reconnection (field line I) protons of ionospheric and magnetosheath origin interdiffuse along the field line as was assumed in previous chapters. At reconnection (II) the southern polar region is connected to the northern region by a field line. Considering the low energy plasma, it is readily seen that the closed field lines have no source of
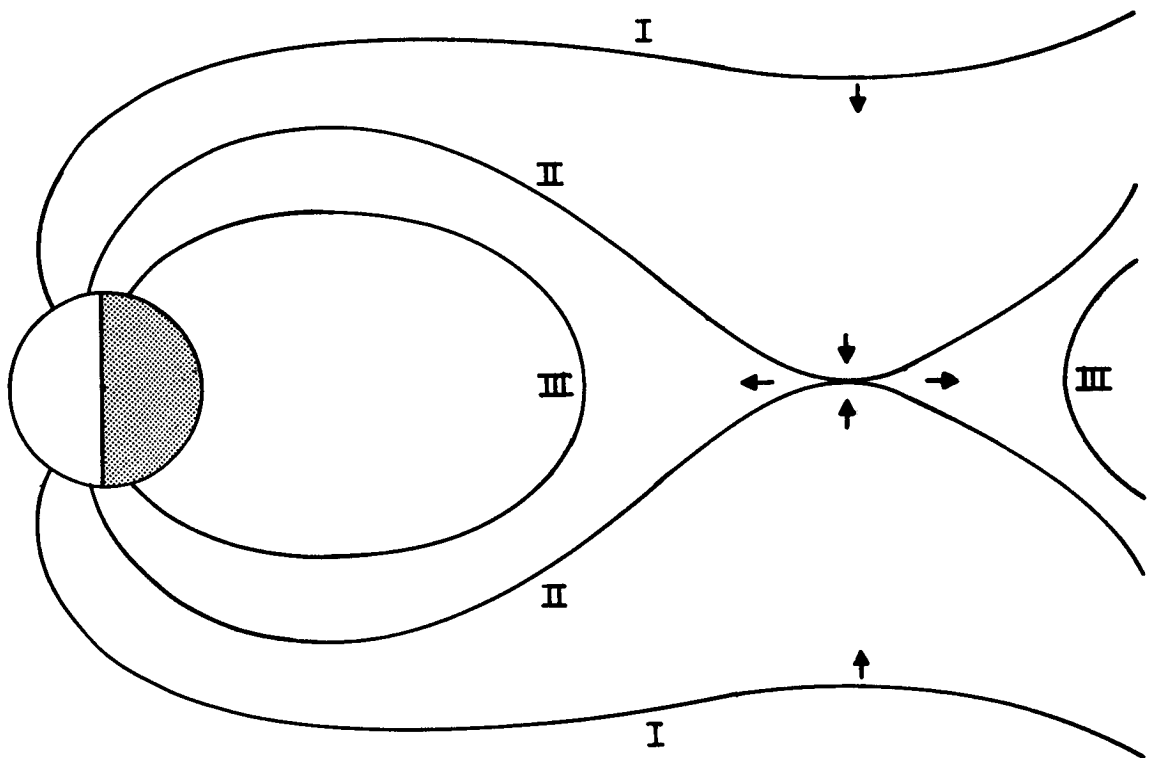
→ PLASMA FLOW DIRECTION

FIGURE 29.   NIGHT SIDE FIELDS

particles of interplanetary origin -- the interplanetary region of the open field line and its associated plasma drift away from the earth after reconnection (III).

A small fraction of the total proton population on the closed field line has been through the current sheet. This fraction has probably gained an energy of perhaps Kev and may tend to have small pitch angles (Dungey, 1966). These particles will be unimportant in considering motion dependent upon the parallel electric field present, due to the much larger percentage of low energy protons which have not been through the current sheet. The behavior of the electrons will probably be similar. Thus, to a first approximation, the plasma along the closed field line (III) a short time after reconnection is of ionospheric origin. The base levels in the north and south polar ionospheres provide a continual source of plasma, produced by photo-ionization in the ionosphere, for the outer magnetospheric region of the closed field line. In fact, as the closed field line (III) rotates out of the plane of Figure 29 towards the day side, the total electron content along the field line should increase with time due to this continual supply of particles at the base levels, and due to the fact that the field line density was partially depleted by a loss of charged particles to interplanetary space during the open phase of the circulation cycle (Nishida, 1966).

Before reconnection there is a net plasma flow outwards in each hemisphere. On the closed field line formed at reconnection, these outward streams will meet at the equator resulting in some interaction. In order to determine the exact nature of this streaming

motion it must be known whether or not the proton plasma is cold.
The next section will show that it is valid to ignore the thermal
energy when compared to the ordered energy of motion of the proton
flow.

The two outward moving plasma streams meet at the equator
immediately after reconnection. It is well known in plasma theory
that a stream of charged particles is prevented from penetrating
another plasma long before collisions could stop such penetration
(Buneman, 1964). Hence, it is probable that there will be a rapid
spatial change of the plasma streaming velocity at the equator
initially. However, due to a lack of experimental measurements of
this plasma medium, the magnitude of this change is not known.
Hence, the initial velocity profile along the closed field line must
be rather arbitrarily chosen.

Immediately after reconnection, it is assumed that the outward
proton flow velocity has a nonzero constant value on each half of the
considered closed dipole field line. (It was pointed out by Dr. J. W.
Dungey, in a personal communication, that on an open field line this
assumption of constant velocity would be analogous to the situation
in the solar breeze.) It is assumed that the interaction region at
the equator has a very small thickness compared to other characteristic
lengths -- that is, the existence of shocks are postulated. Since
symmetry is assumed about the equatorial plane, the proton flow
velocity at the equator must vanish and shocks are assumed to develop
on either side of the equator. These collisionless plasma shocks,
once formed, will move away from the equator along the field line

towards the earth, as the field line and its "frozen-in" plasma follow the convection circulation pattern towards the day side.

The shocks formed at the equator are collisionless shocks which rely entirely on electrostatic fields for their formation. It is assumed that plasma instabilities will limit the magnitude of the longitudinal viscosity coefficient and hence, yield shocks which can be assumed to be of infinitesimal thickness.

The proton density, temperature and velocity will be discontinuous across the shocks. The electron temperature, on the other hand, is assumed to remain unchanged across the shock because since the longitudinal electron thermal conductivity is of great magnitude (Jaffrin and Probstein, 1964) and much larger than the proton thermal conductivity, the electrons may be heated in passing through the shock but then immediately cooled by thermal conduction to the preshock temperature.

The ionospheric base levels of the closed field line are assumed to be characterized by identical, constant electron temperatures. More rigorous model computations will have to take into account disparate north and south hemisphere electron temperatures, and temperatures which vary with time as the field line circulates towards the day side.

Those electrons with trajectories which pass through the base level can be considered Maxwellian (via Liouville's theorem) since ionospheric particles are in thermal equilibrium and collisions are very rare in the magnetosphere. Interplanetary electrons which become trapped in the closed magnetic field configuration after

reconnection will tend to approach thermal equilibrium with the electrons of ionospheric origin due to collisions near the bases of the considered field line. (It is to be noted that a magnetic-magnetic trap is implied and not a magnetic-electric trap as was treated previously.) Hence, in a first approximation, the trapped electrons and the loss cone electrons are characterized by a Maxwellian distribution function with the assumed constant base level temperature.

The electrons from each hemisphere, due to their high thermal velocities, will quickly interdiffuse along the entire field line and can be considered to occupy all of velocity space at each point. Therefore, the electron density is related to the potential by the exponential Boltzmann factor. This relation will be a good approximation, even though it is assumed that no net current exists, because the plasma (i.e., electron and proton) flow velocity is very small compared to the electron thermal velocity.

4.2 Basic Fluid Equations

Ignoring the shocks for the moment, the equations describing the proton motion along a magnetic flux tube in the outer magnetosphere will be considered. First, it must be determined whether the thermal energy can be ignored in comparison to the ordered kinetic energy of flow.

The characteristic temperature of the protons (and electrons) at a height of approximately 1000 km at high latitudes on the night side is approximately 2000°K (Watt, 1965). This corresponds to a proton thermal velocity of approximately 70 m/sec. Now, since 0^+ ions dominate at this altitude, protons at this base level see an electric field directed upwards which is required to maintain

charge neutrality in the presence of the separative action of gravity. The magnitude of this electric field acceleration of the protons is 8g (Geisler and Bowhill, 1965) where g is the local gravitational acceleration. The total acceleration is then 7g (1g was subtracted due to gravity acting downwards). The kinetic scale height $(\frac{kT}{Mg})$ at high latitudes on the night side above 1000 km is always greater than 100 km (Watt, 1965). Taking the conservatively low value of 100 km, an estimate for the flow velocity upward is obtained by equating the kinetic energy of flow to the thermal energy derived from the scale heights at 1000 km. This yields a flow velocity upwards at the base of 4470 m/sec. Since the proton velocity is assumed constant in each hemisphere initially, it is seen that the proton thermal energy can be ignored in comparison to the ordered kinetic energy.

The proton motion along the flux tube is regarded as a cold proton flow in a well thermalized electron background which is characterized by the temperature T. Since all regions of velocity space are occupied by these electrons, the electron density at any point along the field line is directly proportional to the Boltzmann factor. That is, the electron density is given by

$$n = n_0 \; \exp \; (\; \frac{eV_E}{kT} \; - \; \frac{m_e V_g}{kT} \;)$$

where V_E is the electrostatic potential, V_g the gravitational potential, m_e the electronic mass, and n_0 is the constant of proportionality.

From the above equation it is easily shown that

$$\frac{kT}{n} \text{ grad } n = e \text{ grad } V_E - m_e \text{ grad } V_g.$$

Take the scalar product of this equation with the unit vector defining the direction of the field at any point along the field line considered:

$$\frac{kT}{n} \frac{\partial n}{\partial S} = e \frac{\partial V_E}{\partial S} - m_e \frac{\partial V_g}{\partial S}. \qquad (4\text{-}1)$$

In equation 4-1, S is a length coordinate measured along the field line.

The proton force equation along the field direction is given by:

$$M \frac{dv}{dt} = M \frac{\partial v}{\partial t} + Mv \frac{\partial v}{\partial S} = -e \frac{\partial V_E}{\partial S} + M \frac{\partial V_g}{\partial S} \qquad (4\text{-}2)$$

where M is the proton mass and v is the proton parallel velocity magnitude. Substituting the electric field as calculated from 4-1 into this equation yields:

$$M \frac{dv}{dt} = -\frac{kT}{n} \frac{\partial n}{\partial S} + (M - m_e) \frac{\partial V_g}{\partial S}.$$

But since $M >> m_e$, the Euler's equation pertinent to the proton motion at hand is given by

$$\frac{\partial v}{\partial t} + v \frac{\partial v}{\partial S} = -\frac{kT}{Mn} \frac{\partial n}{\partial S} + \frac{\partial V_g}{\partial S} \qquad (4\text{-}3)$$

where n corresponds to the proton number density (via quasineutrality).

Next, it must be determined what form the continuity equation takes for this fluid motion of protons. This equation corresponds to the motion of a fluid (the protons) in a channel of varying cross section (the magnetic flux tube) and is given by

$$\frac{\partial \rho}{\partial t} + \text{div} (\rho \, \underset{\sim}{v}) = 0$$

where ρ is the proton mass density (i.e., ρ = n M) and where $\underset{\sim}{v}$ is the total proton velocity including both the component of velocity parallel to the magnetic field direction and the convective component perpendicular to the magnetic field direction. Since motion is to be considered in the frame of reference of a field line as it is convected, this velocity is identical to the parallel component in the model under consideration.

Expanding the divergence term in the continuity equation yields

$$\frac{\partial \rho}{\partial t} + \text{grad} \, \rho \cdot \underset{\sim}{v} + \rho \, \text{div} (\underset{\sim}{v}) = 0 \, . \tag{4-4}$$

In the frame of reference of a given field line as it and its "frozen-in" plasma is convected in the magnetosphere the second term in equation 4-4 becomes $v \frac{\partial \rho}{\partial S}$ because in this frame of reference only a parallel velocity exists.

Consider next the divergence term. Figure 30 shows an enlarged diagram of a magnetic flux tube with a constructed segment which will be used to evaluate the velocity divergence. Streamlined potential flow is assumed along the flux tube whose outer surfaces are streamlines. This is consistent with the plasma model developed because loss of protons to another flux tube is prohibited. The upper and lower surfaces of the constructed pillbox are curved surfaces which are normal to the streamlines at all points.
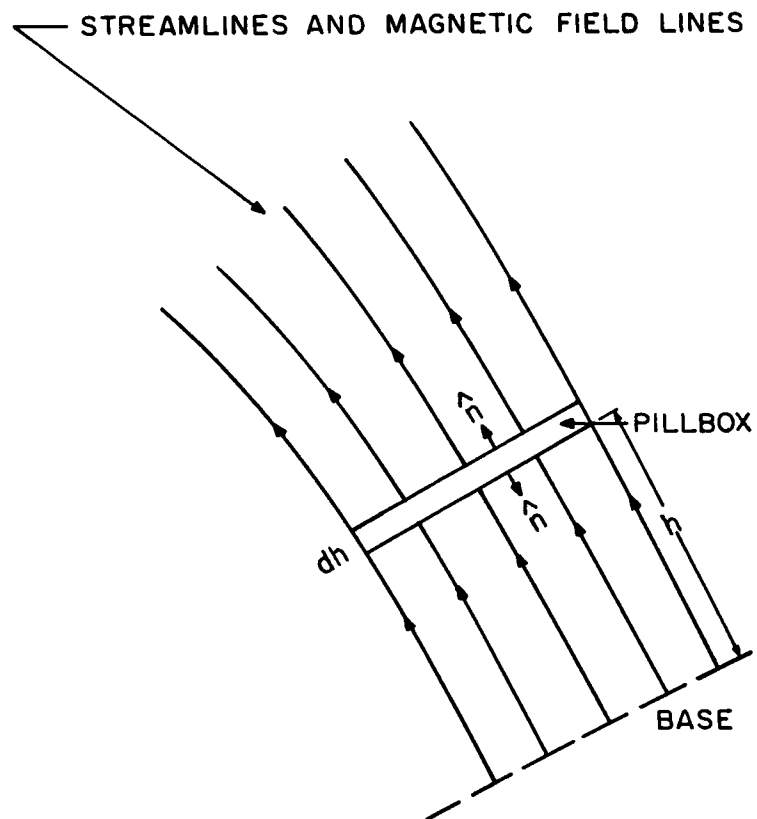
FIGURE 30. FLUX TUBE AND/OR STREAM TUBE

The basic definition of divergence is given by the following equation:

$$\text{div}\ (\underset{\sim}{v}) = \lim_{\Delta V \to 0} \frac{\oint \underset{\sim}{v} \cdot \hat{n}\ dA}{\Delta V}$$

where dA and ΔV are the surface area and volume differentials respectively, and $\hat{n}$ is the unit outward surface normal. Since there is no component of velocity normal to the flux tube walls, the surface integral is given by

$$\oint \underset{\sim}{v} \cdot \hat{n}\ dA = v(S + dS)\ A(S + dS) - v(S)\ A(S)$$

where S is the arc length along the flux tube.

Expanding $v(S + dS)$ and $A(S + dS)$ about the point S by using the Taylor series and substituting the resulting surface integral into the defining formula of the divergence, the divergence of the velocity can be written as

$$\text{div}\ \underset{\sim}{v} = \lim_{dS \to 0} \left(\frac{v(S)\ \frac{\partial A}{\partial S}\ dS + A(S)\ \frac{\partial v}{\partial S}\ ds + 0(dS^2)}{AdS} \right)$$

where $0(dS^2)$ are the terms of higher order than the first in dS and the differential volume element dV for the pillbox is written as AdS. Taking the indicated limit, the divergence of the velocity becomes in final form:

$$\text{div}\ \underset{\sim}{v} = \frac{v}{A}\ \frac{\partial A}{\partial S} + \frac{\partial v}{\partial S}\ .$$

Given this expression for the divergence, the continuity equation 4-4 becomes

$$\frac{\partial \rho}{\partial t} + v \frac{\partial \rho}{\partial S} + \frac{\rho v}{A} \frac{\partial A}{\partial S} + \rho \frac{\partial v}{\partial S} = 0 \; . \qquad (4\text{-}5)$$

From the basic definition of the magnetic flux tube, the cross sectional area is inversely proportional to the magnitude of the magnetic induction. Therefore

$$\frac{dB}{B} + \frac{dA}{A} = 0$$

or

$$\frac{1}{A} \frac{\partial A}{\partial S} = - \frac{1}{B} \frac{\partial B}{\partial S} \; .$$

Using this in equation 4-5, the continuity equation takes the form

$$\frac{\partial \rho}{\partial t} + v \frac{\partial \rho}{\partial S} + \rho \frac{\partial v}{\partial S} = \frac{\rho v}{B} \frac{\partial B}{\partial S} \; . \qquad (4\text{-}6)$$

Using subscript notation to denote partial differentiation, defining a pressure $p = n \, k \, T$ and noting that $g = \frac{-\partial V_g}{\partial S}$, Euler's equation (equation 4-3) and the continuity equation 4-6 can be written in the following compact forms:

$$\rho v_t + \rho v v_S + p_S = -g \rho$$

and $\qquad\qquad\qquad\qquad\qquad\qquad\qquad\qquad\qquad (4\text{-}7)$

$$\rho_t + v \rho_S + \rho v_S = \frac{\rho v}{B} B_S \; .$$

It should be emphasized that p is not a real thermal proton pressure. It corresponds to the force of the parallel electric field acting on the protons. The protons are considered as cold and therefore have no internal thermal pressure. This latter assumption is true only

for the preshock protons (i.e., protons on the earth side of the shock). Passage through the shock will thermalize the protons and hence require a real pressure component. This situation will be investigated in subsequent sections.

A sound speed c can be defined for the proton flow by the usual relationship $c^2 = \frac{dP}{d\rho}$. Since the electron temperature T remains constant, $c^2 = \frac{kT}{M}$ = constant in the present model. Also incorporating the magnetic field terms into one symbol $F = \frac{1}{B}\frac{\partial B}{\partial S}$ for convenience, the equations of flow 4-6 can be written as

$$\rho v_t + \rho v v_S + c^2 \rho_S = -\rho g$$

and   (4-7)

$$\rho_t + v\rho_S + \rho v_S = \rho v F \ .$$

These equations are identical in form to the one dimensional isentropic equations of fluid dynamics with the addition of an external gravitational field and a varying channel width. It now remains to set up a method of solution and the appropriate boundary conditions for the set of equations 4-7.

4.3 Solution of the Fluid Equations

The system of equations 4-7 is a system of quasilinear partial differential equations of the first order for the two dependent variables v and ρ which are functions of the two independent variables t and S. Before a method of solution can be found, it must be determined whether this system of equations is elliptic, parabolic or hyperbolic.

For a system of two equations with the general form

$$L_1 = A_1 \rho_S + B_1 \rho_t + C_1 v_S + D_1 v_t + E_1 = 0$$

$$(4\text{-}8)$$

$$L_2 = A_2 \rho_S + B_2 \rho_t + C_2 v_S + D_2 v_t + E_2 = 0$$

the nature of the equations is elliptic, parabolic or hyperbolic depending on whether the quantity $ac - b^2$ is greater than, equal to, or less than zero respectively, where the quantities a, b, and c are defined by $a = [AC]$, $2b = [AD]$, and $c = [BD]$ with the abbreviation $[XY] = X_1 Y_2 - X_2 Y_2$. The derivation of this relation can be found in "Supersonic Flow and Shock Waves" by R. Courant and K. O. Friedrichs (Interscience Publishers), Chapter II, Section 22.

The factors a, b, and c are easily determined by comparing equations 4-8 with 4-7. A small manipulation then yields $ac - b^2 = -\rho^2 c^2$ which is always negative. Therefore, the proton flow equations 4-7 are always hyperbolic -- in both the supersonic and subsonic domains. Thus, the notion of characteristics may be used to solve these equations.

A characteristic direction represented by the ratio $t_\sigma : S_\sigma$ where t and s are functions of σ alone is defined as such a direction in which there exists a linear combination of L_1 and L_2 (equations 4-8) for which the derivatives of v and ρ are in the _same_ characteristic direction. For the special case of equations 4-7, the characteristic equations are directly obtainable. Form a linear combination of these two equations:

$$v_t + v v_S + \frac{c^2 \rho_S}{\rho} + g + \lambda (\rho_t + v \rho_S + \rho v_S - \rho v F) = 0.$$

Rearranging terms, this becomes

$$v_t + (v + \lambda\rho) v_S + \lambda\rho_t + (\lambda v + \frac{c^2}{\rho}) \rho_S - \lambda\rho vF = -g \ . \qquad (4-9)$$

The conditions for which equation 4-9 involves the derivatives u_σ, ρ_σ of u and ρ in only one direction given by (t_σ, S_σ) is then evidently

$$S_\sigma = (v + \lambda\rho) t_\sigma \qquad \text{and} \qquad \lambda S_\sigma = (\lambda v + \frac{c^2}{\rho}) t_\sigma \ .$$

Therefore, two values exist for the multiplicative factor λ:

$$\lambda = \pm \frac{c}{\rho} \ ,$$

and hence, there are two characteristic directions for the flow equations which are given by

$$S_\alpha = (v + c) t_\alpha \quad \text{and} \quad S_\beta = (v - c) t_\beta \quad . \qquad (4-10)$$

The corresponding characteristic equations for ρ and v are found from 4-9 to be

$$v_\alpha + \frac{c}{\rho} \rho_\alpha - cvFt_\alpha + gt_\alpha = 0$$

and $\qquad\qquad\qquad\qquad\qquad\qquad\qquad\qquad\qquad\qquad\qquad\qquad\qquad\quad$ (4-11)

$$v_\beta - \frac{c}{\rho} \rho_\beta + cvFt_\beta + gt_\beta = 0 \ .$$

where $F = \frac{1}{B} \frac{\partial B}{\partial S}$, c, and the gravitational acceleration g are known quantities.

The four characteristic equations replace the original two flow equations 4-7. The value of the characteristic equations lies in their simple form. Each equation contains derivatives with

respect to only one of the two new independent parameters (α and β)
and the coefficients do not depend on these parameters.

If the external force of gravity and the magnetic field
term F were zero, the derivatives of t in equations 4-11 would not
be present and the ρ-v characteristics could be obtained explicitly
(for a thorough analysis of the force free one dimensional isentropic
flow see Courant and Freidrich's text). In the present model, the
derivatives of t are present and the method of finite differences
must be used to solve the characteristic equations 4-10 and 4-11.

Assume that values of ρ and v are specified along some bound-
ary curve (this curve cannot be a characteristic) in S-t space (see
Figure 31). Then the directions of the characteristic curves
(equations 4-10) passing through the boundary curve are known at
the boundary. Assuming that the velocity varies slowly near the
boundary, the characteristics can be approximated by the straight
lines $\frac{dS}{dt} = v_a - c$ (β characteristic) and $\frac{dS}{dt} = v_b + c$ (α charac-
teristic), where the velocity v_d corresponds to the velocity speci-
fied at the point (S_d, t_d) on the boundary curve and where the
English alphabetic subscripts denote boundary conditions and not
partial differentiation. Since differentiation is to be denoted
explicitly in the work to follow, this change of notation should
cause no difficulty.

Consider a point (S,t) near the boundary curve. This point
is crossed by an α characteristic and by a β characteristic. If the
point is sufficiently close to the boundary, these characteristics
can be taken to be two of the linear segments defined in the previous
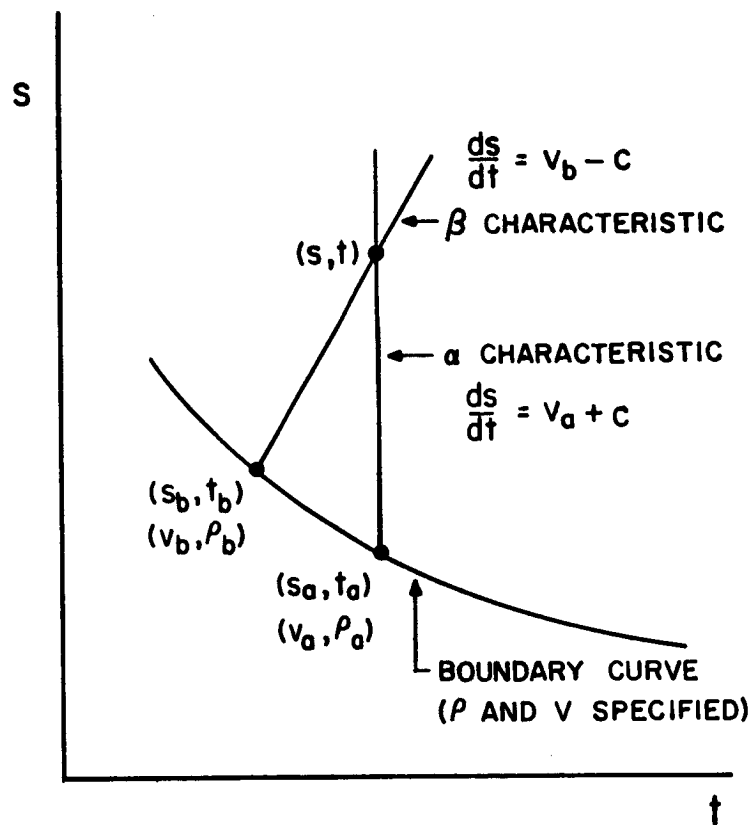
FIGURE 31. LINEAR CHARACTERISTICS

paragraph. Figure 31 shows a construction of an α and a β characteristic intersecting at the point (S,t).

The first of equations 4-11 is valid only along an α characteristic in S-t space. Therefore, the finite difference form of this equation is determined by considering the change in variables between the points (S,t) and (S_a,t_a) which are the endpoints of the linearized α characteristic. The finite difference form of this equation is therefore written

$$v - v_a + \frac{c}{\rho_a} (\rho - \rho_a) - (cv_a\bar{F}_a - \bar{g}_a)(t - t_a) = 0 \qquad (4\text{-}12)$$

where the subscripts denote boundary values and the quantities $\bar{F}_a$ and $\bar{g}_a$ represent values of F and g determined at the midpoint of the α characteristic (i.e., at $(S + S_a)/2$). The unsubscripted variables denote conditions at the point (S,t). Similarly, the finite difference form for the second of equations 4-11 along the β characteristic is

$$v - v_b - \frac{c}{\rho_b} (\rho - \rho_b) + (cv_b\bar{F}_b + \bar{g}_b)(t - t_b) = 0. \qquad (4\text{-}13)$$

Equations 4-12 and 4-13 are two simultaneous equations for the unknowns ρ and v at the point (S,t). Solving these equations for ρ and v yields:

$$v(\rho_a + \rho_b) = \rho_a[v_a + c + (cv\bar{F}_a - \bar{g}_a)(t - t_a)] +$$

$$\rho_b[v_b - c - (cvF_b + g_b)(t - t_b)] \qquad (4\text{-}14)$$

and

$$\rho = \frac{\rho_a \rho_b}{c(\rho_a + \rho_b)} [v_a - v_b + 2c + (cv_a \bar{F}_a - \bar{g}_a)(t - t_a) +$$

$$(cv_b \bar{F}_b + \bar{g}_b)(t - t_b)] . \qquad (4-15)$$

The finite difference forms of the linearized S-t characteristics discussed previously are

$$S - S_a = (v_a + c)(t - t_a) \text{ for the } \alpha \text{ characteristic}$$

and $\qquad\qquad\qquad\qquad\qquad\qquad\qquad\qquad\qquad\qquad\qquad\qquad$ (4-16)

$$S - S_b = (v_b - c)(t - t_b) \text{ for the } \beta \text{ characteristic.}$$

Given an appropriate boundary curve on which the quantities ρ and v are specified, the values of ρ and v at all points adjacent to the boundary are determined as follows. First, a point (S,t) is specified at which a solution is desired. Equations 4-16 are then used to determine at which points the characteristics passing through (S,t) pass through the boundary. This can easily be done if the boundary curve is the curve S = constant or t = constant as it shall be in the model under consideration (see the next section). Since the characteristics' endpoints are now known, the magnetic field and gravitational quantities $\bar{F}$ and $\bar{g}$ appearing in equations 4-12 and 4-13 can be determined. Equations 4-12 and 4-13 then determine uniquely (assuming no shocks develop) the values of the proton density and velocity at a point (S,t) near the boundary curve.

A more accurate solution can be obtained by an iterative technique. Having found v and ρ in the manner described previously at the point (S,t), a more accurate solution at the same point is

obtained by considering the characteristics of equations 4-16 with the boundary point velocities replaced by the average of the boundary velocity and the newly determined velocity. A solution is then obtained using these new characteristic directions. This solution can then be used to modify the slopes and obtain a still more accurate solution. When performing this iterative technique, care must also be taken that the density and velocity terms in the characteristic finite difference equations which did not arise from differentiation be replaced by the average values calculated. In the actual numerical computations performed for this plasma model only two iterations were performed due to the exceedingly long computing time required.

4.4 Physical Parameters and Boundary Conditions

The flow equations 4-7 were developed as part of a model which, it is believed, characterizes the nature of plasma flow along a closed magnetospheric field line which reconnected at the night side of the earth and is convected towards the day side. However, the derivation of these flow equations in section 4-2 was done without specifying the exact nature of the magnetic field configuration and the acceleration term g. These equations are therefore valid for the general case in which a cold proton stream moves with the thermal electron background along the direction of the magnetic field and under the influence of a parallel electric field and an external force characterized by the acceleration g (it is implicitly assumed that the plasma is of very low density). The boundary conditions required for a solution of the equations must therefore be chosen with a definite magnetic and gravitational field configuration in mind.

A magnetic flux tube immediately after reconnection on the night side is of concern here. Initially there is a net flow of protons of assumed constant speed 4.47 km/sec (see section 4.1) upwards along the field direction from both hemispheres. These streams meet at the equator (see top of Figure 32) to form shocks which then move along the flux tube towards the polar regions. The protons on the earth side of the shock are cold and therefore described by the previously developed flow equations. The solution on the earth side of the shock is not affected by the shock itself. However, the protons on the equator side have passed through the shock and are no longer cold particles and therefore do not satisfy the developed equations. Since the flow on the earth side of the shock is unaffected by the shock itself, the cold proton solution can be determined along one-half of the flux tube (only half of the flux tube is needed due to the assumed symmetry about the equatorial plane) as a function of time and after the shock path is determined the cold proton solution on the earth side can be retained.

The cold proton flow along an open flux tube of the type shown on the bottom of Figure 32 will actually be considered. A dipolar flux tube section from one of the polar regions to the equator becomes a tube of nonvarying cross section (i.e., B remains constant) on the opposite side of the equatorial plane. The constant area section, it will be seen, has no influence on the flow along the dipolar part of this flux tube. This open field line solution, it must be noted, has no bearing on the day side models
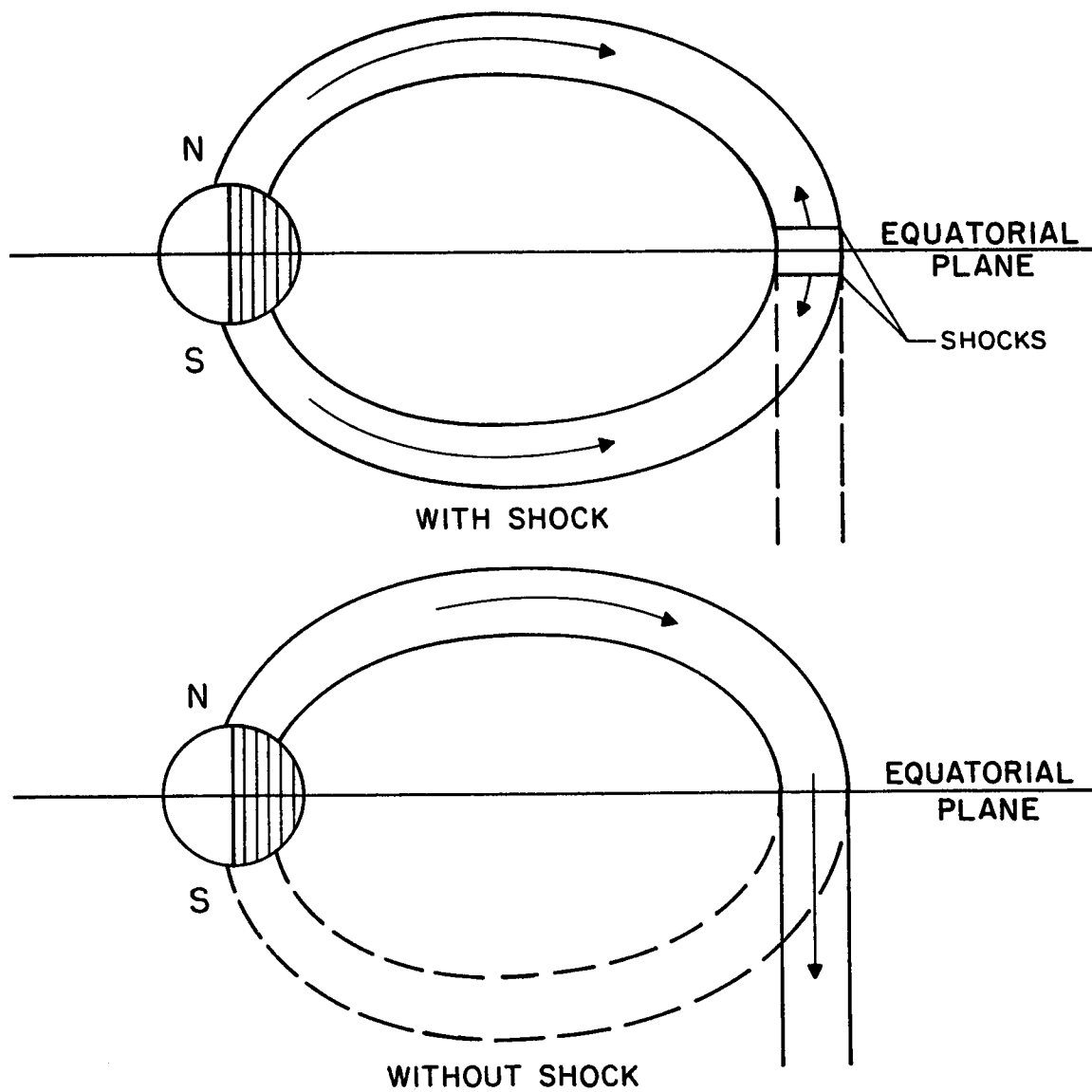
FIGURE 32. FLUX TUBE MODEL

developed previously due to the assumed absence of protons moving

towards the earth in the present model.

After reconnection, the closed field line and its associated

plasma moves around the earth to the day side. Due to this circula-

tion it may seem appropriate that an outward centrifugal force be

included in the flow equations. However, because it is not presently

known at what rate the circulation takes place and because the dif-

ferent parts of the field line may rotate about the earth with dif-

ferent angular velocities, whereas a nonchanging field configuration

is assumed here, it was decided not to include this term in the fluid

equations developed for the cold protons. The effects of this force

will be discussed qualitatively later as a decrease in the downward

gravitational acceleration.

The circulation of plasma in the outer magnetosphere occurs in

the trough region (see Chapter I). Therefore, it is imperative that

the magnetic field line chosen for the proposed model lie beyond

four or five earth radii at the equatorial crossing point. A di-

polar field line which intersects the earth at a latitude of 67° was

chosen -- its geocentric distance at the equatorial crossing point

is 6.55 earth radii. The exact formulas for the variation of the

magnetic induction and its gradient along this dipolar field line

are found in the appendix along with the component of gravitational

acceleration parallel to the field direction.

Using the method of characteristics to solve the quasilinear

partial differential flow equations 4-7 requires stipulation of the

velocity and proton density along a noncharacteristic boundary curve

in S-t space. A natural choice for the boundary curve is the broken

line formed by the S axis and a line parallel to the t axis which

passes through $S = S_o$, where S_o is the distance along the field line

from the surface of the earth to the chosen base level of the line

of force. Physically, this corresponds to specifying the proton den-

sity and velocity at every point along the field line at time $t = 0$

(immediately after reconnection) and specifying these quantities at

the base level as a function of time. The base level at S_o must be

chosen at a high enough altitude so that protons are the dominant

positive ion. This is required because a neutral proton-electron

plasma was assumed in deriving the flow equations. The value $S_o =$

1,400 km satisfies this criterion and will be used in the calculations

to follow.

It is now to be shown qualitatively that such boundary con-

ditions will be sufficient to determine the flow parameters along the

entire field line, if chosen properly. Initially (i.e., at $t = 0$)

the proton velocity is assumed to be directed away from the earth

with a constant magnitude of 4.47 km/sec along the field line. It is

to be remembered that unless otherwise stipulated, the field line

referred to is the open line of Figure 32. Since the sound speed c

is defined by $c^2 = \frac{kT}{M}$ and the characteristic electron temperature is

$2000^{\circ}K$, the numerical value of the speed of sound is 4.06 km/sec.

Thus, the initial flow is "supersonic" and the characteristics

(equations 4-10) have the general form shown in Figure 33 for the two

characteristics emerging from the base level at $t = 0$. The
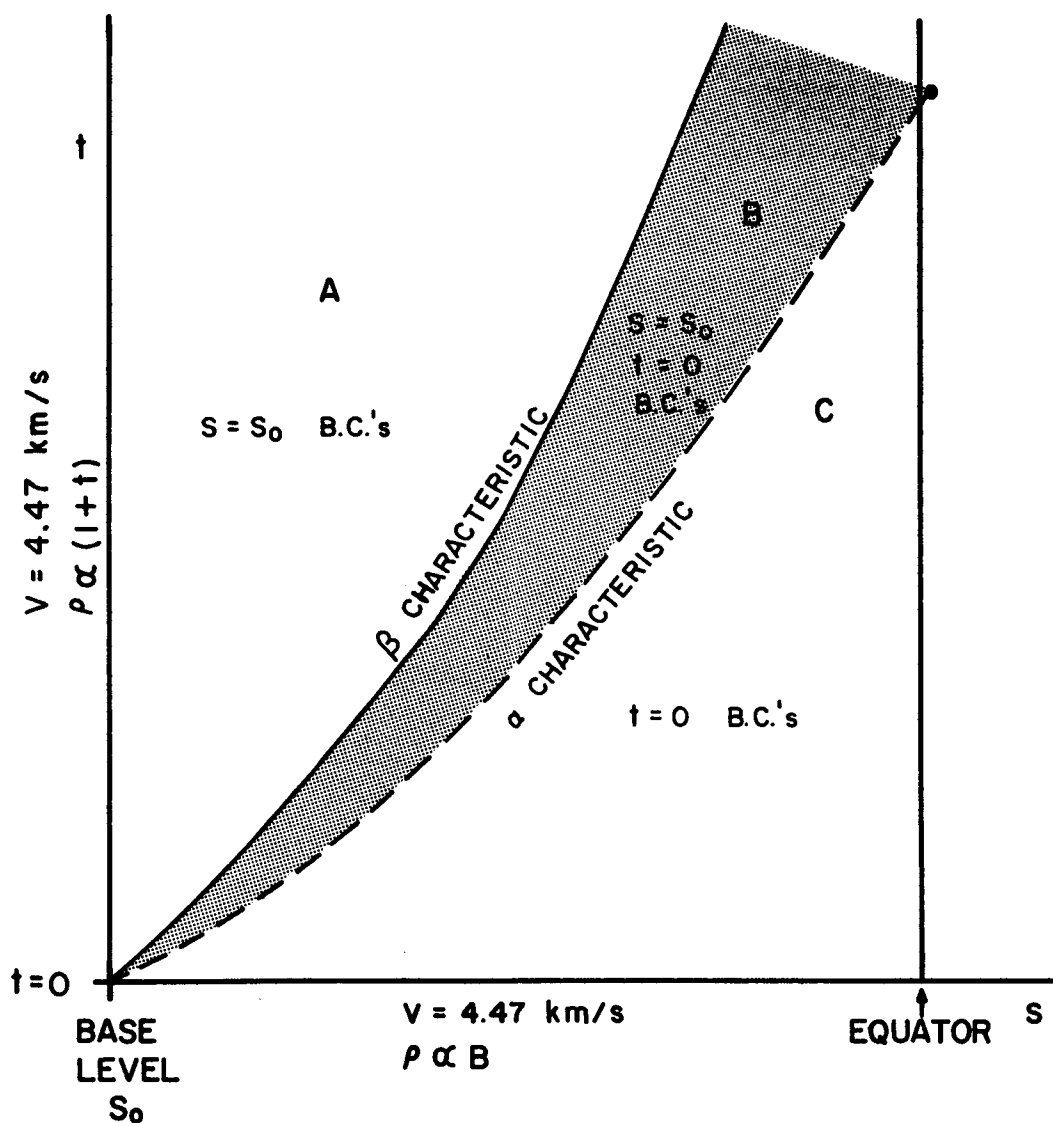
FIGURE 33. BOUNDARY CONDITIONS

characteristics plotted are only approximate. The flow equations must
be solved to determine the exact nature of these curves.

The specification of proton density along the field line at
t = 0 should be made from experimental data. However, the data avail-
able is insufficient for this purpose. Therefore, an assumed profile
must be used. Since the closed field line lies in the magnetospheric
trough region, the density at the equator should be very small. A
value of one proton/cc at the equator agrees with the observed whis-
tler data (Carpenter, 1966). In the polar regions, densities as low
as 300/cc have been found at altitudes near 1000 km (Taylor et al.,
1967). Taking the density as directly proportional to the magnetic
induction along the considered field line (67° base latitude) and
assuming the density at the equatorial crossing point is one proton/cc,
the density at S_{o} is of the order of magnitude of 300/cc. Therefore,
the variation of the density along the field line initially is assumed
proportional to the magnetic field.

As the closed dipole field line and its associated plasma move
toward the day side of the earth, the base level proton density in-
creases due to increased photoionization at and below the base level.
This increase is assumed to be a linear function of the time in hours.
That is $n = n_{o} (1 + t$ (in hours)). A more realistic model may have
an exponential increase in density superimposed on this variation to
correspond to possible very rapid increases at sunrise. The more
gradual increase may restrict the validity of the proposed model to
the night part of the circulation cycle. The velocity at the base

level is assumed constant at the previously calculated speed of 4.47 km/sec.

If all of the characteristics in S-t space have the same form as the two characteristics emanating from the origin in Figure 33, all of S-t space can be covered by a net of characteristics. If shocks do not develop, no two α characteristics will ever intersect one another and no two β characteristics will intersect one another. In such a case the flow profile can be calculated uniquely along the field line as a function of time by means of the scheme of integration developed in the previous section with the boundary conditions indicated. The three spatial regions A, B and C in Figure 33 indicate points which are determined by the boundary conditions at S_o alone, by boundary conditions on both axes near their intersection, and by boundary conditions on the t = 0 axis alone, respectively.

Should shocks develop from compression waves, similar characteristics will intersect and at the intersection points the method of characteristics will not yield unique solutions to the flow equations. Methods for calculating the development of shocks from compression waves can be found in Courant and Friedrichs' text (1948).

As long as the flow remains supersonic, the slopes dt/dS of both types of characteristics remain positive. Therefore, in the open flux tube which has a constant cross section beyond the equator, the developing waves will propagate away from the dipolar segment into interplanetary space. Conditions on the constant field portion do not propagate towards the earth. Therefore, the solution on the dipolar portion of the open field line is identical to the solution

of the cold proton flow along the closed field line. It now remains

to determine the actual development of the proton flow velocity and

density along the open field line with the boundary conditions

developed in this section.

4.5 Numerical Solution of Flow

The numerical technique described in section 4.3 is applied

to the boundary conditions described in the previous section to

determine the flow development. Numerical computations were perform-

ed on the IBM 360 Computer at the Pennsylvania State University.

In a flow problem of this nature, the most natural pattern

of iteration is to determine the density and velocity profiles along

the entire field line at specified times. That is, from the bound-

ary conditions specified in the previous section, the flow is deter-

mined at all points on the straight line $t = \Delta t$ in S-t space. These

new values are then used to determine the solutions on the line

$t = 2\Delta t$, and so forth.

Preliminary computations using this scheme with the finite

difference solution developed in section 4.3 showed that the largest

time interval Δt which could be used without yielding spurious dis-

continuities, due to a failure of the approximation of the deriva-

tives by finite differences, was 0.2 minutes. This value was used

in the computations. The distance between points on the line

$t = $ constant at which the flow variables were determined was taken

as 0.04 earth radii. This spatial separation corresponds to

division of the considered 67° dipole field line into 200 parts

between the base level and the equator.

The computing time required for the complete determination of the flow along the dipole part of the open field line at a given time, from the data determined at a time Δt earlier and/or the prescribed boundary conditions was approximately 30 seconds.

The resulting density and proton velocity profiles along the dipolar part of the considered open field line appear in Figure 34 and Figure 35 respectively for a time period of four hours. Further computations were not performed due to the formation of a shock discontinuity at the base shortly after four hours which propagates toward the equator and requires a treatment different than the flow solution used.

This shock formation appears in the density profile as a rapid rise in proton density with altitude just above the base level followed by a rapid spatial decrease. The velocity, on the other hand, tends to approach the speed of sound (4.06 km/sec) as its minimum value. As the velocity approached the speed of sound, similar characteristics began to approach one another until at the speed of sound they intersected, yielding a multiple valued solution indicative of a shock. When formed, this shock will probably be driven along the field direction towards the equator.

Since there are shocks hypothesized initially at the equator on the closed field line, it appears that further computations may involve the almost impossible numerical problem of determining the time development of the interactions between four shocks (remember that shocks form in both hemispheres on the closed field line). If the equatorially generated shocks, on the closed field line,
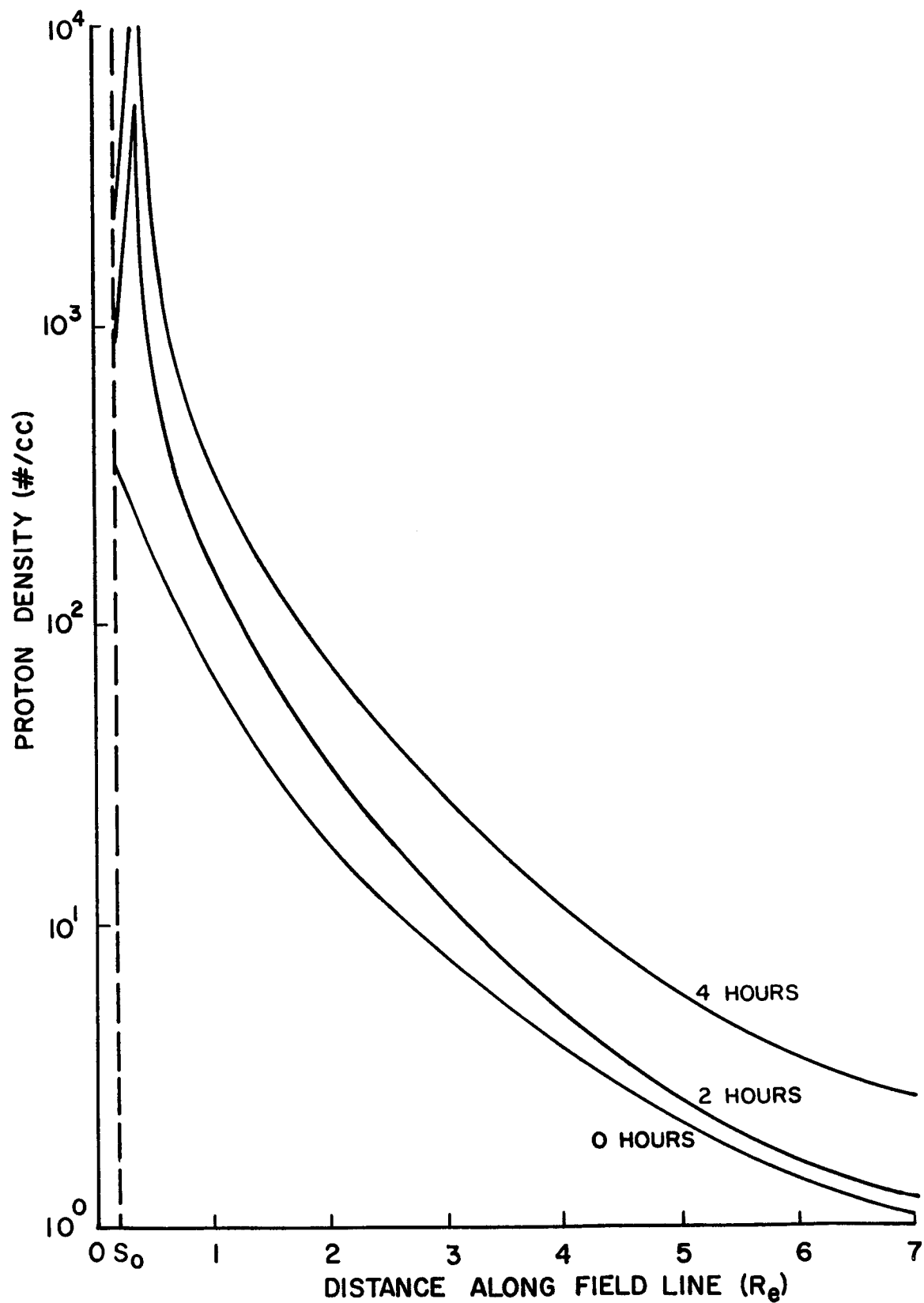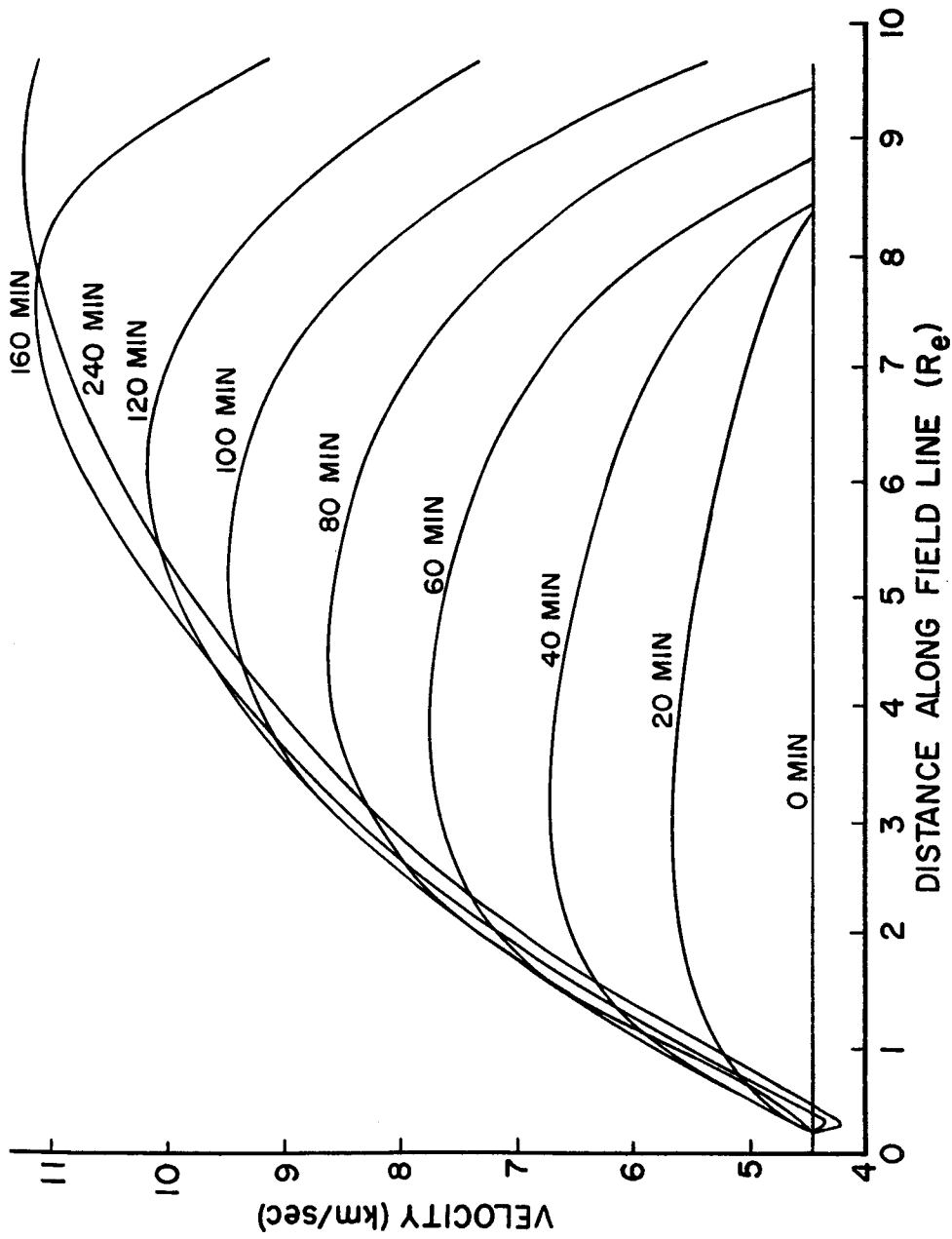
FIGURE 34. DEVELOPMENT OF DENSITY PROFILE

FIGURE 35. VELOCITY PROFILE DEVELOPMENT

however, should reach the earth before the shocks form at the base

levels, they may disturb the medium enough so that these shocks do not

form. In fact, it appears that this will happen, so that it is not

necessary to develop the motion of this base generated shock further.

Also, it is to be seen that the formation of this shock is due mainly

to the geometry chosen. Therefore, it may not really occur in a more

realistic model.

That the proton velocity should tend to decrease with altitude

to a minimum value and then increase with altitude at heights above

the point of the minimum is reasonable can be seen most readily from

an examination of the steady state flow equations. From equations

4-7, the time independent equations describing the proton flow are:

$$v \frac{\partial v}{\partial S} = -\frac{1}{\rho} \frac{\partial P}{\partial S} - g$$

and   (4-17)

$$v \frac{\partial \rho}{\partial S} + \rho \frac{\partial v}{\partial S} = \frac{\rho v}{B} \frac{\partial B}{\partial S}$$

where p = nkT as defined previously.

Integration of the second of equations 4-17 yields $\rho v \sim B$. Sub-

stituting this result into the first equation and using the definition

of the speed of sound $c^2 = \frac{dp}{dS}$ yields the following equation after a

few manipulations:

$$(v - \frac{c^2}{v}) \frac{dv}{dS} = -\frac{c^2}{B} \frac{\partial B}{\partial S} - g \; .$$ (4-18)

For a dipole field line which intersects the earth at a latitude

of 67° (see the appendix for the field equation) and a sound speed of

4.06 km/sec, the right hand side of equation 4-18 is negative below
approximately 0.3 Re, zero at 0.3 Re and positive at distances along
the field line greater than this. Therefore, considering the left
hand side of the equation, it is seen that at altitudes below this
critical point the velocity v decreases with increasing altitude if
it is supersonic (as is assumed in the model presented). Above the
critical point the velocity must remain supersonic if the speed is
supersonic at the critical point. Therefore, the velocity above the
critical distance from the earth increases with increasing altitude
according to equation 4-18. The time dependent analysis shows this
tendency near the base level. These results are indicative of flow
in a channel with a throat (see Liepmann and Roshko; 1957). The
expanding flux tube in the present case is effectively constricted
near the base level by the gravitational force. Time independent
computations of this nature have been applied also to describe the
hydromagnetic expansion of the solar corona (Parker, 1963).

Having explained the results near the base of the field line,
it remains to describe the physics of the situation above the
critical point. The proton density increases with time as expected
due to the continual movement of plasma upwards along the field line
from the base regions.

The protons (Figure 35) are accelerated along the field line
away from the earth. This acceleration is due to the upwardly
directed parallel electric field present (the upward force exerted
on a proton due to the parallel electric field present is propor-
tional to $-\frac{1}{n}\frac{\partial n}{\partial S}$ -- see equation 4-1). It is expected from the

previous analysis of the time stationary equations that the accelera-
tion should be directed away from the earth because a supersonic flow
in the region above the critical point implies an increase of velocity
with altitude.

After a time period of approximately three hours, the increase
of velocity at stationary points far above the base level no longer
occurs. This transition is due to the fact that the electric field
will drive the protons in such a manner as to reduce the field magni-
tude. Also the deceleration of particles at the critical point
yields a source of particles of lower initial velocities for the
distant regions.

The velocity profiles of the protons (Figure 35) steepen with
time as they propagate away from the equator (the equator is located
at a distance of 8.03 Re along the field line from the earth) along
the constant field portion of the open field line into interplanetary
space. This corresponds to a compression wave which will eventually
form a shock traveling away from the earth into a medium character-
ized by a constant density and velocity. (Initially, it was assumed
that $v = 4.47$ km/sec everywhere on the open field line and that
$n = 1$ proton/cc at the equator and beyond.)

Now that the flow has been determined on the open field line,
the shocks hypothesized at the equator on a closed field line after
reconnection (see Figure 32) can be considered since the above re-
sults remain valid in the regions corresponding to the earth sides
of the shocks in both hemispheres.

4.6 Shock Relations

The hypothesized discontinuity of velocity at the equator, corresponding to a collision of proton streams traveling with constant velocities along the considered field line away from the earth is to be considered now. Due to the symmetry of the problem, it is expected that two shocks will form at the equator -- each to travel along the field line, away from the equator, towards the polar regions, as the field line circulates towards the day side of the earth. Due to the symmetry about the equator, only one shock is to be treated. The motion of the other shock is determined by a simple reflection through the equatorial plane.

Since a symmetrical model is to be developed, it is imperative that the velocity of the proton flow at the equator vanish. This condition is required for a solution as will be seen in the work to follow.

The shock discontinuity propagates towards the earth along the dipole field line. The shock motion and the corresponding terminology commonly used to describe it are drawn in Figure 36. As the shock propagates down the tube, it meets a plasma characterized by the subscript o, which passes through the shock and emerges on the downstream side of the shock with new flow variables which will be indicated by a 1 subscript. In passing through the shock, the entropy of the plasma flow increases. This entropy increase is a conversion of ordered energy into thermal energy in the present model since it had been assumed previously that the protons flowing upwards from
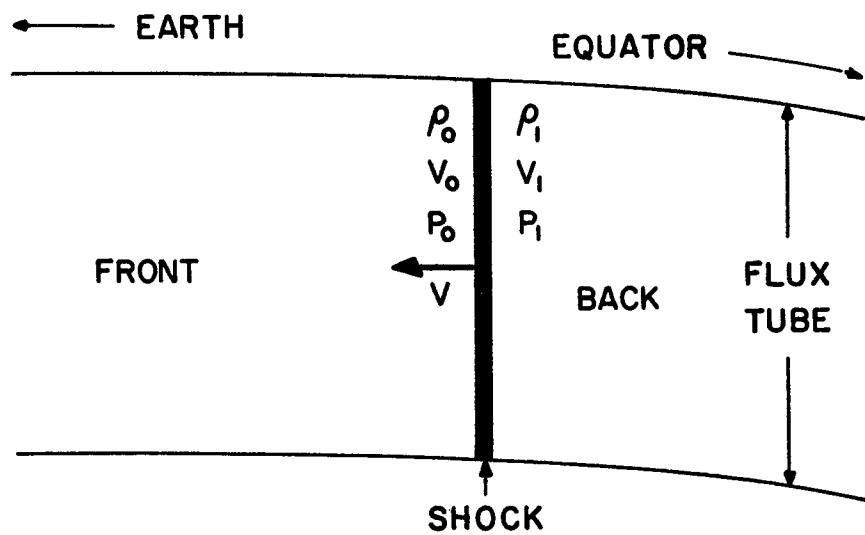
FIGURE 36.   SHOCK VARIABLES

the earth were cold. A thorough analysis of the effect of a shock

on the entropy can be found in the text of Courant and Friedrichs.

Since time varying boundary conditions were imposed at the

base of the circulating field line, it follows that the shock veloc-

ity as well as the medium behind the shock is dependent on time. It

shall be assumed, however, that the shock is thin enough so that the

change in flow variables can be considered instantaneous and the

shock motion regarded as quasistatic.

Given the shock velocity V (positive away from the earth) and

the pressure p_o, proton flow velocity v_o, and the density ρ_o adjacent

to the shock on the earth side (given the shock location and time,

these flow parameters can be determined from the flow profiles de-

veloped in the previous section), it is desired to have a set of

relations which can be used to determine the plasma variables adja-

cent to the shock on the backside (i.e., the equator side). These

relations are determined by the conservation equations across the

shock.

In the frame of reference in which the shock is stationary

the velocity of the plasma flow is u = v-V where v is a plasma

velocity at the shock in a frame of reference fixed in the plane of

the circulating dipole field line. Subscripts on u and v will in-

dicate whether pre- or postshock velocities are meant. The conser-

vation laws are to be determined in this frame of reference of the

shock.

First consider the mass flow through the shock. Since no ions

are created inside the shock, the proton number flux and the proton

mass flux remain unchanged across the shock. Therefore the conservation law is written

$$\rho_1 u_1 = \rho_o u_o .$$ (4-19)

The proton momentum is changed in passing through the shock due to a difference in the forces acting on the protons upstream and downstream of the shock. Upstream of the shock, there is an effective pressure acting on the protons of $p_o = n_o kT$, which is the electrical force. On the downstream side there is also a thermal pressure component p_t. Therefore, the change in momentum flux across the shock is equated to the pressure difference across the shock. That is,

$$\rho_1 v_1 u_1 - \rho_o v_o u_o = p_o - p_1$$ (4-20)

where $p_o = n_o kT$ and $p_1 = n_1 kT + p_t$ and T is the constant electron temperature.

Since the electron temperature is assumed constant across the shock there will be no change in the internal energy of the electrons (see section 4-1). Also, due to charge neutrality, no electrical potential energy is carried across the shock. On the other hand, the cold protons become thermalized in passing through the shock. The proton energy change is due to the net power applied at the shock. The equation of conservation of energy across the shock can be written as

$$\rho_1 \left(\frac{1}{2} v_1^2 + e_1\right) u_1 - \rho_o \left(\frac{1}{2} v_o^2\right) u_o = p_o v_o - p_1 v_1$$

where e_1 is the internal energy per unit proton mass on the backside
of the shock. Assuming isentropy behind the shock with an adiabatic
index of 5/3, e_1 can be written as $3/2 \; p_t/\rho_1$ (Courant and Friedrichs,
1948). The energy equation can then be written

$$\rho_1 \; (\frac{1}{2} v_1^2 + \frac{3}{2} \frac{p_1}{\rho_1}) \; u_1 - \rho_0 \; (\frac{1}{2} v_0^2) \; u_0 = p_0 v_0 - $$
$$(\frac{\rho_1}{\rho_0} \; p_0 + p_t) \; v_1 \; . \tag{4-21}$$

The jump equations 4-19 to 4-21 are three equations for the
three unknown v_1, p_1, and ρ_1. Usually, in shock problems the shock
velocity is known and these three parameters are the only unknowns.
However, in the present nonsteady shock problem, the shock velocity is
not known. Therefore, the three conservation equations are not suf-
ficient to specify the shock motion. Another equation is needed.
For adiabatic flow behind the shock, as assumed, the pressure is re-
lated to the density by

$$p_t = A\rho_1^{5/3} \tag{4-22}$$

where A, in general, must satisfy

$$\frac{\partial A}{\partial t} + \underset{\sim}{v} \cdot \text{grad } A = 0$$

along the dipole field line from the earth. It now remains to solve
the shock relations for the shock motion and for conditions immedi-
ately behind the shock.

4.7 Shock Solutions

At time t = 0, when the shock is at the equator, the velocity v_1 of the plasma flow behind the shock vanishes -- this is expected due to the symmetry involved. Therefore, equations 4-19 through 4-22 are sufficient to determine p_1, ρ_1, V and A initially.

Substituting $v_1 = 0$ into equation 4-19 yields a relation between the density downstream and the shock velocity (the upstream quantities are known from the cold proton analysis of the previous section) at the equator:

$$\rho_1 = \frac{v_o - V}{-V} \rho_o .$$ (4-23)

From the momentum jump condition (4-20) the backside thermal pressure p_t is determined in terms of the shock velocity and the parameters on the earth side of the shock to be:

$$p_t = p_o \frac{v_o}{V} + \rho_o (v_o - V) v_o$$ (4-24)

where equation 4-23 was used to eliminate the density ρ_1.

The energy conservation jump condition (equation 4-21) at the equator initially is then solved for the shock velocity in terms of the known plasma parameters on the frontside using 4-23, 4-24 and the condition $v_1 = 0$. The equation for V turns out to be a quadratic equation with the solution

$$V = \frac{-B \pm \sqrt{B^2 - 4DC}}{2D}$$ (4-25)

where $D = \frac{3}{2} \rho_o v_o$, $B = -\rho_o v_o^2$, and $C = -\frac{5}{2} p_o v_o - \frac{\rho_o v_o^3}{2}$. There are two solutions for the shock velocity, but this causes no difficulty

because one of the solutions (the solution with the positive sign) will be seen to yield a negative thermal pressure p_t behind the shock and hence, can be ignored.

The initial conditions at the equator immediately after reconnection were set up in previous sections. Due to symmetry $v_1 = 0$ -- this relation was used to determine the above shock equations at the equator at time $t = 0$. The remaining initial conditions at the equator are that the proton density is 1/cc and the upward velocity on the earth side is 4.47 km/sec. Substituting these values in 4-23, 4-24 and 4-25 yields the parameters of the shock motion initially at the equator. The two shocks formed initially which move away from one another toward opposite hemispheres are thus found to have oppositely directed velocities of magnitude -4.54 km/sec (the minus sign denotes motion away from the equator towards the earth). The shocks initially are found to have a backside density which is 1.98/ cc. That is, the density is increased by a factor of approximately two in passing through the shock in the direction of flow.

In the case of general isentropic flow behind the shock, the motion of the shock must be determined by solving equations 4-19 through 4-22 when the position of the shock and frontside conditions are known. Unfortunately, an explicit mathematical solution cannot be obtained in the general case except at the equator where the velocity v_1 vanishes. If v_1 is allowed to vary behind the shock as the shock moves towards the earth, the shock jump conditions must be solved in conjunction with the flow equations behind the shock. However, the proton flow equations behind the shock will not be

identical to the cold proton flow equations used to determine the

flow on the earth side of the shock. The sound speed c, for example,

defined as $\sqrt{\dfrac{dp}{d\rho}}$, will no longer be constant due to the addition

of a thermal component to the pressure which is not a linear function

of density. Another complication in the solution results because a

third characteristic which corresponds to the particle path in S-t space

must be used in addition to the alpha and beta characteristics de-

fined previously. This characteristic is needed whenever general

adiabatic flow is considered (see Courant and Friedrich's text).

These difficulties, in conjunction with the immense computing time

required for a numerical solution, precluded any attempt at a

solution in this general case.

Part of the ordered motion of the proton flow on the front

side of the shock is converted into thermal energy on the backside.

It shall be assumed that all of the ordered energy is converted into

thermal energy so that the plasma on the backside of the shock in

the earth's frame of reference has no ordered velocity. Thus, v_1

shall be assumed to vanish at all points behind the shock.

For vanishing v_1, equations 4-23 to 4-25 yield the shock

velocity and backside parameters as the shock moves along the

field line towards the earth. The numerical procedure to be follow-

ed is one of finite differences. The shock velocity V at the equator

has been determined. Therefore, in a small time interval Δt, the

shock will travel a distance $V\Delta t$ from the equator (a negative dis-

tance corresponding to a negative shock velocity just means that the

shock is moving away from the equator). This time interval is chosen

small enough so that the velocity of the shock does not change significantly in this interval. In the actual computations a time interval of one minute was used. In this interval of time, a particle of velocity 4.54 km/sec travels a distance of approximately 0.04 earth radii. After the new location of the shock is obtained, the preshock flow parameters at that point are determined from the cold proton flow results of section 4.5. Then the jump conditions for $v_1 = 0$ are solved with these values to determine the shock velocity V at this point. This iterative procedure is continued until the shock reaches the earth.

The resulting path of the shock in S-t space for complete thermalisation behind the shock is plotted in Figure 37 as a dashed line. The vertical scale for this curve is labeled on the right. Superimposed on this plot is the shock velocity (solid curve) as a function of the location of the shock on the field line. The slope of the shock path curve at any point is the shock velocity at that point and time. However, the scales required for the time and distance axes obscure the velocity changes -- hence, the inclusion of the explicit velocity curve. It is seen that the shock is initially accelerated in its motion towards the earth until it reaches approximately four earth radii from the base of the field line. At lower attitudes, the velocity is decelerated -- this deceleration is due to the fact that the proton flow velocity on the earth side of the shock in this region is itself decelerated (see Figure 35).

It can also be seen from Figure 37 that the shock reaches the surface of the earth in approximately three hours. Since it was
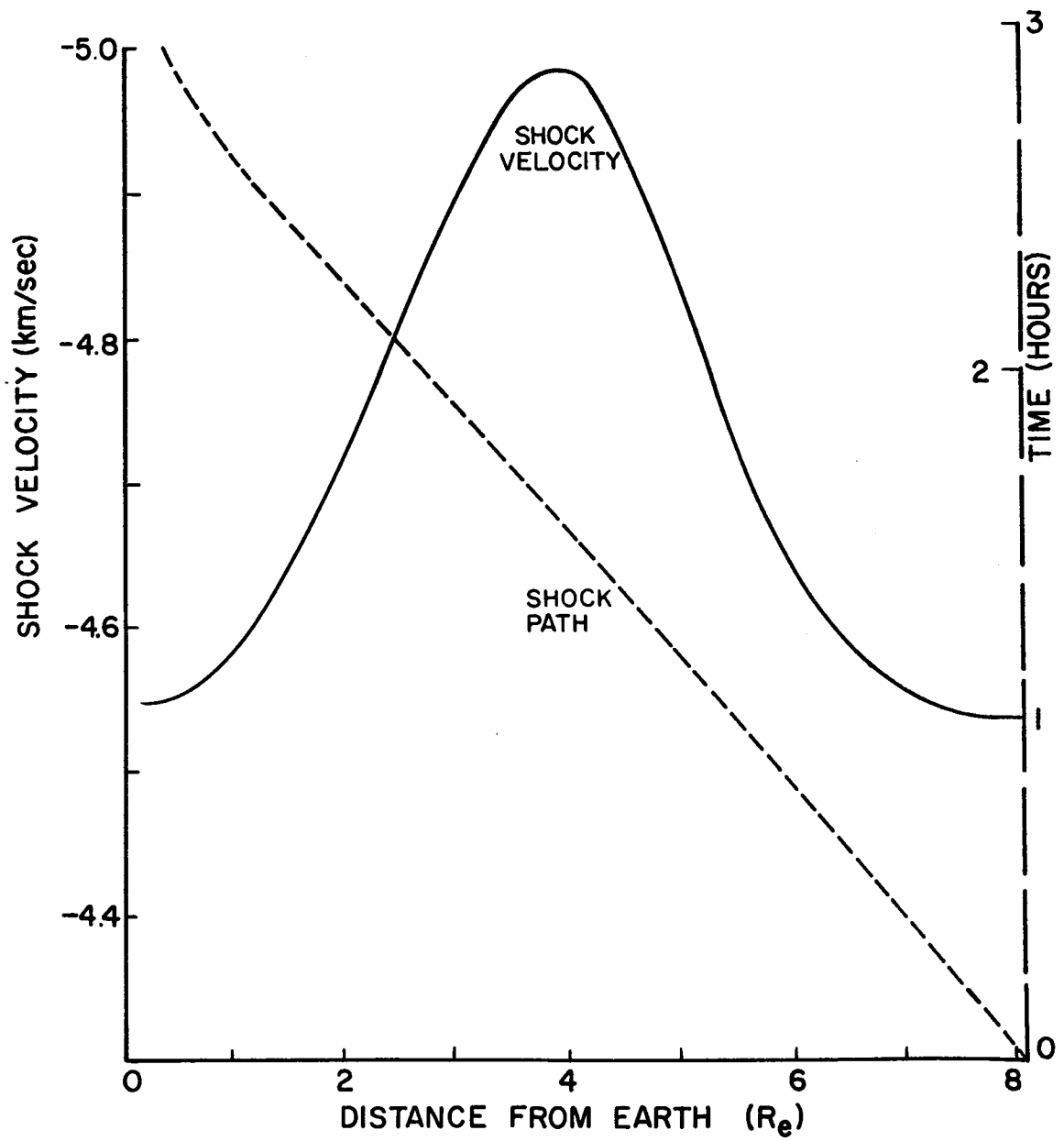
FIGURE 37.   SHOCK PATH AND VELOCITY

previously determined that a shock appears to be forming at the base

level at a time greater than three hours after reconnection, it is

seen that the equatorial generated shock will pass through the com-

pression wave at the base before this shock can form. This passage

may preclude the formation of the base level shock due to disturbance

of the medium by the downcoming discontinuity. Whether or not the

base level shock will form depends on a more critical evaluation of

the boundary conditions at the base level.

The passage of the equatorial shock itself through the base

level also creates a problem of consistency. The flow profile

generated on the backside of the shock is a time stationary profile.

Since the flow velocity is assumed to vanish at every point in this

region, there is no net motion of protons along the field line and

hence the density must remain time independent at any point behind

the shock. (However, there can be, and are, spatial variations of

density in this region.) When this shock passes through the base

level, it leaves a constant valued flow at the base. But a time

varying density was assumed at the base level as one of the bound-

ary conditions previously. Therefore there is an inconsistency

at the base level. This inconsistency is due to the many assumptions

made in the model without detailed physical structure. For example,

the density variation at the base level is determined by the rate

at which the sun's energy photoionizes the neutral particles at and

below the base level. This production will occur after the shock

passes,creating an actual time dependent variation. Thus, the

assumed nature of the shock must be modified in some manner by including this production term in a more rigorous model.

A more serious drawback to the boundary value problem at hand is that the density and velocity were specified at the base level as a function of time. This specification implicitly assumed the non-existence of a temporal discontinuity in the density and velocity at the base level. Therefore, these boundary conditions must be modified by considering the temporal discontinuity in the parameters at the base level due to the passage of the shock. A true boundary value specification will take into account the changes caused by the shock.

The stationary density configuration behind the shock at any time in its motion is a simple decrease from the value immediately on the backside of the shock to the minimum value of 1.98/cc at the equator. Due to the lack of any interesting structure in this variation, the density variation is not plotted.

4.8   Comments on Flow Problem

The flow of protons (and electrons) along closed field lines which circulate in the outer magnetosphere has been approximated by a mathematical model. The assumptions made in this model were many. Due to the lack of experimental data on the characteristics of the low energy plasma in the outer magnetosphere, many of the numerical parameters were specified rather arbitrarily. As more data becomes available, these parameters can be adjusted accordingly.

One of the critical assumptions made is that shocks of infinitesimal thickness form at the equator immediately after

reconnection. If viscosity plays an important part and is not limit-
ed severely by plasma instabilities, there will be no infinitesimal
shock but rather a finite region over which the flow variables change
continuously. Whether shocks actually exist or not in the low energy
plasma distribution along closed field lines in the outer magnetosphere
must be determined by satellite measurements. Should such discon-
tinuities not be found, it would indicate the possible existence of
a large longitudinal viscosity coefficient in the outer magnetosphere.
In such a case, the momentum and energy equations would have to be
solved with the viscosity terms included.

The most important need in this area of physics, at the present
time, is more satellite explorations of the low energy magnetospheric
plasma. Extensive satellite measurements are required in order to
accurately specify the boundary conditions and the initial conditions
of the proton flow, and in order to determine whether the many physi-
cal assumptions made in this dissertation are valid or not.

CHAPTER V

SUMMARY AND CONCLUSIONS

This work is a theoretical study of the motion of low energy plasma in the outer magnetosphere assuming Dungey's open model of the geomagnetic field configuration. The object of the study is to explore the distribution of low energy plasma expected in the open model. Such studies are required in order to determine what type of physical variations may be expected when actual satellite measurements are made of this medium. Also, there is a need, at the present time, to clearly define the problems which must be solved in order to obtain a clear understanding of the plasma processes which take place in this region. In order to make these studies, certain simplified plasma models are devised.

It was assumed that the electric field component parallel to the magnetic field direction is a conservative field. Therefore, the low energy plasma could be considered as frozen to the magnetic field lines in the outer magnetosphere, and the spatial distribution of plasma is determined by considering the evolution of the plasma motion along a line of force, which is followed through the circulation described in the introduction. That is, the motion of the plasma is considered in the one dimensional coordinate system along a field line and to this motion is to be superposed the independent motion in the direction perpendicular to the field direction. In this thesis the parallel motion is explored numerically; whereas, the perpendicular motion is only considered qualitatively. (Direct

experimental measurements of the electric fields and detailed mappings of the magnetic field configuration at high latitudes and high altitudes would be required in order to determine the validity of the frozen-in hypothesis and in order to determine accurately the morphology of the field line circulation.)

There are two distinct phases in the circulation cycle of such a magnetic field line: the open state and the closed state. Each phase requires a different physical model to describe the motion of plasma along the field line. The plasma along an open field line formed by interconnection on the day side of the earth is considered in Chapter II and Chapter III; whereas, a model of the plasma motion along a closed field line formed by reconnection on the night side is considered in Chapter IV.

At day side interconnection, the field line becomes open and forms a direct path by which magnetospheric charged particles can escape into the magnetosheath, and a path by which the hotter magnetosheath particles can enter the magnetosphere and eventually the polar ionosphere. Electrons of magnetosheath and magnetospheric origin, due to their high thermal velocities, rapidly interdiffuse along the entire length of the open field line. Hence, there should be a sharp latitudinal gradient of electron temperature at high altitudes across those geomagnetic field lines which pass through the day side neutral point (see Figure 4) due to the absence of the hot magnetosheath electrons on the closed field lines and due to the rapid traversal of the length of the open field line by these electrons. At low altitudes, this gradient will be much reduced

due to the large number of cooler electrons, of ionospheric origin, which are present.

In the outer magnetosphere the density of the low energy charged particles is very low and collisions can be ignored. In such a plasma electric field components parallel to the magnetic field lines may exist and must be considered in determining the motion of the plasma. The electrons due to their high thermal velocities can be considered in quasistatic equilibrium with the electrostatic potential at any point along the open field line. The proton motion, however, due to the protons' low velocities, must be determined by considering the past history of the parallel electric field.

A simplified model which may describe the proton motion along the open field line formed at interconnection is developed by approximating the velocity distribution function of the magnetospheric and magnetosheath protons by block functions. The parallel electric field which accelerates the protons is determined by using the principle of quasineutrality and the electron density-potential profiles derived from a consideration of the loss cones occupied by the electrons along the field lines. If the magnetosheath density is less than the magnetospheric density near the point of reconnection (i.e., near the neutral point) a parallel E field directed away from the earth developes in the interdiffusion region. This implies that there will be electrons on the open field line which are trapped between an electrical potential barrier near the magnetopause and the magnetic mirror near the earth. The existence of these trapped electrons were inferred from, but not included in the

computations of Chapter II. However, they were included in the computations of Chapter III, in which the electron density - potential profiles were derived at points along the open field line, under the reasonable assumption that the trapped electrons were of ionospheric origin. If the electron density distribution (or the proton density via quasineutrality) along an open field line in the magnetosphere were measured experimentally, these computed results could be used to obtain the variation of the parallel electric field along the field line.

The physics of the low energy plasma changes when the magnetic field line closes by reconnection on the night side. Considering the closed field line which is formed at reconnection, the particles of interplanetary origin are quickly lost in the ionosphere so that only charged particles of ionospheric origin are assumed to be on the closed field line. There is before reconnection a net outflow of protons from each hemisphere along the field direction. Therefore, on the closed field line formed by reconnection, these two streams of protons meet at the equator initially and the formation of a shock is postulated at the equator. To be precise, due to the assumed symmetry of the plasma motion about the equatorial plane, two shocks form -- one of which travels along the closed dipole field away from the equator towards the north pole region, and the other towards the south pole region.

Numerical solutions of the derived proton flow equations along the closed field line show that the protons are accelerated along the field line away from the earth by the parallel electric field present.

They are also accelerated upwards due to that fact that their velocity is initially supersonic (with respect to a sound speed characteristic of the problem) and the flow is in a diverging channel (i.e., a diverging magnetic flux tube).

The motion of the shocks is explored for the simple situation in which the ordered proton velocity is completely randomized by the passage of the shocks. It is found that the shocks will reach an altitude of 1000 km above the earth in the polar regions in a time period of approximately three hours after being formed at reconnection on the night side. The effects of the passage of such a shock would be a rapid spatial change of density and temperature of the low energy plasma.

Near the base levels of the closed field line formed by reconnection on the night side, compression waves develop which steepen into shocks approximately four hours after reconnection. These compression waves (and shocks) arise due to the supersonic flow of protons in a channel with an effective constriction near the base. The constriction (or throat as it is commonly called) forms due to the effect of gravity and is identical in nature to that which occurs near the sun and is responsible for the supersonic coronal expansion (Parker, 1963).

The computations of the motion of the equatorial formed shocks indicate that these shocks will reach the earth three hours after reconnection, assuming the proton flow is completely randomized by their passage. Hence, the compression waves formed at the base are destroyed by the downcoming shocks and shocks may never

form at the channel constrictions. However, if the assumed values
of the physical parameters used in the flow model should be found in
need of revision from experimental measurements, and if the motion
of shocks generated at the equator which do not completely thermalize
the proton motion is considered, a series of two or more traveling
disturbances in the form of interacting shocks may exist along the
closed field line at all times during the closed phase of the con-
vection cycle.

The model studies performed in this thesis are only initial
approaches to a complete understanding of the physics of the low
energy magnetospheric plasma. These studies have defined many of
the problems which must still be considered in this plasma medium.
It is suggested that further studies be undertaken as follows:

1. Extensive experimental measurements of the low energy
plasma density and energy distribution in the magnetosphere and in
the polar regions are needed in order to determine the exact forms
of the initial and boundary conditions applicable to the model
studies, and in order to evaluate the assumptions used in these
studies. The model studies indicate that the experimental data
should be ordered along magnetic field lines. In fact, given the
density profile along a field line, the results of this thesis can
be used to determine the variation of the parallel electric field
along this same field line.

2. Direct experimental measurements of the electric fields
in the magnetosphere must be undertaken in order to determine to
what degree the assumption of a conservative parallel electric field

is valid, and in order to determine the exact form of the convection

pattern described in Chapter I.

3. The approximate model of proton motion along an open

field line, which was developed in Chapter II, should be applied to

the model of the electron distribution developed in Chapter III using

a more realistic magnetic field configuration than was used in the

second chapter.

4. The paths of the shocks formed at reconnection on the

night side should be computed, using the flow model developed in

Chapter IV, in the general case of isentropic flow behind the shocks.

5. The effect of a nonvanishing longitudinal viscosity co-

efficient on the plasma flow along a closed field line should be

explored. That is, to the proton flow equations developed in Chapter

IV should be added the viscosity term. It is to be noted that the

use of viscosity will also require the use of the differential energy

conservation equation since viscous stresses will yield a finite

region of continuous change in place of the shock.

6. An extensive theoretical investigation of the structure

of plasma shocks generated by electrostatic fields should be under-

taken in order to determine the processes required for their forma-

tion.

BIBLIOGRAPHY

1. Abramowitz, M., and Stegun, I. A., <u>Handbook of Mathematical Functions</u>, National Bureau of Standards, 1964.

2. Alfvén, H., and Fälthammer, C-G., <u>Cosmical Electrodynamics</u>, Oxford Press, 1963.

3. Angerami, J. J., and Carpenter, D. L., J.G.R., <u>71</u>, 711, 1966.

4. Angerami, J. J., and Thomas, J. O., Radioscience Laboratory Report SEL-63-110, The Stanford University, 1963.

5. Biermann, L. Z., Astrophys., <u>29</u>, 274, 1951.

6. Block, L. P., Electron and Plasma Physics Report Nr 65-13, The Royal Institute of Technology, Stockholm, 1965.

7. Booth, A. D., <u>Numerical Methods</u>, Butterworth's Scientific Publications, 1955.

8. Bonetti, A., Bridge, H. S., Lazarus, A. J., Rossi, B. and Scherb, F., J.G.R., <u>68</u>, 4017, 1963.

9. Brice, N. M., J.G.R., <u>72</u>, 5193, 1967.

10. Buneman, O., Phys. Fluids, Supplement, 53, 1964.

11. Carpenter, D. L., J.G.R., <u>67</u>, 135, 1962.

12. Carpenter, D. L., J.G.R., <u>68</u>, 1675, 1963.

13. Carpenter, D. L., Rev. Geophys., <u>2</u>, 415, 1964.

14. Carpenter, D. L., J.G.R., <u>71</u>, 693, 1966.

15. Chapman, S., Cowling, T. G., <u>The Mathematical Theory of Non-Uniform Gases</u>, Cambridge University Press, 1964.

16. Chapman, S., and Ferraro, V. C. A., Terrest. Mag. and Atmos. Elec., <u>36</u>, 77, 1931.

17. Chapman, S., and Ferraro, V. C. A., Terrest. Mag. and Atmos. Elec., <u>37</u>, 147, 1932.

18. Chapman, S., and Ferraro, V. C. A., Terrest. Mag. and Atmos. Elec., <u>38</u>, 79, 1933.

19. Coleman, P. J., Davis, L., and Sonett, C. P., Phys. Rev. Letters, <u>5</u>, 43, 1960.

20. Courant, R., and Friedrichs, K. O., <u>Supersonic Flow and Shock Waves</u>, Interscience Publishers, 1963.

21. Dungey, J. W., Phys. Rev. Letters, <u>6</u>, 47, 1961.

22. Dungey, J. W., Scientific Report No. 269, Ionosphere Research Laboratory, The Pennsylvania State University, 1966.

23. Fairfield, D. H., Report No. X-612-67-174, Goddard Space Flight Center, 1967.

24. Fairfield, D. H., and Cahill, L. J., Jr., J.G.R., <u>71</u>, 155, 1966.

25. Fälthammer, C-G., Electron and Plasma Physics Report, The Royal Institute of Technology, Stockholm, 1964.

26. Geisler, J. E., and Bowhill, S. A., Aeronomy Report No. 5, The University of Illinois, 1965.

27. Gringauz, K. I., Bezrukikh, V. V., Ozerov, V. D., and Rybchinskii, R. E., Dokl. Acad. Nauk. SSSR, <u>131</u>, 1301, 1960.

28. Jaffrin, M. Y., and Probstein, R. F., Phys. Fluids, <u>7</u>, 1658, 1964.

29. Levy, R. H., Petschek, H. E., and Siscoe, G. L., Avco Everett Research Laboratory Report No. 170, 1963.

30. Liepmann, H. W., and Roshko, A., <u>Elements of Gasdynamics</u>, John Wiley and Sons, Inc., 1957.

31. Nishida, A., J.G.R., <u>71</u>, 5669, 1966.

32. Parker, E. N., Astrophys. J., <u>128</u>, 664, 1958.

33. Parker, E. N., Astrophys. J., <u>132</u>, 821, 1960.

34. Parker, E. N., <u>Interplanetary Dynamical Processes</u>, Interscience Publishers, Inc., 1963.

35. Persson, H., Scientific Report Nr. 65-07, The Royal Institute of Technology, Stockholm, 1965.

36. Schatten, K. H., and Wilcox, J. M., J.G.R., <u>72</u>, 5185, 1967.

37. Sonnerup, B. U. Ö., and Cahill, L. J., Jr., J.G.R., <u>72</u>, 171, 1967.

38. Speiser, T. W., Scientific Report No. 222, The Ionosphere Research Laboratory, The Pennsylvania State University, 1964.

39. Speiser, T. W., J.G.R., $\underline{72}$, 3919, 1967.

40. Taylor, H. A., Jr., Brinton, H. C., and Smith, R. C., J.G.R., $\underline{70}$, 5769, 1965.

41. Taylor, H. A., Jr., Brinton, H. C., and Pharo, M. W., III, Report No. X-621-67-559, Goddard Space Flight Center, 1967.

42. Watt, T. M., J.G.R., $\underline{70}$, 5849, 1965.

43. Wilcox, J. M., Schatten, K. H., and Ness, N. F., J.G.R., $\underline{72}$, 19, 1967.

44. Whipple, E. C., and Troy, B. E., paper presented at American Geophysical Union Meeting, Washington, D. C., April, 1965.

APPENDIX

MAGNETIC AND GRAVITATIONAL TERMS

The coordinate systems used to define a magnetic dipole field line are shown in Figure 38. The distance along the line of force from the earth to the point in question is labeled s and corresponds to the distance coordinate used in the text.

Angerami and Thomas (Appendix; 1963) derived a relationship between the distance along the field line S_1 from its equatorial crossing point and the latitude ϕ of the given point. This is expressed as

$$S_1(\phi) = \frac{RE}{2\sqrt{3}} \left[\ln(Y + \sqrt{1+Y^2}) + Y\sqrt{1+Y^2} \right] \quad \text{(A-1)}$$

where $Y = \sqrt{3} \sin \phi$, ϕ is the latitude and RE is the geocentric distance to the equatorial crossing point of the considered field line. The coordinate s is related to S_1 by

$$s(\phi) = S_1(\phi_o) - S_1(\phi) \quad \text{(A-2)}$$

where ϕ_o is the latitude at which the field line intersects the earth.

The differential ds is related to the latitude by

$$ds = -RE\sqrt{1+3\sin^2\phi} \cos\phi \, d\phi . \quad \text{(A-3)}$$

Another relation which is needed is the magnetic induction along a dipole field line specified by the equatorial crossing distance RE:
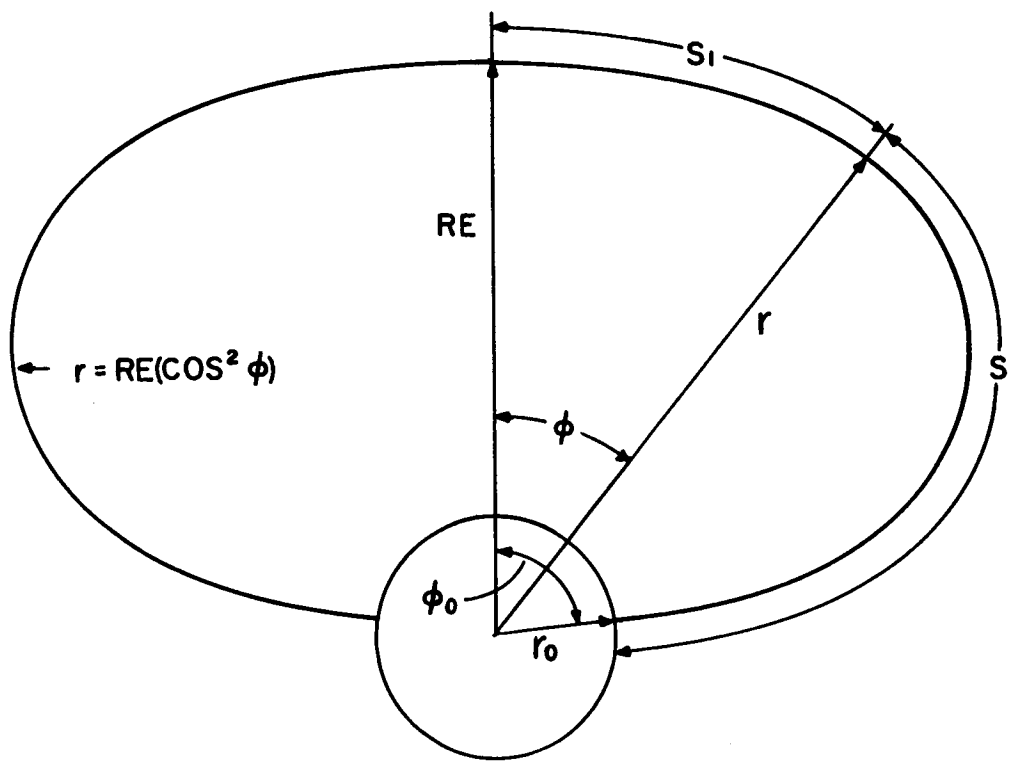
FIGURE 38. MAGNETIC DIPOLE FIELD LINE

$$B = \left(\frac{M}{RE^3 \cos^6 \phi} \right) (1+3 \sin^2 \phi)^{\frac{1}{2}} \qquad (A-4)$$

where the magnetic moment M for the earth is approximately 0.31 gauss- (earth radii)[3].

The flow equations developed in the text involve the factor $F = \frac{1}{B} \frac{\partial B}{\partial s}$. Since $\frac{dB}{ds} = \frac{dB}{d\phi} \frac{d\phi}{ds}$, equations A-4 and A-3 are used to determine the expression for F at any point along the field line:

$$F = \frac{- 3 \sin \phi}{RE (1+3 \sin^2 \phi)^{\frac{1}{2}}} \left[\frac{1}{1+3 \sin^2 \phi} + \frac{2}{\cos^2 \phi} \right]. \qquad (A-5)$$

Since the natural parameter in the plasma fluid model under consideration is s, a numerical analysis technique must be used to obtain the latitude corresponding to s from the equation A-2 before B or F (equations A-4 and A-5) can be stipulated. Newtons iteration scheme (Booth; 1955) was used to accomplish this inversion in the actual computations.

Next, the gravitational acceleration g along the magnetic dipole field line is required. Again, Angerami and Thomas (1963) derived this expression. If g_o is defined as the gravitational acceleration at the earth's surface (i.e., g_o = 9.8m/sec^2), and ϕ_o is the latitude at which the field line intersects the earth, the component of the gravitational acceleration along the field line is given by

$$g = g_o \frac{\cos^4 \phi_o}{\cos^4 \phi} \cos \beta$$

where $\qquad (A-6)$

$$\beta = \frac{2}{\cos \phi} \frac{\sin \phi}{\sqrt{1+4 \tan^2 \phi}} .$$